

Design and Validation of a Device to Measure the Cutting Edge Profile of Osteotomes

By

**Eamonn Price
(B.Eng)**

Institute of Technology, Sligo

**A Thesis submitted in fulfilment of the degree of
Master of Engineering**

2005

**Mr. Ger Reilly
Dr. B.A.O. McCormack
Supervisors**

Dedicated to My Son Jeremy

Now we will make up the lost hours

Declaration

I declare that I am the sole author of this thesis and that all the work presented in it, unless otherwise referenced, is my own. I also declare that this work has not been submitted, in whole or in part, to any other university or college for any degree or qualification.

I authorise the library of Sligo Institute of Technology to lend this thesis.

Signed: 

Date:17-10-2005.....

Acknowledgements

I would like to acknowledge the help and support of Mr Ger Reilly, Dr. Brendan McCormack and Dr. John Donavan.

Thanks to Mr. Andrew Macey for his support and allowing me to attend at hip operations which proved both informative and enlightening.

My thanks to Dr. Ger O'Connor at the national Centre for Laser Applications for his in-depth knowledge of laser systems. To Prof. Hossien Valizadeh for information on the applications of lasers.

Special thanks to Mr. Ray Tobin for his technical assistance especially with Labview software, and for his ability to see a solution where it appears none exists.

My thanks to all the staff of the engineering workshop for their assistance with the development of the prototype particularly when I arrived at the workshop at ten to five on a Friday evening John, Seamus, Sam, David and Jimmy thank you.

Thanks to Gordon Muir for machining jigs and to Michael Fox for the supply of calibrated gauges and for the supporting paperwork, to Noel Duncan for manufacture of sample blades.

The transition back to college life was made that much easier by the help and support of the lads in the research office Anthony, Ashkan, Cormac, Hamid, Bahman and Shane thanks for your support and the lively and varied conversation, particular thanks to John Hession for all your help. Thanks to Margeret O'Dwyer for proof reading the Thesis.

The Engineering office staff deserve special mention for all the encouragement and practical help that they have given to me over the past two years Mary, Carmel, Phylis, Cathronia, Evelyn, Michelle and Veronica thank you for putting up with my continuous questions and your often noisy neighbours.

This Thesis is part of wider research group involved in the research of cutting of Biomaterials and Biocomposites. I would like to thank the other members of the group for the transfer of ideas and data which has improved the understanding of the complexities of the cutting process.

I would like to thank my family for the support and encouragement which allowed me to complete my studies.

**This Research Project has been financed by the Irish Government under
the National Development Plan, 2000 – 2006
With co-financing by the
European Commission under the
European Regional Development Fund**

Publications and presentations resulting from this study

E.Price, G.A.Reilly, B.A.O. McCormack, A.C.Macey 2003. At the Cutting Edge of Surgical Instruments.

Presented at the 4th Annual Multidisciplinary Research Conference, Research and education foundation Sligo General Hospital

E.Price, G.A.Reilly, B.A.O. McCormack, A.C Macey 2004. Techniques for Investigation of Surgical Cutting Instruments.

Presented at the Materials and Processes for Medical devices conference & Exposition, St.Paul,Minnesota USA

+

Contents

Declaration	I
Acknowledgements	II
Publications and presentations resulting from this study	IV
Contents	V
List of Figures	VIII
List of Tables	XIII
Abstract	XIV
List of Symbols, Abbreviations and Glossary	XV
Chapter 1	1
1.1 A history of blades	1
1.2 The cutting process	2
1.3 Approaches to bone cutting.....	4
Chapter 2.0	8
2.1 The cutting process	8
2.2 Cutting sharpness	8
2.3 Why measure sharpness?.....	10
2.3.1 Qualitative analysis of cutting sharpness	10
2.4 Models of the cutting process	13
2.4.1 Aspects of the Bone Cutting Process.....	14
2.4.2 Orthogonal cutting of bone	14
2.4.3 Chip formation	15
2.4.4 Orthogonal cutting forces.....	15
2.5 Methods used to measure blade geometry (Quantitative analysis of blade sharpness).....	17
2.5.1 Contact measurement.....	17
2.5.2 Non-Contact measurement	18
2.6 Patent searches	20
2.7 Concluding remarks	21
Chapter 3.0 Current state of the art	22
3.1 Current state of the art in surface profilometry	22
3.2 Contact measurement:	23
3.2.1 CATRA sharpness tester	23
3.2.2 Co-ordinate measurement machine.....	26
3.3 Non-contact measurement:	27
3.3.1 Shadow Graph.....	27

3.3.2 Vision systems	28
3.3.3 Confocal microscope	28
3.3.4 Autofocus laser measurement	32
3.3.5 Scanning electron microscope	35
3.3.6 Dynamic force microscope	38
3.4 Conclusions	40
Chapter 4.0 Design of measurement device	43
4.1 The Design Process	43
4.2 Phase I Conceptual Design	44
4.2.1 Design Brief	44
4.2.2. Information Gathering	44
4.2.3 Objective Tree Analysis	45
4.2.4 Functional Analysis	46
4.2.5 Product Design Specification	48
4.3 Phase II Concept generation	50
4.3.1 Concept (a)	50
4.3.2 Concept (b)	51
4.3.3 Concept (c)	52
4.4 Evaluation of Concepts	52
4.4.1 Morphological analysis	54
4.5 Component selection	56
4.5.1 Lasers	56
4.5.2. XY Slides	61
4.5.3 Control of XY Slides	64
4.5.4 Blade clamp design	64
4.5.5. Software Design	65
4.5.6 Program Design – Laser testing	66
4.5.7 Program Design – Slide and laser interoperability	70
4.6 Phase III Detail Instrument Build	75
4.6.1 Component configuration	75
4.7 Instrument Testing	78
4.7.1 Laser interference study	78
4.8 User interface	80
4.9 Final layout of components	83
Figure 4.47 Layout of components	83
Chapter 5.0 Instrument Testing	84
5.1 Instrument Evaluation Study	84
5.2 Gauge R and R Study	86
5.3 Clamp Modification Design	92
5.4 Program Modification Design	97
5.5 Results single side scans	101

5.6 Results double side scans.....	103
5.7 Verification of Results.....	104
5.8 Measurement of osteotome.....	105
Chapter 6.0 Conclusions.....	108
6.1 Main conclusions and proposals for further work	108
References	110
Appendix A Machine evaluation study	
Appendix B Calibration sheets	
Appendix C Mechanical drawings	

List of Figures

Figure 1.1	Blade fitted with bone handle	1
Figure 1.2	A very early capital amputation saw	2
Figure 1.3	Orthogonal cutting	3
Figure 1.4	Cutting edge geometry	3
Figure 1.5	Osteotome cutting bone	4
Figure 1.6	Osteotome in use, is struck with mallet	5
Figure 1.7	Osteotome removed from service	5
Figure 1.8	Osteotome in use at Sligo General Hospital during a hip replacement operation	6
Figure 1.9	Variation in wedge angle caused by inappropriate re-grinding procedures	6
Figure 1.10	SEM Image of blade showing a blade which is sharpened to a smaller tip radius than is recommended	7
Figure 2.1	Cutting edge parameters showing wedge angle and cutting edge radius	8
Figure 2.2	Scalpel blade edge	9
Figure 2.3	Classifications of cutting edges for periodontal curettess	10
Figure 2.4	Wire edge formed after prolonged use of enamel hatchet blades	11
Figure 2.5	Surface quality resulting in poor cutting edge quality	11
Figure 2.6	Model of orthogonal cutting showing system of balanced cutting forces	13
Figure 2.7	Hills model of indentation cutting showing slip line fields	14
Figure 2.8	Expanding core and median crack during indentation of brittle materials	16
Figure 2.9	Schematic arrangements for obtaining Fourier transformation	19
Figure 2.10	Blade angle measurement	19
Figure 3.1	Sample blades used in all the studies of the various technologies	22
Figure 3.2	Blade being tested on CATRA blade sharpness tester	23
Figure 3.3	Schematic operation of CATRA blade sharpness tester	24
Figure 3.4	Results of tests on CATRA sharpness tester	24

Figure 3.5	CATRA sharpness tester	26
Figure 3.6	Starrett HD400 shadowgraph	27
Figure 3.6(a)	Image from vision systems	28
Figure 3.7	Blade set-up for scanning with confocal microscope	29
Figure 3.8	Depth of field is reduced due to the diffused light	30
Figure 3.9	Image generated by confocal microscope	31
Figure 3.10	Blade scanned on side to reduce the effects of light scatter	32
Figure 3.11	Jig fixture used for setting blade flank in horizontal direction	32
Figure 3.12	Blade scanned on side using NanoFocus confocal laser scanner	33
Figure 3.13	The limitations of spot size	34
Figure 3.14	Scanning Electron Microscope at Institute of Technology Sligo	35
Figure 3.15	Blade set-up in Scanning Electron Microscope	36
Figure 3.16	Image generated by Scanning Electron Microscope	37
Figure 3.17	Image of top of blade using Scanning Electron Microscope	37
Figure 3.18	Dynamic Force Microscope	38
Figure 3.19	Operation of dynamic force microscope	38
Figure 3.20	Sample blade in vertical direction being scanned with Dynamic Force Microscope	39
Figure 3.21	Image of scalpel generated by Dynamic Force Microscope	39
Figure 3.22	Comparisons of various measurement technologies	40
Figure 4.1	The design process outlining the stages during the design of the prototype	43
Figure 4.2	Methods used to gather information	45
Figure 4.3	Objective tree analysis	46
Figure 4.4	Functional analysis showing the outline functions required of the measurement device	47
Figure 4.5	Functional analysis extended beyond scope of this thesis	47

Figure 4.6	Product design specification	48
Figure 4.7	Device designed to rotate blade 180 degrees	50
Figure 4.8	Sequence of operation of the blade clamp	51
Figure 4.9	Goniometer concept	51
Figure 4.10	Concept of device to scan both sides of a blade simultaneously	52
Figure 4.11	PSD Beam spot is used to determine the beam spot centre	57
Figure 4.12	CCD :Detection of the peak value	57
Figure 4.13	Principle of operation of laser triangulation	58
Figure 4.14	Arrangement of laser triangulation head relative to blade	58
Figure 4.15	Keyence LK-31 laser head controller	59
Figure 4.16	68-pin shielded connector	59
Figure 4.17	Data flow from laser heads to laptop	60
Figure 4.18	Slide unit M-111.1DG	62
Figure 4.19	XY slide configured from two PI. M-111 high resolution motorized translation stages	62
Figure 4.20	Aligning the slides using dial gauge	63
Figure 4.21	Aligning the clamp unit using dial gauge	63
Figure 4.22	Mercury II C-862 single-axis DC-motor controller	64
Figure 4.23	Design for blade clamping unit	64
Figure 4.24	Operation of clamp unit	65
Figure 4.25	Clamp unit fitted to XY slide	65
Figure 4.26	Labview program to run one laser head	66
Figure 4.27	Zero datum for blade	67
Figure 4.28	Span setting for blade	67
Figure 4.29	Using slip gauges to calibrate laser heads	68
Figure 4.30	Outline of program to scan blade using one laser	70

Figure 4.31	Data as displayed in Microsoft Excel	71
Figure 4.32	Calculation of wedge angle	71
Figure 4.33	Outline of program to scan blade using two lasers	72
Figure 4.34	Graph of data points scanned into excel	73
Figure 4.35	Calculation of wedge angle of blade	74
Figure 4.36	Proposed layout of laser heads relative to blade clamp device	75
Figure 4.37	Support frame	76
Figure 4.38	Aligning laser head	77
Figure 4.39	Effect of laser head misalignment	77
Figure 4.40	As blade flanks are scanned no interference is experienced by the lower laser	78
Figure 4.41	As blade is scanned some diffused from the top laser is picked up by the lower laser	79
Figure 4.42	Measurement errors as a result of diffused light from laser	79
Figure 4.43	Laser head reorientation changed to eliminate the problem associated with laser light scatter.	80
Figure 4.44	User interface screen	81
Figure 4.45	Maximum force/wedge angle for HDRPF 40PCF	82
Figure 4.46	Maximum force/cutting edge radius for HDRPF of varying densities.	82
Figure 4.47	Final layout of components	83
Figure 5.1	Results of instrument evaluation study	85
Figure 5.2	Concepts of precision and accuracy	86
Figure 5.3	Original design for blade clamping unit	92
Figure 5.4	Modified blade holder	93
Figure 5.5	Reproducibility and Repeatability study	97
Figure 5.6	Original calculation of wedge angle of blade	98
Figure 5.7	Effect of using just four data points to calculate the wedge angle of blade	98
Figure 5.8	Schematic of point parameters for regression calculation	99

Figure 5.9	Instrument evaluation study without regression formula	100
Figure 5.10	Instrument evaluation study with regression formula	100
Figure 5.11	Comparison of results	101
Figure 5.12	Single side of blade, tip radius 500 μ m	102
Figure 5.13	Single side of blade, tip radius 300 μ m	102
Figure 5.14	Single side of blade, tip radius 100 μ m	102
Figure 5.15	Double scan of sample blade radius 500 μ m.	103
Figure 5.16	Double scan of sample blade radius 300 μ m.	103
Figure 5.17	Double scan of sample blade radius 100 μ m.	103
Figure 5.18	Results of scans on sample blades	104
Figure 5.19	12mm osteotome set up for scanning	105
Figure 5.20	Results of scan on 12mm osteotome	106

List of Tables

Table 2.1	Qualitative systems for analysis and classification of cutting edge sharpness for periodontal instruments	21
Table 3.1	Summary of operating specifications	57
Table 4.1	Product Design Specification	49
Table 4.2	Weighted analysis matrix for measurement device	53
Table 4.3	Morphological Chart	54
Table 4.4	Component selection for measurement head	54
Table 4.5	Component selection for blade clamp	55
Table 4.6	Component selection for XY slide drive	55
Table 4.7	Specifications for the components for the measurement system	56
Table 4.8	Calibration of laser head	68
Table 4.9	Results of scans on slip gauges	69
Table 4.10	Results of second series of tests using slip gauge	69
Table 5.1	Table of results for Machine evaluation study	85
Table 5.2	Summary of results for R and R study	88
Table 5.3	Results of calculation of moving range for R and R study	90
Table 5.4	Summary of results for R and R study (2)	94
Table 5.5	Verification of Results for prototype measurement Instrument	104

Abstract

Design and Validation of a Device to Measure the Cutting Edge Profile of Osteotomes

By Eamonn Price B.Eng.

The cutting capacity of a cutting instrument is normally defined as its sharpness, which defines the ability of the cutting edge to cut the target material. Many factors therefore affect the ability of a blade to cut, including the target material, the manufacturing process, and the cutting forces associated with cutting technique employed (Kalder S., 1997).

In this study of techniques for measurement of the cutting edge profile various methods were used to measure blade profiles and found that no one method of measurement was capable of quantifying all the geometric parameters of the cutting edge of the blade.

SUB³ (Sharpness of Unserrated Blades for Biomaterials and Biocomposites) is a research project focusing on the specification of sharpness measurement for surgical blades. A component of the work of the SUB³ project is the design and build of a prototype device for blade profile measurement. This project contributes a device capable of measuring the profile and wedge angle of the cutting flanks of a surgical osteotome.

The aim of this thesis is to investigate the measurement of sharpness with particular relevance to non-contact measurement of the geometric parameters of the surfaces of the cutting instrument.

All relevant current methods of profile measurement were investigated to establish a suitable method for the measurement of the geometric properties of a surgical osteotome using legacy technology, and also to establish if it could be developed using existing components of measurement systems. If the technology does not exist it is proposed to design and build a working prototype non-contact profile measurement device capable of measuring the wedge angle of a surgical osteotome.

List of Symbols, Abbreviations and Glossary

Symbols

R_a	<i>Arithmetic mean of the absolute departures profile from the mean line.</i>
z	<i>Depth of field.</i>
w	<i>Beam spot size.</i>
λ	<i>Wavelength.</i>
μm	<i>Micron</i>
nm	<i>Nanometer</i>
Å	<i>Angstrom</i>
α	<i>Rake angle</i>
β	<i>Clearance angle</i>

Abbreviations

CCD	Charged Coupled Device.
CMM	Co-ordinate Measurement Machine.
DFM	Dynamic Force Microscope.
DAQ Card	Data acquisition card.
LASER	Light Amplification by the Stimulated Emission of Radiation.
PDS	Product Design Specification.
PSD	Position Sensitive Device.

SEM	Scanning Electron Microscope.
SUB ³	Sharpness of Unserrated Blades for Biomaterials and Biocomposites.
WLI	White Light Interfometer.
P/T ratio	Precision-tolerance ratio.

Glossary of Terms Related to Cutting and Measurement of Sharpness

Accuracy	Ability to measure the true value correctly on average.
Blade	Cutting instrument, used to cut target material.
Blunt material.	Dulled edge/not suitable for purpose of cutting target material.
Burr	Rough edge left on blade edge after sharpening/cutting.
Chip	Shaving of target material removed by the cutting process.
Chipping	Action of removing target material by a pecking cutting action.
Chopping	To cut/split resulting from a blow from a cutting instrument.
Cut	To open up target material.
Cut depth	Depth to which the blade is inserted into the target material.
Cutting tip	Geometry at cutting edge.
Diffused light	Light which is diffused from a sample surface while it is being scanned.
Blade flanks	Sides of cutting blade, forming the wedge angle.
Osteotome	Surgical cutting instrument used for the cutting of bone.

Precision	A measure of the inherent variability in the measurements.
Sharpening	Procedure for reproducing or repairing the cutting edge of the cutting instrument.
Spot size	The diameter of the spot from the light source used in the measurement head.
Target material	Material to be cut.
Wedge angle flanks.	Included angle of blade, measured between the cutting
Wire edge	Burred edge formed by the sharpening process or by blade wear.

Chapter 1

1.1 A history of blades

Blades have been used since stone-age man first learned how to use flint to produce cutting instruments and date back some 2 million years, however recognisable blades were made out of stone from five hundred thousand years ago (500,000-10,000 B.C.)

Four to seven thousand years ago (5000-2000 B.C.), stone blades were being polished and were fitted with crude handles, which were made of wood or animal hides to protect the users hand (Figure 1.1).



Figure 1.1 Blade fitted with bone handle (www.agrussell.com/.../glossary/c.html)

Metal blade knives were first made from copper and subsequently bronze in the years 3000-700 B.C., and they have had many features that are still retained today. After the Bronze Age it was discovered that an iron blade had a much sharper and long-lasting edge, and iron knives were widely made from about 1000 years before the birth of Christ. The Romans in particular developed many different types of knife to suit a wide number of uses (including ritual animal sacrifices and knives for cutting hair). Knives were considered to be very important possessions and people had personal eating knives which they carried with them. It was not unusual for people to be buried with their personal eating knives.

Throughout the ages many variations of cutting instruments were developed, the Japanese in particular were noted for the *chokuto* which is a broad, straight, and single edged blade.

The design of osteotomes dates back to the 17th or 18th century. These tools were copied from those used in the wood industry. Surgeon's tools only included a few technical improvements compared with those commonly used for cutting other materials (Giraud et al., 1991) Blades were also developed for

industry and for surgery and many of the early surgical instruments were simply copies of cutting instruments used for cutting metal or wood (Figure 1.2).



Figure 1.2 A very early capital amputation saw from Jacobean England 1606-1621. (<http://antiquescientifica.com/articles%205.htm>)

As cutting involves the interaction between the blade, and the target material it was historically the operator who decided the type of cutting tool to use, the cutting procedure, and when to replace or regrind the cutting tool. Increasingly it is becoming more important to standardise the sharpening interval and procedure for sharpening, particularly on reusable surgical cutting tools.

1.2 The cutting process

Cutting is a complex process involving the interaction between the cutting instrument normally a cutting tool or blade, the target material, the cutting environment, and the user or cutting system. It has been proposed in respect of metal cutting tooling that each of these parameters have an integrated role in the optimisation of the cutting process and on the role of appropriate tool selection in the efficacy of cutting (Kaldor S. and Venuvinod P.K., 1997). We use the term sharpness to define the capacity of the cutting instrument to cut the target material with a high level of efficiency. We use the term bluntness as an antonym to sharpness. To understand the need for inspection and control of cutting instruments some understanding must be gained on the cutting process.

The most basic type of cutting is of an orthogonal nature. This type of cutting involves a tool with a plane cutting face, and a single straight cutting edge (Figure 1.3).

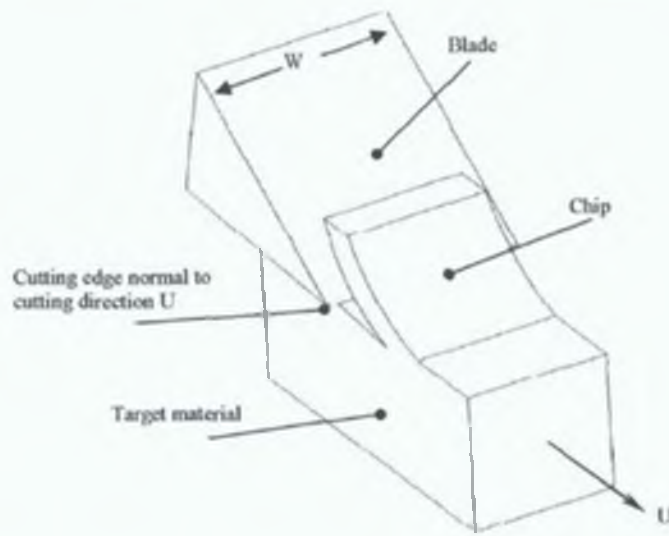


Figure 1.3 Orthogonal cutting; the cutting tool has a plane cutting face and a single, straight cutting edge. (Oxley P.L.B., 1989)

The geometry of the cutting edge is defined as the cutting width (w) (Figure 1.3) and by the two angles α and β (Figure 1.4). The angle α at the front of the cutting tool face is the rake angle, and may be positive (Figure 1.4a) or negative (Figure 1.4c).

The rake angle has a pronounced effect on the cutting process, causing an increase in cutting energy for many materials. (Merchant M.E., 1944)

The angle β between the base of the cutting tool and the target material is known as the clearance angle, it is of less importance in the mechanics of chip formation, however it can influence the rate of wear of a cutting tool.

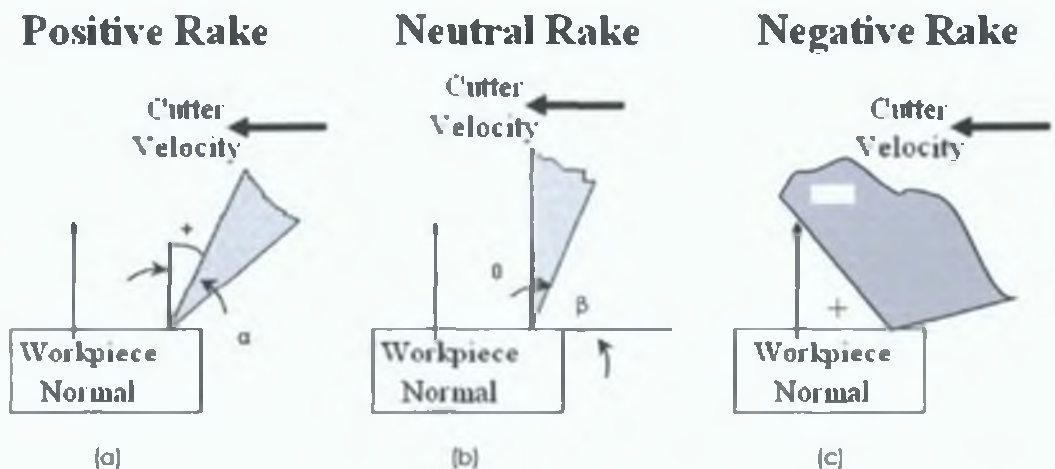


Figure 1.4 Cutting edge geometry (a) Positive rake angle, (b) Neutral rake angle, (c) Negative rake angle

1.3 Approaches to bone cutting

Surgical cutting may be divided into two broad categories, that of power cutting and of manual cutting.

1.3.1 Power cutting

Power cutting used in the surgical field, includes the use of, power drills, reciprocating saws, oscillating saws and reamers. Issues with power cutting include the generation of heat, cutting force and the use of coolant.

The inspection of these devices is not covered in this thesis.

1.3.2 Manual cutting

Manual cutting in the surgical field involves the use of, scalpels, scissors, chisels, gouges, hand reamers, osteotomes, as well as other such "hand" operated instruments.

This thesis will concentrate on the use and inspection of surgical osteotomes.

Osteotomes are used in surgical procedures such as hip joint replacement, and procedures where bone removal is required, surgical osteotomes are used with an orthogonal or indentation cutting action (Figure 1.5). The osteotome is impacted with a mallet as illustrated in (Figure 1.6), or by hand when cutting softer bone.

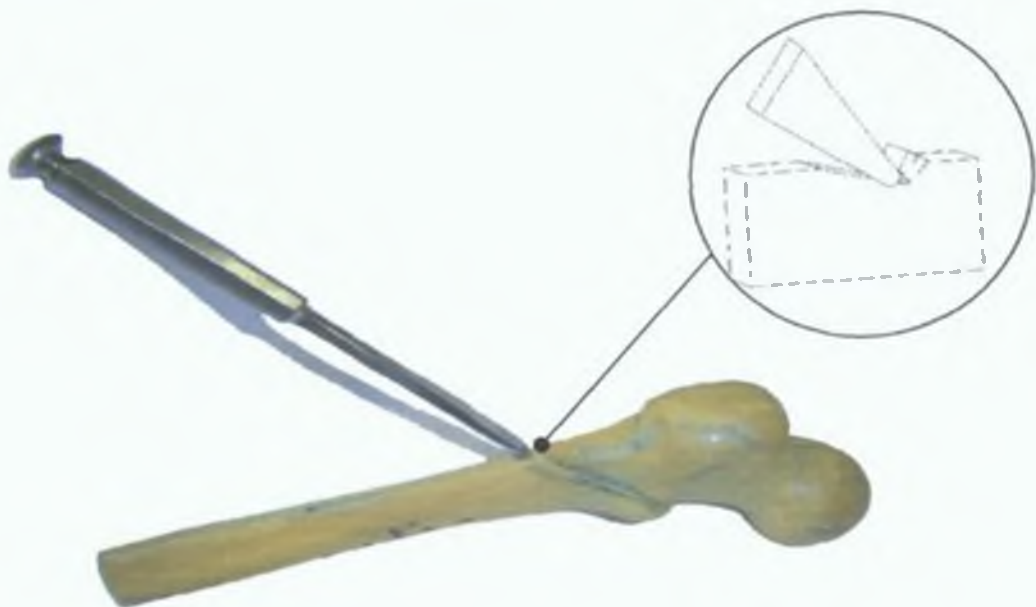


Figure 1.5 Osteotome cutting bone illustrating the orthogonal nature of the cutting process

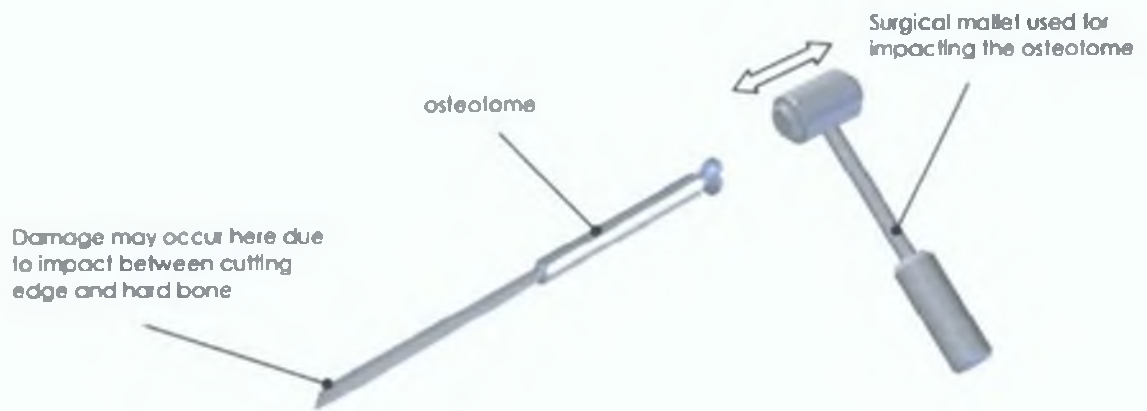


Figure 1.6 Osteotome in use, is struck with mallet, this may cause wear/ chipping to the edge of the blade

Factors which affect the ability of a surgical osteotome to cut, include the cutting procedure, the material type, and the blade geometry. It is common for the osteotome to become damaged during a surgical procedure, this can be blunting of the tip or in extreme cases chipping may occur to the tip of the osteotome. This chipping is to be avoided during a surgical procedure, as fragments of the tip may become imbedded in the open wound causing infection (Figure1.7).



Figure 1.7 Osteotome removed from service, showing signs of chipping of the blade tip, this particular osteotome should not have been used, hence the requirement for procedures for the inspection and maintenance of surgical cutting equipment



Figure 1.8 Osteotome in use at Sligo General Hospital during a hip replacement operation. Note the use of the surgical mallet to impact the osteotome.

The frequency of use of a chipped osteotome may be reduced by regular inspection of the cutting edge of the osteotome. Any deviation from the original tip profile of the osteotome should result in the osteotome being removed from service and resharpened.

It should also be noted that during the re-sharpening procedure the original shape of the tip should be preserved, to minimise the tendency to increase the wedge angle during the re-sharpening procedure creating a blunter wedge (Figure 1.9).

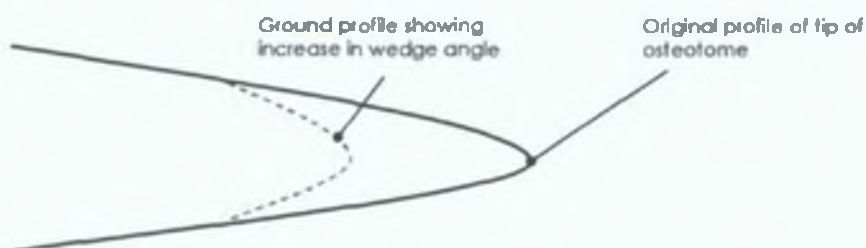


Figure 1.9 Variation in wedge angle caused by inappropriate re-grinding procedures

It should be also be noted that the tip radius of the blade should be preserved during the re-sharpening process, as a reduction in the tip radius may cause premature wear and chipping of the blade edge

Figure 1.10 illustrates the problem of a wire edge associated with a blade having an inappropriate tip radius. A wire edge occurs when cutting edge folds over on itself, in extreme cases the wire edge may break away.

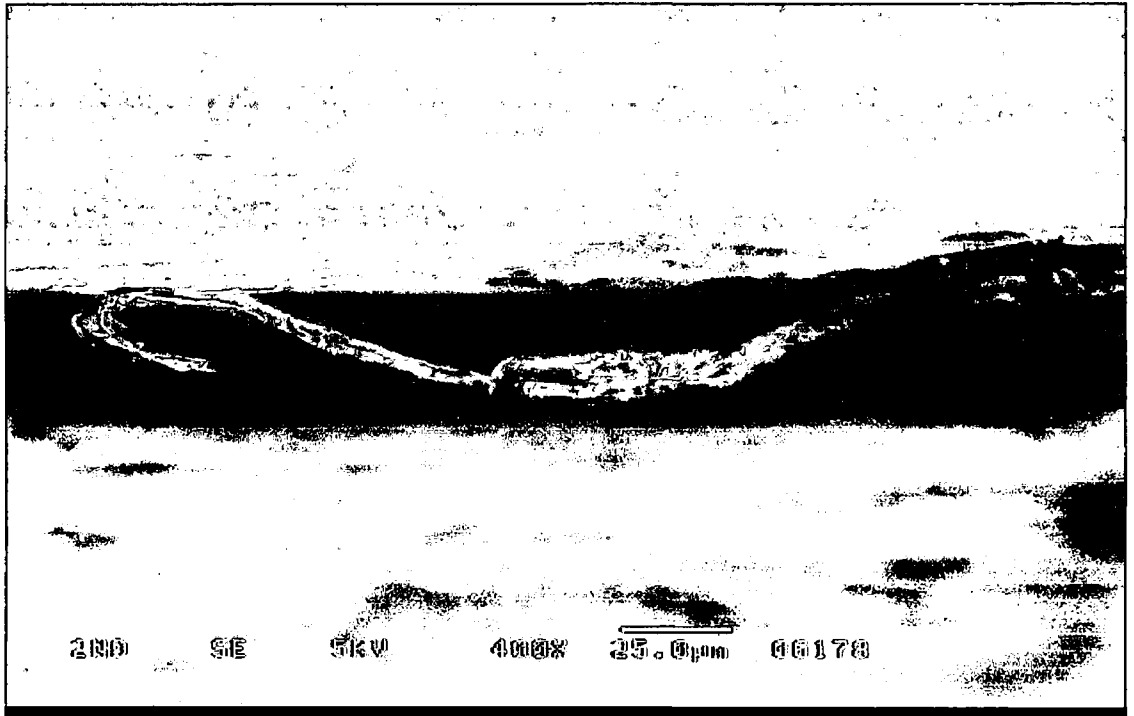


Figure 1.10 SEM image of wire edge on blade cutting edge

Chapter 2.0

2.1 The cutting process

The cutting process involves the cutting device (a blade or other cutting instrument) and the target material which is to be cut.

It is widely accepted that the quality of cut made by cutting instruments is dependent on number of variables, such as the properties of the material being cut, the blade material type, cutting edge geometry, friction and the type and direction of cutting force applied required. This force will produce a slicing, paring, chopping or shearing action depending on the direction of the applied force.

2.2 Cutting sharpness

The cutting instrument geometry will vary depending on the type of cutting whether it is used for cutting metal, wood or tissue will dictate the type of geometry of the blade.

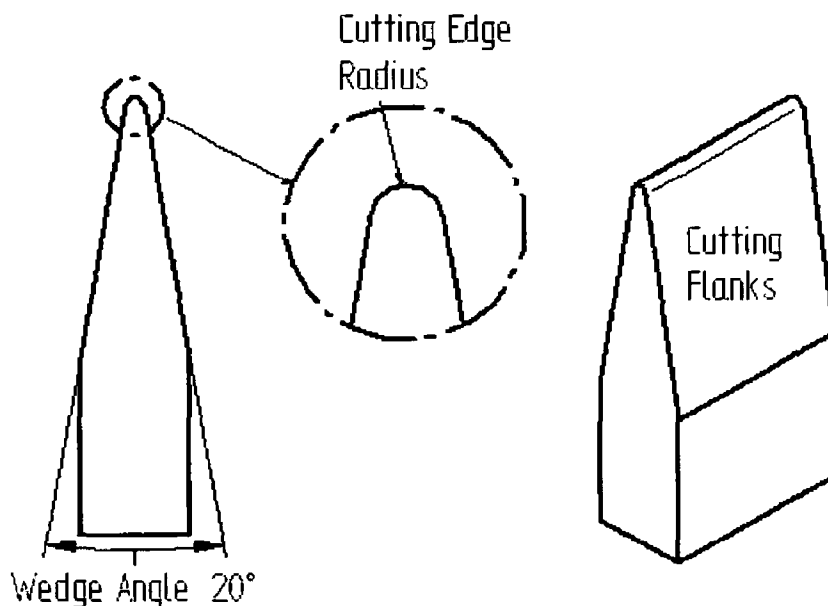


Figure 2.1 Cutting edge parameters showing wedge angle and cutting edge radius (Reilly et al 2004a)

The cutting component of the instrument is normally defined in a blade or pointed feature consisting of at least two cutting surfaces forming an included wedge angle. The intersection of cutting surfaces creates a single line of

intersection. This edge is not finitely sharp and the apex may be curved or filleted as shown in Figure 2.1 (Reilly et al., 2004a).

As indicated it is generally assumed that the cutting edge has a finite sharpness and that the edge is constructed of two intersecting flat planes formed by the grinding process. Manufactured sharpened edges generally produce a wedge angle not below 20° or above 90° as these are defined as limits of functionality for most cutting instruments used in slicing chipping and paring (Wehymer, 1987). Flat planes resulting from the sharpening process and creating such a line or edge of intersection may be referred to as the cutting surfaces of the blade. It has being shown in the case of instruments such as scalpel blades, which are considered to have an extremely sharp cutting edge that the radius on this edge is submicron in size and so quality and geometry of surfaces and edges are limited by the sharpening process. Images retrieved from a specialist sharpening company illustrate the size of edge features on sharpened scalpel edges (Figure 2.2).



Figure 2.2 Scalpel blade edge, field of view $20\mu\text{m}$, annotated radii $0.21 - 0.31\mu\text{m}$, source MDW Technologies (<http://www.mdwtech.com/imaging/images.html>)

2.3 Why measure sharpness?

When used for cutting of biological tissue, the characteristics of the blade and the condition of the cut surfaces may have long term consequences. For example, experiments carried out by (Izmailov et al., 1989) on 200 animals using 300 scalpels showed that incisions made with a scalpel of tip radius 0.8 microns heal better than an incision made with a scalpel of tip radius of 12.5 microns.

(Izmailov et al., 1989) showed that blunting of the cutting edge will occur during the normal use of cutting instruments therefore some method must be put in place to measure the sharpness of cutting instruments to ensure that the blade performs in an optimised condition or is re-sharpened as it loses its cutting edge. (Huebscher et al., 1989) states that a sharp scalpel is the first precondition of good postoperative wound healing.

2.3.1 Qualitative analysis of cutting sharpness

Most attempts to classify sharpness based on qualitative analysis of SEM micrographs provide limited geometrical analysis of the edge or its angular features, as quantitative analysis of the edge is difficult using this technique.

Relevant research into the quality of periodontal curettes classifies the various types of cutting edges as, a fine edge, a wire edge or a dull edge is illustrated in (Figure 2.3).

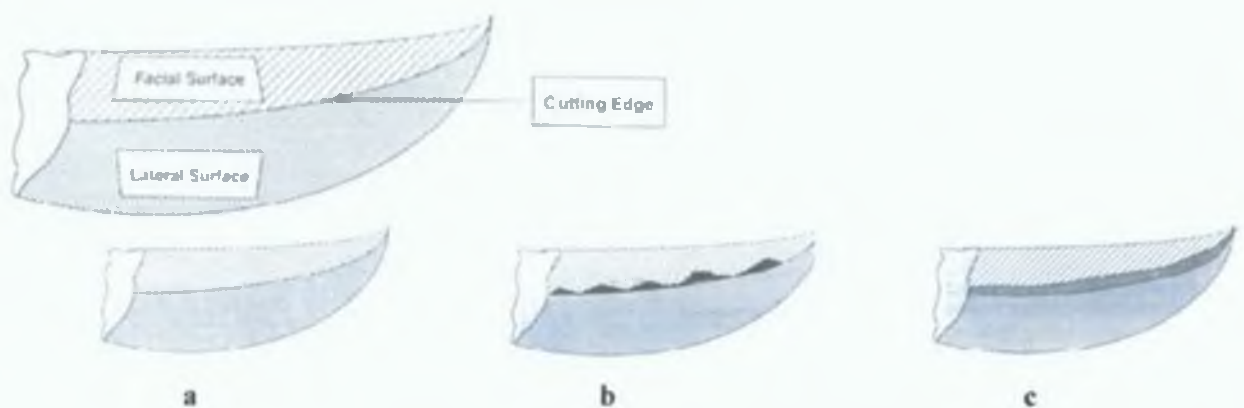


Figure 2.3 Classifications of cutting edges for periodontal curettes (a) fine edge, (b) wire edge, (c) dulled edge (Balevi, 1996).

The type of burred edge formed by the sharpening process has also been described as a wire edge and has been illustrated by Scanning Electron Microscope (SEM) (Antonini, 1977; Smith, 1989). The edge is formed when the sharpening process utilised is unsuitable for complete burr removal at the cutting edge, or when the cutting surfaces are not polished by fine grinding, honing or polishing abrasives following primary formation. The wire edge may also result from excessive wear of a cutting edge that is incapable of withstanding use and has rolled over on a cutting surface, (Figure 2.4) (Antonini, 1977; Smith, 1989)

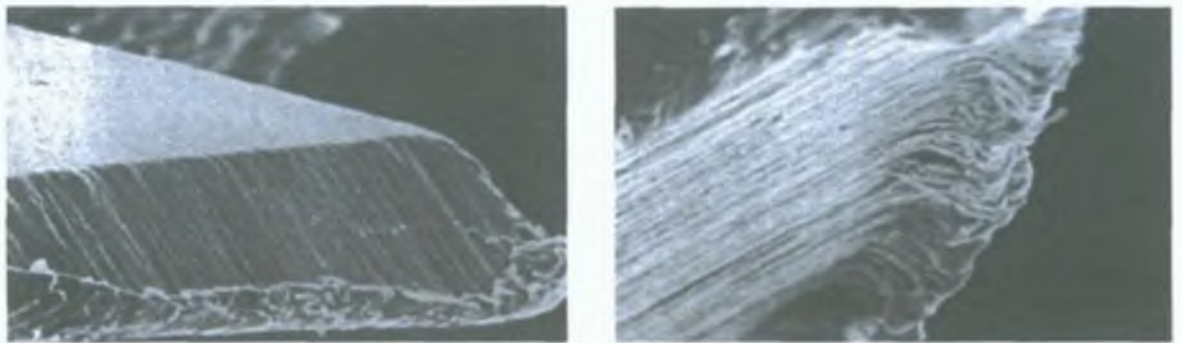


Figure 2. 4 Wire edge formed after prolonged use of enamel hatchet blades (Antonini, 1977; Smith, 1989)

Further SEM analysis of the cutting edge has illustrated other factors deemed relevant to the cutting ability of the instrument. These factors result from the sharpening process utilised and relate to the smoothness of either cutting surface (Vincent and Doting, 1989; Rossi, 1998). The features normally referred to are material treatment in manufacture (Wadsworth, 2000) and roughness of the cutting surfaces resulting in incomplete or poor definition of the cutting edge (Figure 2.5)

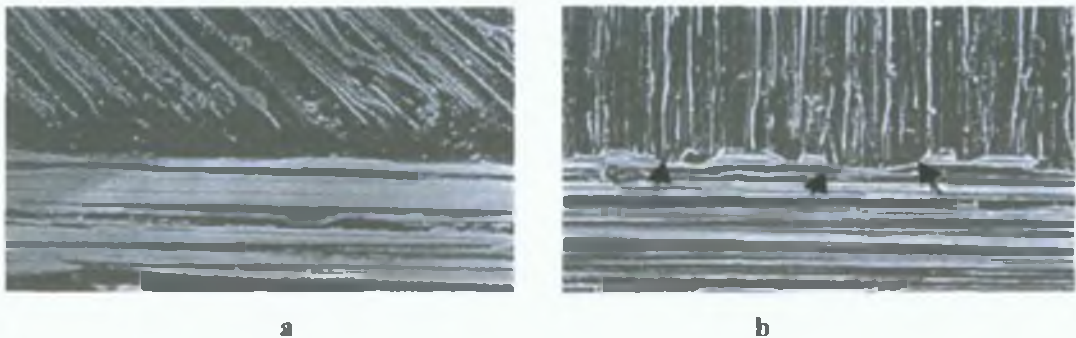


Figure 2. 5 Surface quality resulting in poor cutting edge quality (Rossi, 1998).

These studies which involved sharpness analysis of periodontal files, hatchets, and curettes have shown that the quality of the cutting edge prior to use has a significant affect on the durability of the cutting edge and on the quality of the cut surface on the target material (Smith, 1989; Vincent and Doting, 1989; Pasquini, 1995; Balevi, 1996; Rossi, 1998; Akura, 2001). These studies attempted a classification of sharpness based on observed characteristics of the cutting surfaces and cutting edges and the systems used to classify the sharpness are detailed in Table 2.1. It was also observed in these studies that instruments supplied as new or sharpened by manufacturers were not worthy of the highest sharpness grading and were in some instances deemed blunt and unsuitable for use in experimental tests.

Table 2.1 Qualitative systems for analysis and classification of cutting edge sharpness for periodontal instruments

Researcher	Instrument Studied	Classification System	Range of System
Smith et al (1989)	Enamel Hatchets and Hoes	Observational (Qualitative)	No comparative system
Tal et al (1989)	Periodontal curets	Qualitative	1 (sharp) to 3 (severe attrition)
Pasquini et al (1995)	Periodontal files	Qualitative	1 (dullest) to 5 (sharpest)
Rossi et al (1998)	Periodontal curets	Qualitative	0 (poor) to 2 (sharp)

2.4 Models of the cutting process

The term cutting sharpness is used to describe the capability of a cutting instrument to cut a particular type of material. Much research has been carried out in relation to the cutting of engineering materials, and the interaction between the cutting edge geometry and the cutting forces applied over a range of metals. Engineering models of cutting provide information on how the geometry of the cutting edge of the instrument has an effect on the measurable parameters of the process. Two such cutting models are applicable to the description of the mechanics of the cutting of bone using osteotomes. Orthogonal cutting describes a cutting process for a single pointed cutting instrument where the cutting edge of the instrument is aligned at right angles to the direction of the cutting motion and where the mechanics of the cutting process can be resolved by considering the cutting action as a two dimensional process (Figure 2.6).

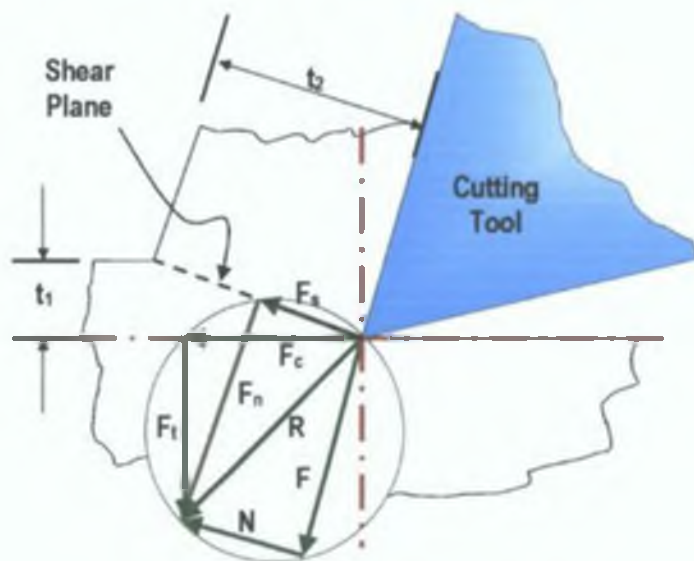


Figure 2. 6 Model of orthogonal cutting showing system of balanced cutting forces

Indentation cutting describes a process where the cutting instrument cuts by perpendicular penetration into the work piece and where the wedge angle of the cutting instrument is positioned to be symmetrical about the line of the cutting force (Figure 2.7).

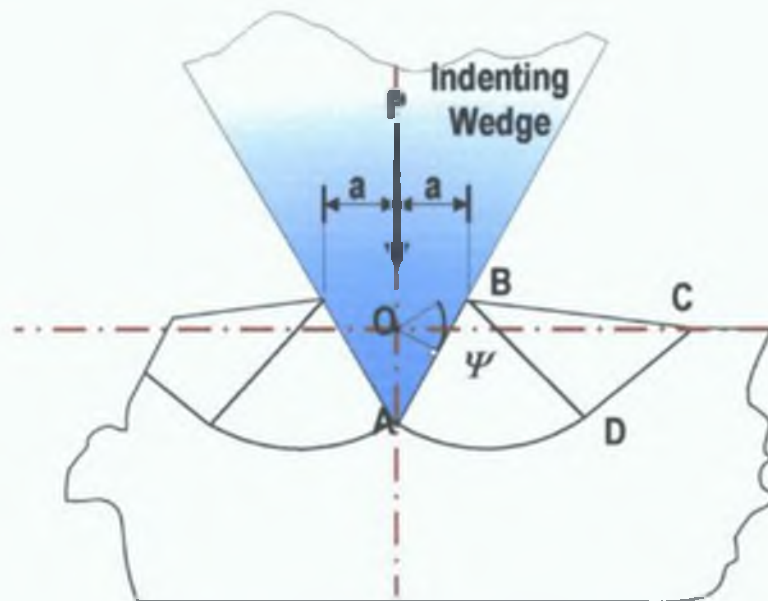


Figure 2.7 Hills model of indentation cutting showing slip line fields

2.4.1 Aspects of the Bone Cutting Process

There are a number of key features of the bone cutting process that have merited comment in the literature (Giraud et al 1991). In order of the occurrence of the event in the cutting process these are:

- (a) Deformation during initiation of the cutting process
- (b) Plasticity of the bone during machining
- (c) Chip formation at the tool material interface
- (d) Cutting force measurement as a factor of cutting criteria

2.4.2 Orthogonal cutting of bone

The concept of orthogonal cutting has potential applications to drilling, milling, chopping, chipping, and reaming of bone. It is necessary to state at the outset that bone is considered to be a brittle material, and moreover micro structurally and mechanically anisotropic and also liable to failure by brittle fracture through

crack propagation. This means that the application of cutting models developed for ductile metals may have limited application to an analysis of bone cutting.

2.4.3 Chip formation

The orthogonal cutting of bone involves the initial indentation of the bone by the tool, the formation of a chip by the movement of the tool in the material, and the fracture of the chip by the continuous cutting process. During the first stage a bone material subjected to indentation cutting parallel to the osteon direction can undergo recoverable plastic deformation due to the behaviour of mucopolysaccharides (proteoglycans) (Jacobs et al., 1974). It is known that proteoglycans can alter the collagen fibril structure and the rate of mineralisation in bone (Martin et al., 1998). During the second stage of cutting it was originally proposed that a continuous bone chip is formed across a shear plane that extends from the uncut surface of the bone to the original top surface of the bone material. This chip was thought to slide along the rake face of the cutting tool in a manner similar to continuous chip formation in metal cutting (Jacobs et al., 1974) but subsequent studies show that this observation was incorrect and that the chip formation involves a series of discrete fracture processes ahead of the cutting tool tip (Wiggins and Malkin, 1978).

2.4.4 Orthogonal cutting forces

Previous studies of orthogonal cutting have identified two key forces, the cutting force (force in the direction of cutting) and the thrust force (force perpendicular to the direction of cutting) that may be experimentally measured during the cutting operation (Merchant, 1944) as indicators of the tool geometry material interaction. In studies on bovine bone it has been shown that increasing the depth of cut increases the cutting forces while increasing the rake angle from a negative rake to a high positive rake can significantly decrease the cutting force measured in all cutting directions (Jacobs et al., 1974; Wiggins and Malkin, 1978). These relationships have also been similarly determined for human bone (Itoh et al., 1983). Wiggins & Malkin (1978) demonstrated that the first of these relationships is not linear and also that the decrease in cutting forces with increase in rake angle was more pronounced at larger depths of cut whereas Jacobs et al. (1974) had earlier proposed a linear relationship between

increasing depth of cut and increasing forces. Jacobs et al (1974) had not however considered depths of cut above $48\mu\text{m}$ in their studies. During orthogonal cutting of bone the cutting force is always higher than the thrust force and is greatest when cutting in a transverse direction and least when cutting in a parallel direction relative to the longitudinal axis of the bone (Itoh et al., 1983; Pal and Bhadra, 1986; Wiggins and Malkin, 1978). This is due to the anisotropy of bone and the fact that the preferred direction for crack propagation is parallel to the osteon direction. Wiggins & Malkin (1978) also determined that there is a decrease in specific cutting energy with increase in rake angle for cutting of both human and bovine bone in all cutting directions relative to the osteon direction. Brittle materials subjected to an indentation load undergo a two stage process of fracture involving penetration of the material during which the material underneath the indenter becomes compacted in a core which is separated from a volume of elastic material by an intermediate zone. During the first loading phase the core expands outwards creating a median vent crack underneath the indenter tip. Further loading of the material in the second phase results in opening and propagation of the crack leading to material fracture (Figure 2.8) (Lawn, 1975; Lawn, 1977). This model of crack initiation and propagation has been shown to apply to the cutting of bone (Reilly and Taylor 2003).

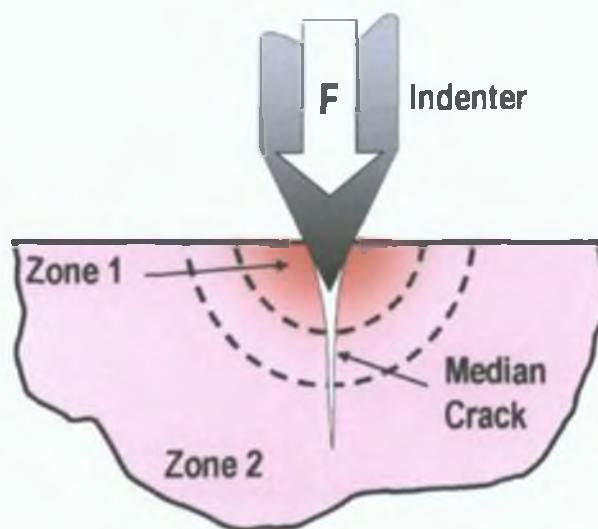


Figure 2.8 Expanding core and median crack during indentation of brittle materials (Lawn, 1975;)

2.5 Methods used to measure blade geometry (Quantitative analysis of blade sharpness)

As has been described in Section 2.3 it may be seen that many factors affect the ability of a blade to cut a particular material. These include the blade material type, the target material type, friction and the blade geometry.

If the blade material, target material and friction remain constant then it is possible to get an indication of the sharpness of a blade by measuring the geometric profile of the blade.

Various methods of measuring the profile of a cutting instrument have been proposed in research literature, these can be divided into two broad categories that of contact measurement and non-contact measurement.

2.5.1 Contact measurement

Contact measurement is one of the most established methods of profile measurement, methods include stylus form tracers, CMM's (Co-ordinate Measurement Machines), A non-destructive method for measuring the edge radius of the blade is described by Arcona (1996). The method involves creating an impression of the blade edge using a replica material in this case a vinyl polysiloxane impression material manufactured by 3M Corporation. When the mould is cured it is sectioned and viewed under a microscope. To test the effectiveness of this method a blade was sectioned and measured in a scanning electron microscope, the comparison was made by using a template to measure the void left in the plastic mould and comparing this to a best fit circle on the scanning electron microscope image, the measurement of $1.7\mu\text{m}$ measured by the mould compared favourably with the $1.6\mu\text{m}$ measured with the scanning electron microscope. Some drawbacks of this method include the subjective nature of the measurement of the void in the plastic mould. Also the need to produce a mould of the blade edge results in a slow measurement process.

Budinski (1997) describes a method in which soft solder (50% Pb, 50% Sn) is impacted on the blade edge; this indented solder is subsequently sectioned with a microtome and viewed under an optical microscope. This method has limitations primarily due to the contact nature of the test which may damage the blade edge, also it is only possible to view one cross section of the blade at a time.

A contact profilometer used to measure the tip radius of a metal cutting tool insert is described by Barry (1993) this technique describes the jig set-up to allow for the limited travel of the stylus profilometer used.

Shortfalls of this method include the range of the vertical stylus travel; this limits the profiles which can be measured to 30-40 μ m.

2.5.2 Non-Contact measurement

Non-contact measurement may be carried out by various methods including: white light interferometry, confocal microscopy, laser profilometry, dynamic force, microscopy scanning electron microscopy.

A goniometric laser model developed by CATRA (Cutlery and Allied Trades Association) is used to provide a non-contact analysis of blade sharpness. This device although limited to measurement of the wedge angle can, with training allow the operator to determine the grind finish and direction of grind.

A similar device was designed by the author with a view to automating the process, however it was limited in its applications for this particular project (Chapter 4).

Brosse et al (1996) describes a method in which a 10mW linearly polarised He-Ne Laser is used to measure the surface roughness of metal specimen samples, some limitations of this are restrictions in the depth of surface roughness which can be measured. The maximum surface roughness which could be measured in this experiment is 550nm.

Shetty (1982) devised a technique for inspecting surgical scalpels, the system uses laser diffraction as shown in Figure 2.9.

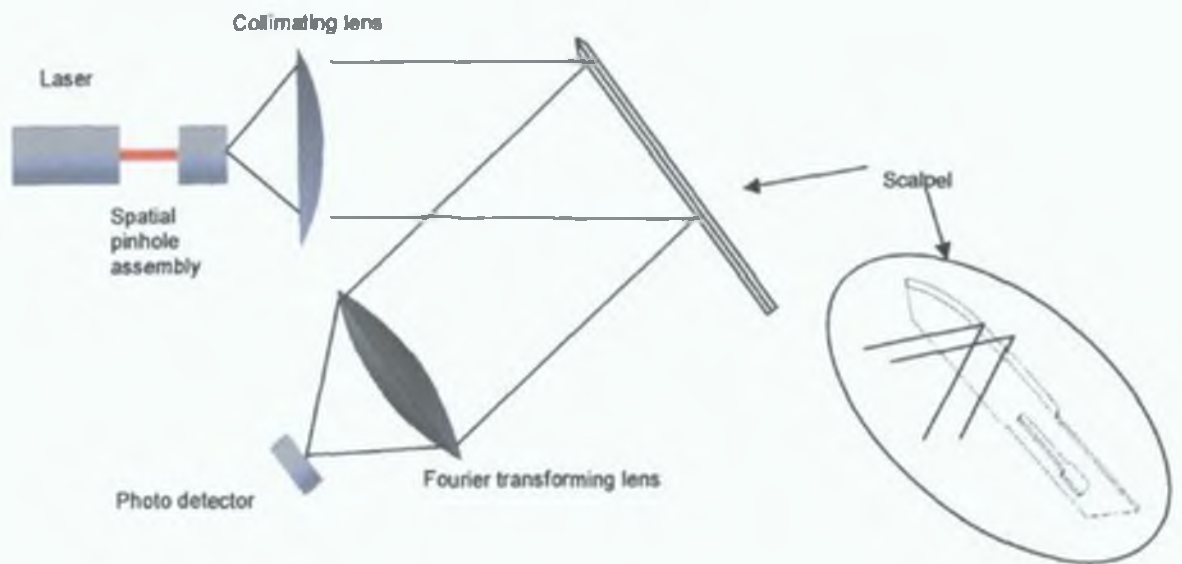


Figure 2.9 Schematic arrangements for obtaining fourier transformation (reflection) of side face of blade. (Shetty 1982)

This system uses a 1 mW helium-neon laser, a spatial pin hole assembly, a collimating lens, a Fourier transforming lens, and a detector system. This arrangement only gives detail on the surface finish of the blade. Shetty (1982) indicates that the number of "blips" displayed on a graph gives an impression of the surface finish of the blade.

He carried out further experiments to measure the angle of a scalpel using the arrangement outlined in (Figure 2.10).

The scalpel is oriented along the laser beam as shown, the angle is calculated from the diffraction pattern generated, this technique only gives the tip angle but gives no indication of the wedge angle.

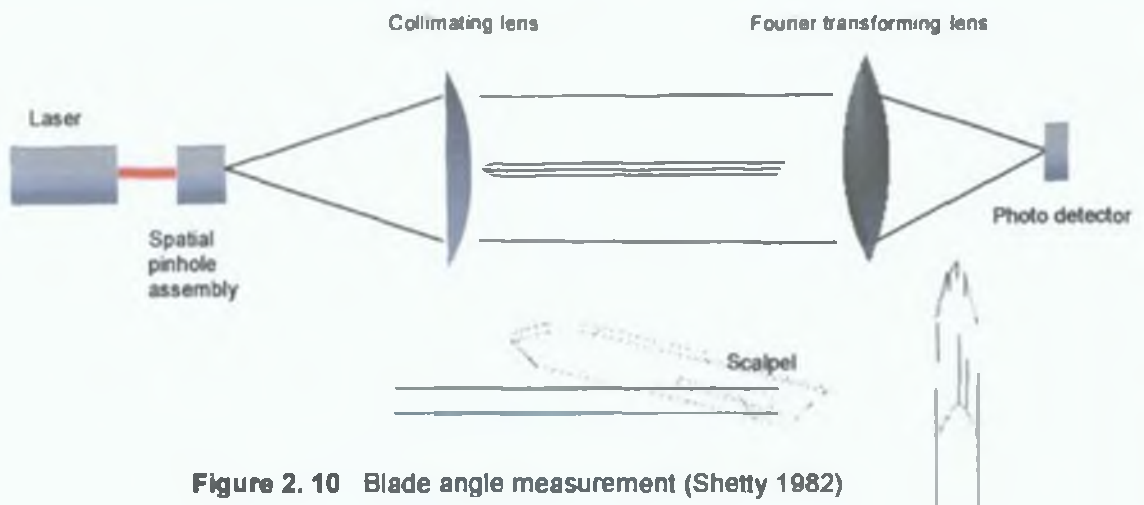


Figure 2.10 Blade angle measurement (Shetty 1982)

Bing Li (2003) describes a technique in which a series of ten triangular displacement lasers are used to measure the surface of a rear view mirror for an automobile vehicle. He describes this system as a multi light-knife measuring system. The lasers were fastened on an adjustable device, which could be set to give an equal distance between the bordering beams, ensuring the beams are synchronously parallel. The multi light-knife was produced by one long cylinder lens to ensure the uniformity of the multi light-knife.

In the measuring system, the distance between the camera and the object is 300mm, the width is 100mm, and the depth is 200mm. The resolution of the CCD camera and the Image Frame Grabber is 800×600 pixels.

A novel contact/non-contact hybrid measurement system as described by Shengfeng (2001) bridges the gap between contact and non-contact systems, although scanning in the non-contact mode is limited to a range of 500µm to 1mm and this may have implications for measurement of macro and micro geometric features of the cutting instrument.

2.6 Patent searches

One objective of this research involves the design and build of a non-contact blade measurement system. In order to determine if such a device exists a patent search was carried out first by the author and then a more comprehensive search carried out by Tomkins & Co., patents specialists. The results of both searches are presented. Patent (Graff, 1993) describes an apparatus for measuring the cutting sharpness of a knife; this apparatus measures the blade area presented at the tip of the blade (tip radius). The apparatus consists of an electrical capacitance probe having an active sensor area, changes in the cutting edge area (tip radius) are measured by changes in capacitance between the cutting edge and the sensor area in successive measurements. The sensor probe includes a central capacitance sensor lamination having an elongated active sensor area. The capacitance between the sensor area and the cutting edge is measured and this determines the sharpness of the blade. This method does not take into consideration the wedge angle of the blade which has been shown to affect the cutting process in studies carried out by researchers in the SUB³ group (Duffy 2003).

Other capacitive measurement techniques are reported in Patent (Pigage et al, 2005) which involves the measurement of the radial trueness of the position of cutter blades retained in an indexer of a gear cutting machine. The capacitance of the air gap between the probe and the face or edge of the cutter blade is used to determine the radial trueness of the blade position in the indexer. This device does not measure the actual sharpness of the tool cutting edge. In the Patent (Thompson Robert A., 1986) a capacitive sensor is used to measure the distance between the tool face and the freshly cut surface of the material being cut. Any wear of the tool face gives a reduction in the measured distance from the tool face to the material surface.

2.7 Concluding remarks

Research to date has mainly concentrated on the measurement of surface roughness using contact and non-contact techniques. Profile measurement research is limited to contact measurement using various forms of stylus profilometers. Research literature pertaining to the non-contact measurement of all the geometric parameters of a cutting blade is limited.

As stated previously in the introduction the aim of this research is to produce a device to measure all the geometric parameters of a surgical cutting instrument. The geometric parameters are then compared with research data which is built up on the cutting process by the larger research group. The ability of the blade to cut a particular material can then be determined from its geometric properties, if all other cutting parameters (such as friction, blade material, target material and cutting speed) remain constant.

Chapter 3.0 Current state of the art

3.1 Current state of the art in surface profilometry

This chapter will focus on the current state of the art of profile measurement systems. Research was conducted into the ability of off-the-shelf profile measurement systems, to measure the profile of a blade. In order to get an accurate representation of the ability of the various methods it was decided to use custom made sample blades in the evaluation of the various technologies (Figure.3.1).

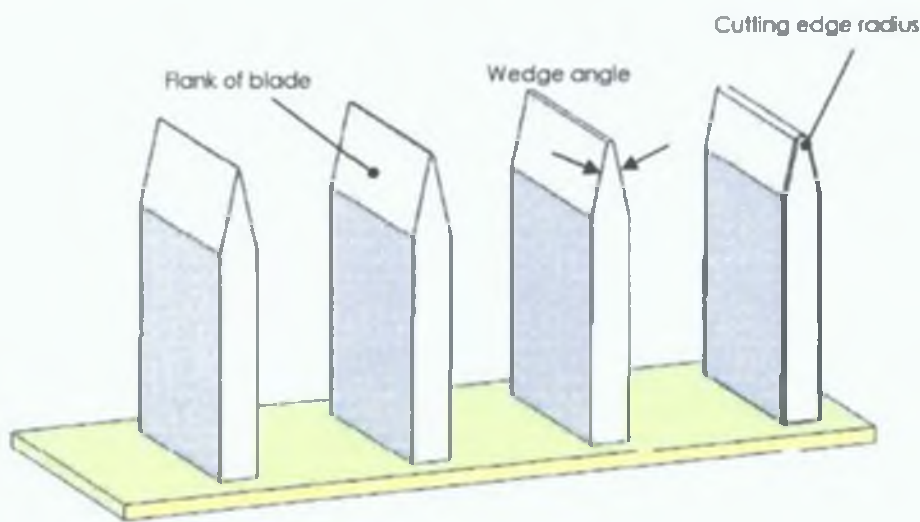


Figure 3.1 Sample blades used in all the studies of the various technologies

The blades used in the evaluation process had varying cutting edge radii from $7\mu\text{m}$ to $300\mu\text{m}$. The included wedge angle was varied from 15° to 60° . Blades were manufactured from cobalt high speed steel, and were ground to the required angles using form grinding techniques. Blades with largest cutting edge radii were manufactured using wire erosion to a surface finish R_a of $4.32\mu\text{m}$ (measured with a Newview 5000 surface profiler). Each method of profile measurement was evaluated for its ability to measure the cutting edge radius and the gross wedge angle of the blade.

3.2 Contact measurement:

3.2.1 CATRA sharpness tester

A contact sharpness measurement device (Figure 3.2) designed at Sheffield Hallam University in conjunction with CATRA (Cutlery & Allied Trades Research Association, 2003)

Technology Background

This method uses impregnated paper to test the sharpness of cutlery. The method of test involves the lowering of the test material (synthetic paper) onto the blade. The blade is oscillated back and forth underneath the paper and the depth of paper cut is recorded. The sum of the depth of the first three cuts gives the cutting index for that particular blade. This device is used to determine the sharpness index of a particular blade. Thus this is a comparative test, it does not give the actual profile details of the blade. The main disadvantage of this particular method is the destructive effect of the process on the blade

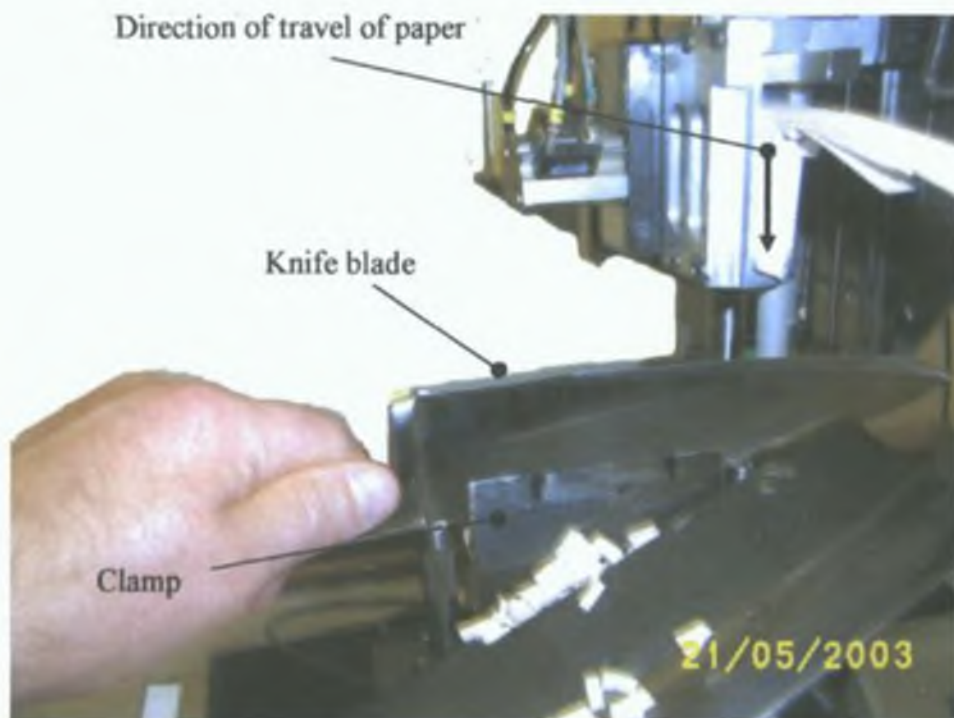


Figure 3. 2 Blade being tested on CATRA blade sharpness tester

Test Setup

A number of evaluation tests were carried out on the site at CATRA. It was not possible to use the sample blades on this particular test, because, the clamping device could not accommodate the sample blades. Blades were supplied by

CATRA to carry out the evaluation tests. The test carried out involved the comparison of two different profiles of blades, the first blade tested was a stainless steel domestic knife (Figure 3.3).

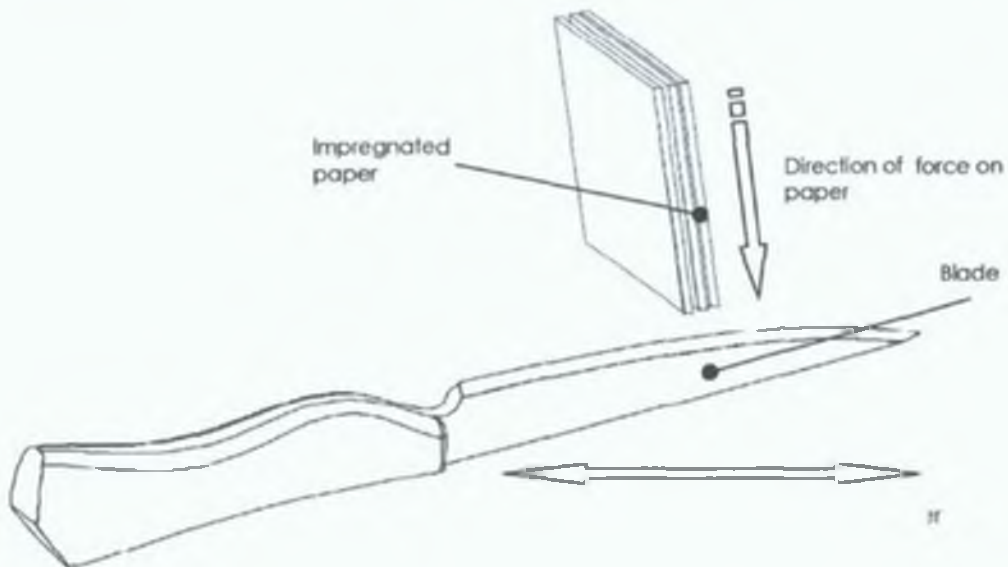


Figure 3.3 Schematic operation of CATRA blade sharpness tester

Results

Results of the sharpness and longevity tests using blades supplied by CATRA are shown in Figure 3.4.

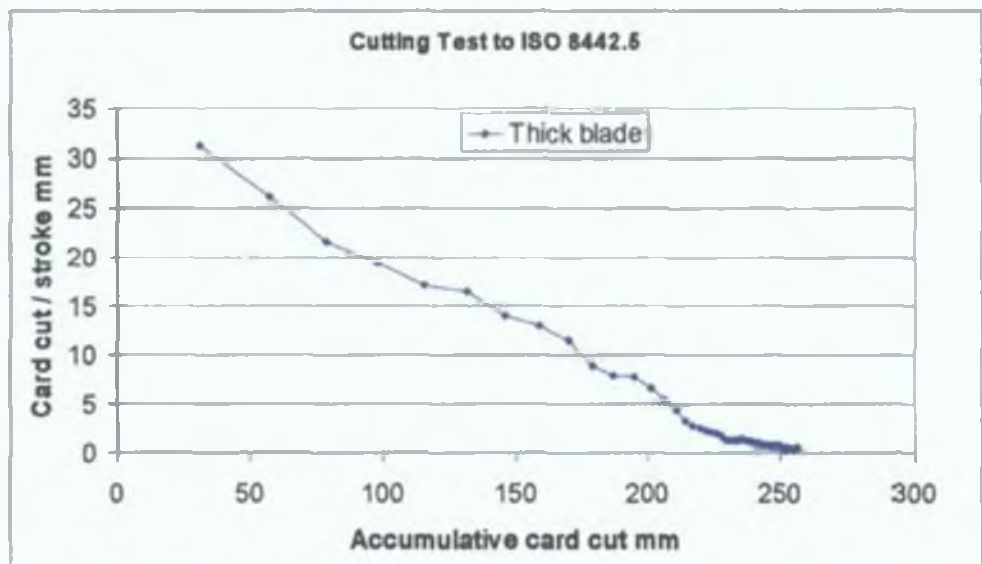


Figure 3.4 Results of tests on CATRA sharpness tester, vertical axis shows the depth of penetration of the card on each stroke.

The test result shown in Figure 3.4 shows the wear behaviour of a typical blade, as the blade is oscillated under the impregnated paper. The first pass gave a cutting depth of 31.3mm. (Results sheet in Appendix A), the second pass gave a cutting depth of 26.1mm and the third pass gave a cutting depth of 21.7mm. The sum of the first three passes gives the cutting index which in this case was 79.1mm. The limit for this type of blade is 50mm so this blade would have passed this test.

The CATRA sharpness tester also gives the longevity of the blade which is cumulative depth the blade cuts into the impregnated paper over the preset number of cycles (in this case 60 cycles) the total depth in this test was 256.2mm. The longevity limit for this blade is 150mm so this blade would pass this test.

CATRA also supply a device to measure the sharpness of razors, scalpel blades and surgical needles. (Figure 3.5)

The test utilises the constant cut depth method in which the blade is pushed perpendicularly into the test media without oscillation or longitudinal movement. The cutting force is recorded as a measure of the sharpness, which means the lower the force the sharper the blade. The test media is 8 mm square silicon rubber, which is bent around a 20 mm former and the cut is made into the outer periphery of this bend. This causes the rubber to open up as the blade penetrates, reducing the frictional contact between the flanks of the blade and the rubber and so confining contact to the tip of the blade edge only.

As the blade contacts the rubber and penetration of the blade occurs into the rubber the force increases to a maximum at which stage cutting starts to take place. The cutting force then falls to lower level. It is the maximum penetration force which is used as the sharpness value. Sample scalpel blades were tested in this device.



Figure 3.5 CATRA sharpness tester, force based test.

As with the previous test method the results are a comparative value. This device is designed for a production environment and it is not capable of blade profile measurement.

3.2.2 Co-ordinate measurement machine

Technology Background

The co-ordinate machine tested was the MAXIM CNC ultra high-speed Co-ordinate measuring machine. The machine uses a Renishaw R1 probe with a 1mm. ruby ball stylus. In general CMM's are universal devices for geometrical quality inspection of workpieces in manufacturing. However generally CMMs are very large, expensive and very slow because of the point-by-point mode by which they capture data, they require a specially trained operator and continuous environmental control.

Test Setup

The sample blades were placed in a vertical orientation relative to the scanning probe.

Results

Results from the machine gave the wedge angle of the blade and the tip radius, the smallest tip radius that could be measured was 0.028mm, however the

blade edge diameter which can be measured is limited by the diameter of the stylus.

3.3 Non-contact measurement:

3.3.1 Shadow Graph

Technology Background

The shadow graph evaluated was the Starrett HD400. The measurement scales have a 0.001mm resolution and angular measurements have a 1 minute of arc resolution.



Figure 3.6 Starrett HD400 shadowgraph

Test Setup

The sample blades were placed on the machine bed, no clamping was necessary blue tack was used to limit the blade vibration during machine use.

Results

Interpretation of blade geometry feature involves subjective evaluation of the images of the blade profile projected on the shadow graph screen. Accurate

and consistent evaluation of the geometric features are affected by clarity of resolution and skill of operator thus this process could result in operator error.

3.3.2 Vision systems

Technology background

Vision systems that were evaluated included the Mitutoyo Quick vision ELF, the "Venture" vision inspection system by Aberlink, the Starrett "Vicon 3020202", and the 0V² Optical-video conversion adaptor from Starrett.

Test Setup

No special jig was required to clamp the blades in position during the scan.

Results

All of these systems gave high quality results, however the machines were special purpose and could not be easily adapted to suit our purposes.

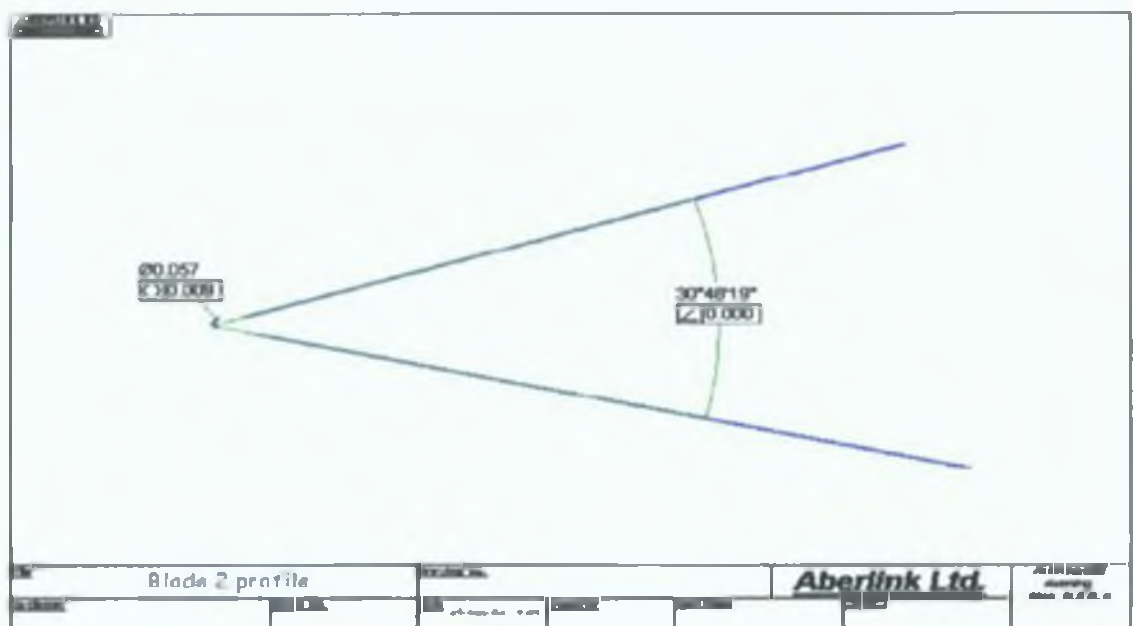


Figure 3.6(a) Image generated from vision systems

3.3.3 Confocal microscope

Technology background

The confocal microscope evaluated in the study was the Nanofocus CF2001 the confocal point sensor uses a point light source and detector pinhole to

discriminate depth. The laser beam emitted from the point light source is focused on a specimen through an objective lens that moves rapidly up and down. A detection signal is only generated when the maximum amount of possible light goes through the pinhole. A precise height measurement of the illuminated point is achieved by continuously scanning along the Z axis.

Test Setup

The sample blades were set-up in a vertical direction on the anti-vibration table as shown in Figure 3.7, and held in position with blue tack.

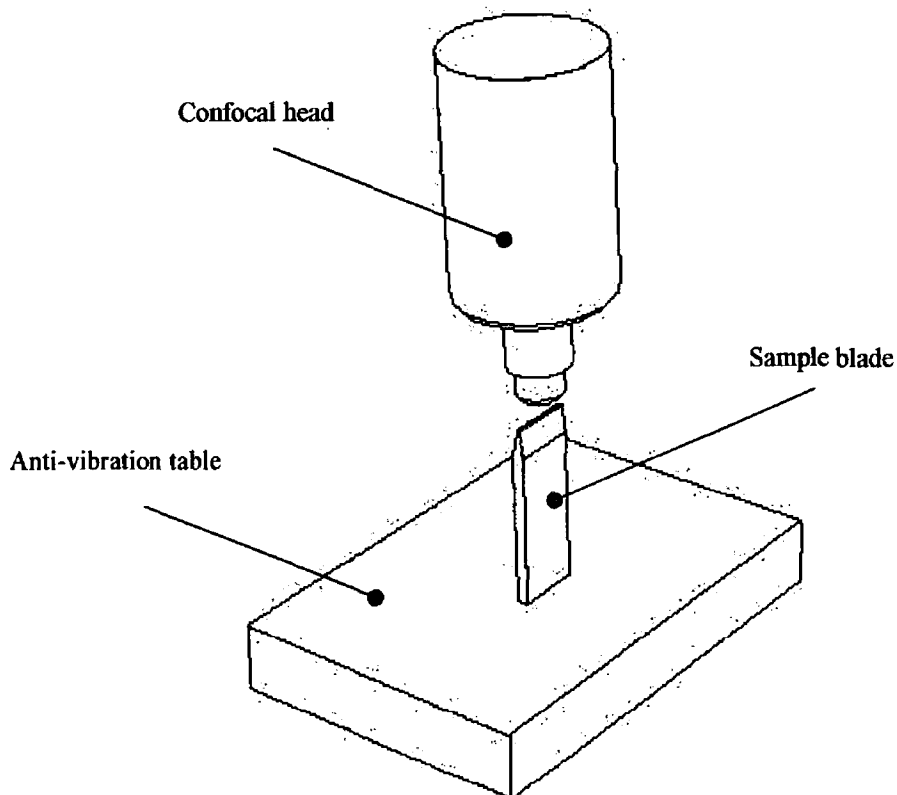


Figure 3.7 Blade set-up for scanning with confocal microscope

All the sample blades were scanned using this system with similar results. Different surface finishes were also tested, a disadvantage of this system was that it was found that angles of more than 20° from the horizontal (Figure 3.9) were not capable of being picked up by the measuring head. This is primarily due the light delivery and receiver being incorporated in the same source

(Figure 3.8) meaning that some light is not received from the sample blade, this is caused by the angle of inclination of the blade flanks.

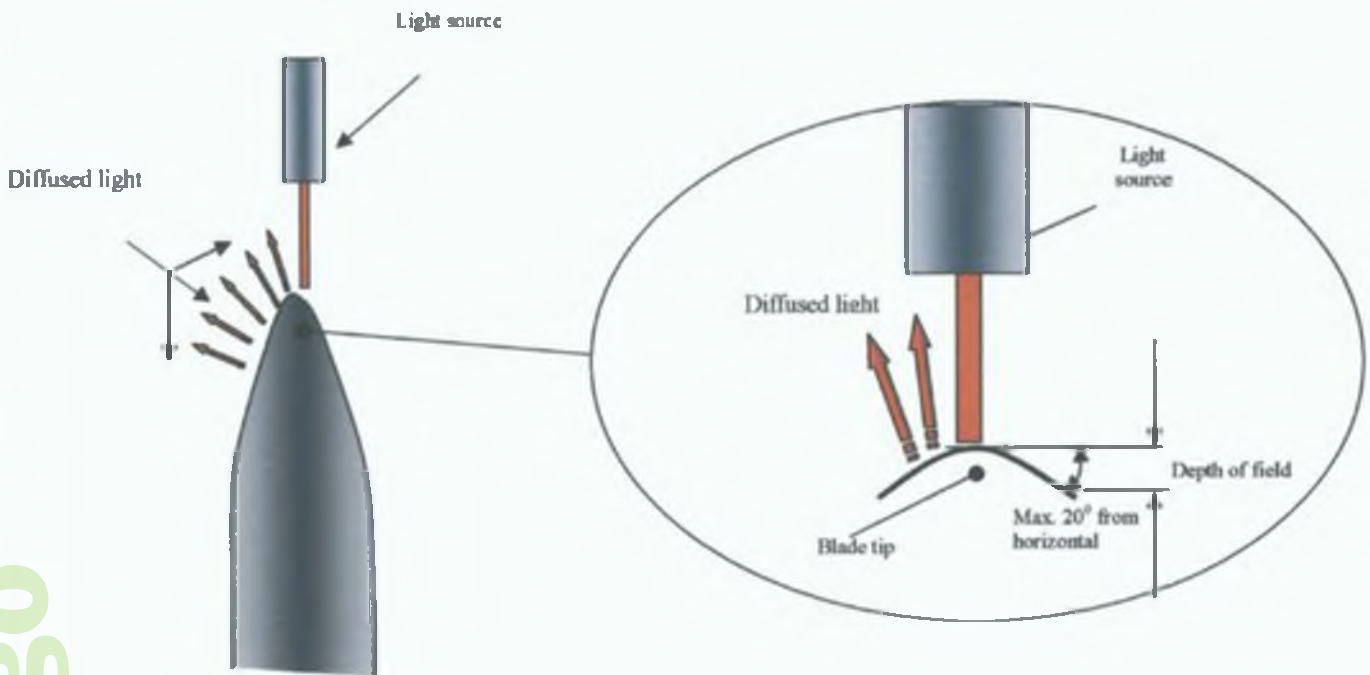


Figure 3.8 Depth of field is reduced due to the diffused light The Maximum angle from horizontal that is possible to measure is approximately 20° from the horizontal

Results

For the applications of this project the confocal microscope proved unsuccessful because of the problems associated with scattered light. This is illustrated in Figure 3.9. These problems with the confocal microscope prevented a complete image of the blade being generated it can be clearly seen that data is generated on the tip of the blade however no data is generated on the flanks of the blade. It was a requirement of the system that data be collected on the flank angles.

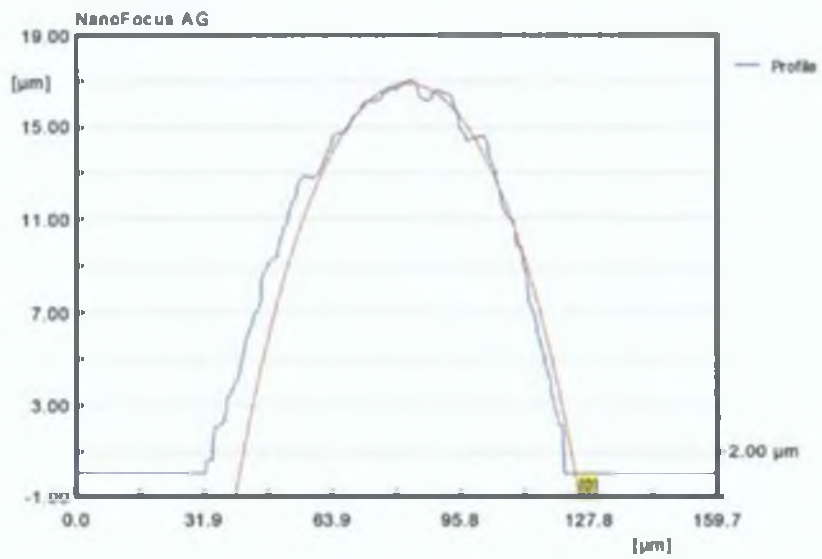
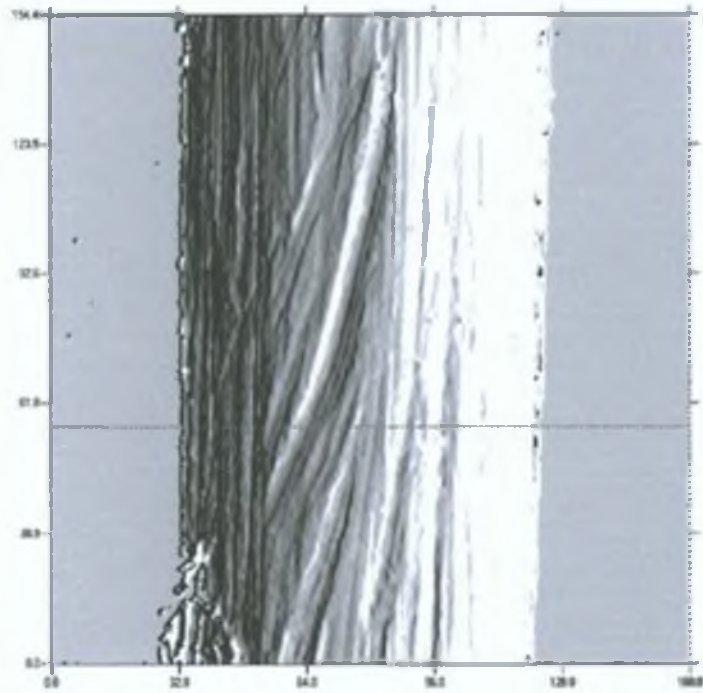


Figure 3.9 Image generated by confocal microscope it can be seen that the flanks of the blade are not detected due to the diffused light.

3.3.4 Autofocus laser measurement

Technology background

The laser autofocus system evaluated was the AF2000 by NanoFocus, in this system concentrated light is focused from a laser diode onto the surface of the sample.

Similar problems encountered with this system as indicated previously with the angle of the blade causing diffused light, meaning that conclusive measurements of total blade profile could not be obtained.

Test Setup

To overcome the problem of scattered light the blade was turned on its side and scanned one side at a time as shown in Figure 3.10.

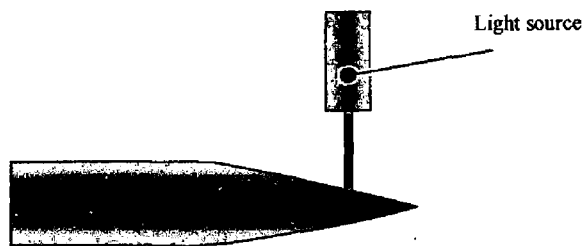


Figure 3.10 Blade scanned on side to reduce the effects of light scatter.

The first problem occurring with this procedure is due to the accurate alignment of the blade during scanning. A solution was to use an adjustable jig system (Figure 3.11) this arrangement allowed the blade to be scanned with the blade flanks horizontal in order to obtain the best possible image of the blade.

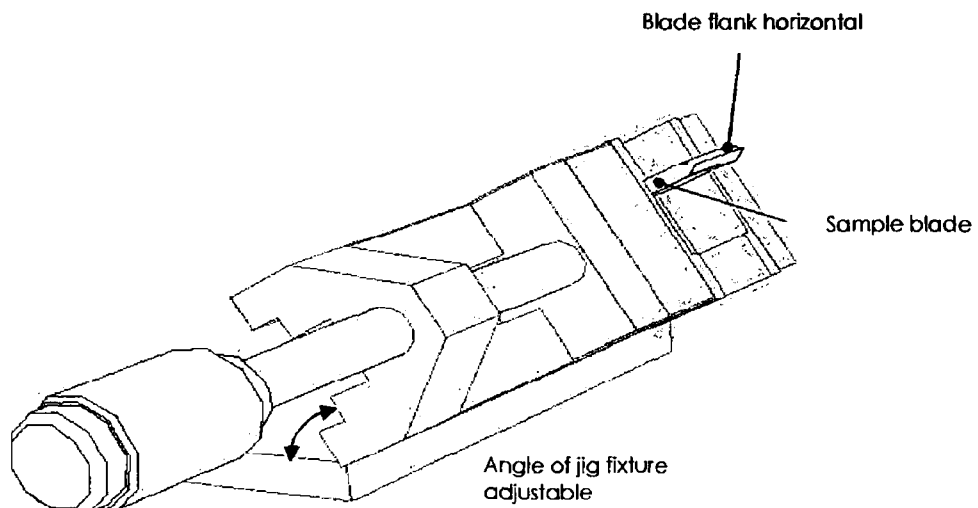


Figure 3.11 Jig fixture used for setting blade flank in horizontal direction

Results

A scanned image of the blade on its side is shown in (Figure 3.12) the detail in this image is of a high resolution however a second problem with this technology is highlighted in that no information is gathered on the tip radius of the blade.

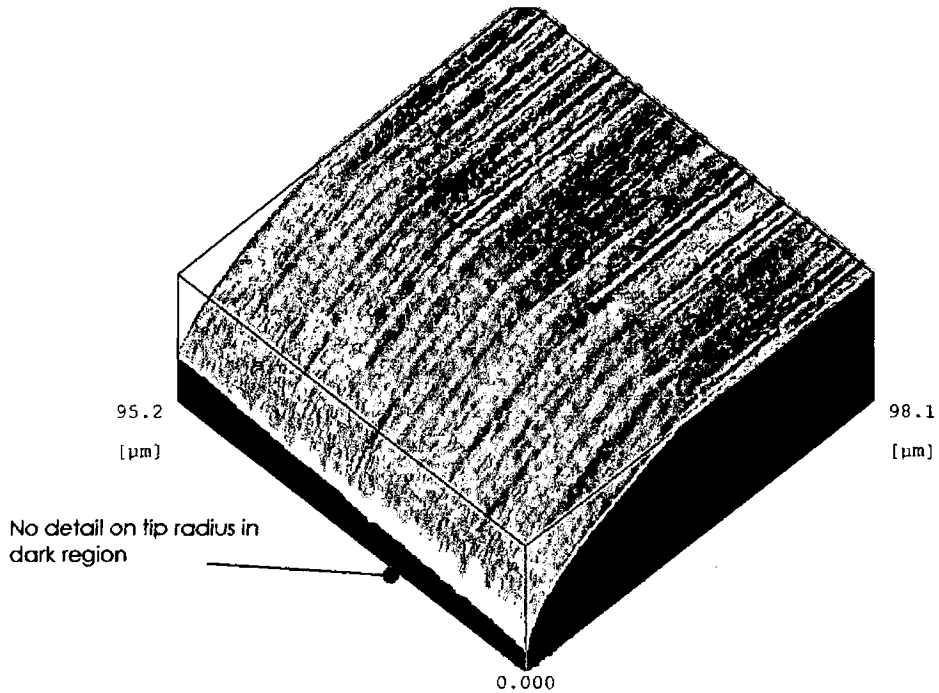


Figure 3.12 Blade scanned on side using NanoFocus confocal laser scanner.

The third issue associated with laser light technology is the problem of the spot size of the laser light; the lasers examined in this study have a minimum diameter of one micron (Figure 3.13). A general ratio for obtaining enough data to determine the profile of a blade is 10 to 1. This means that the smallest diameter that this technology can measure is approximately seven to ten microns.

In our tests it was just possible to measure a blade of tip width $7\mu\text{m}$. However, this was the smallest width in which enough data could be obtained to give an accurate representation of the blade tip.

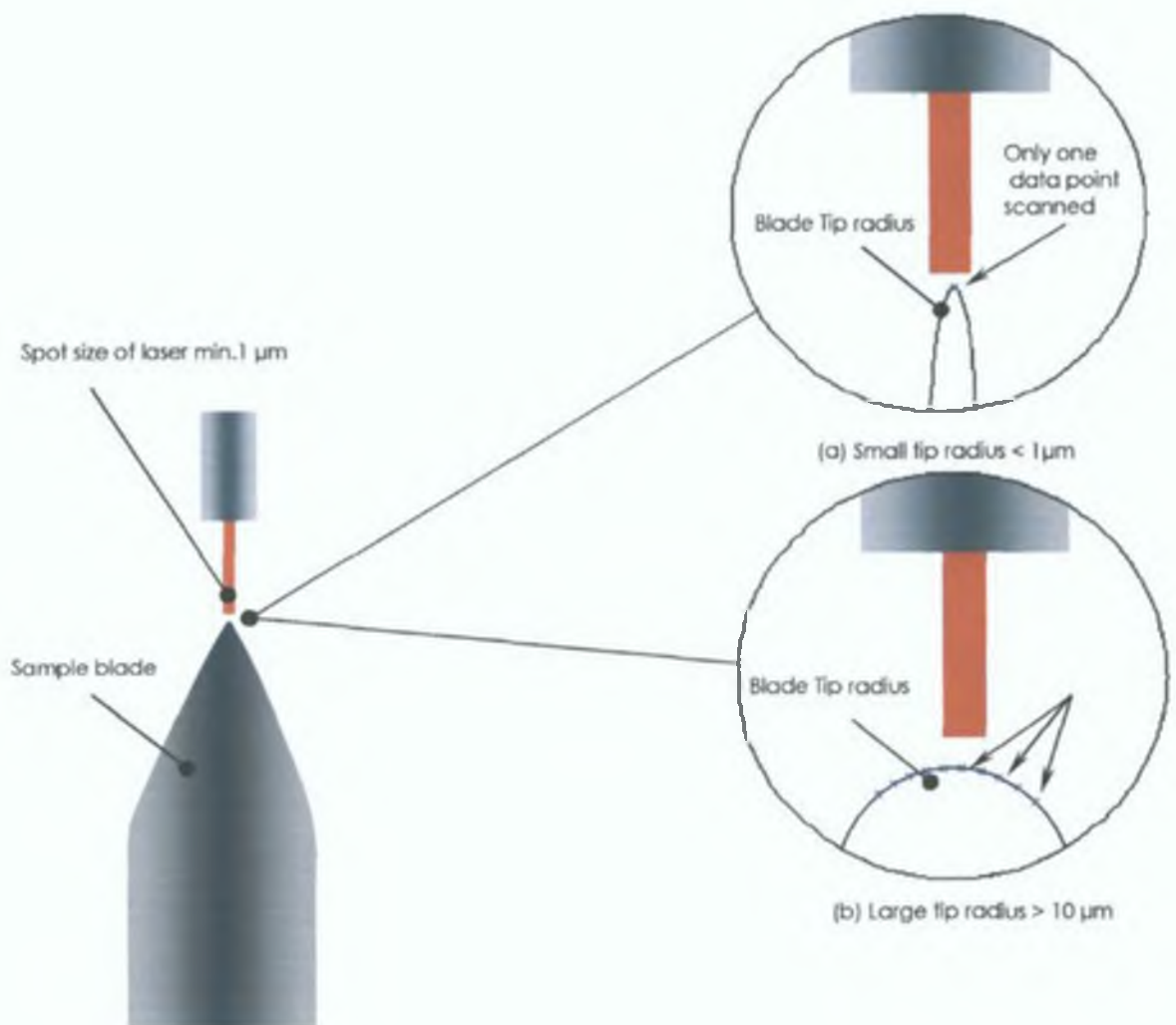


Figure 3.13 The Limitations of spot size are illustrated, a minimum of a ten to one ratio is required in order to obtain enough data points to determine the tip radius

3.3.5 Scanning electron microscope

Technology background

The Scanning Electron Microscope creates magnified images of surfaces by using electrons instead of light waves (Figure 3.14) Scanning electron microscopy operates by bombarding the blade with a beam of electrons and then collecting the slow moving secondary electrons that the specimen emits. These are collected, amplified, and displayed on a cathode ray tube, the electron beam and the cathode ray tube scan synchronously so that an image of the surface of the blade is formed.



Figure 3.14 Scanning Electron Microscope at Institute of Technology Sligo

After the air is pumped out of the column, an electron gun (at the top of the column) emits a beam of high energy electrons. This beam travels downward through a series of magnetic lenses designed to focus the electrons to a very fine spot.

Near the bottom, a set of scanning coils moves the focused beam back and forth across the specimen, row by row. As the electron beam hits each spot on the sample, secondary electrons are knocked loose from its surface. A detector counts these electrons and sends the signals to an amplifier. The final image is built up from the number of electrons emitted from each spot on the sample.

Test Setup

The scanning electron microscope used in the evaluations is a Topcon SM 600 based at the Institute of Technology Sligo. The sample blades were set-up as shown in Figure 3.15. The blades were scanned in both the side position and the vertical position. However the chamber size limits the size of sample that can be scanned.

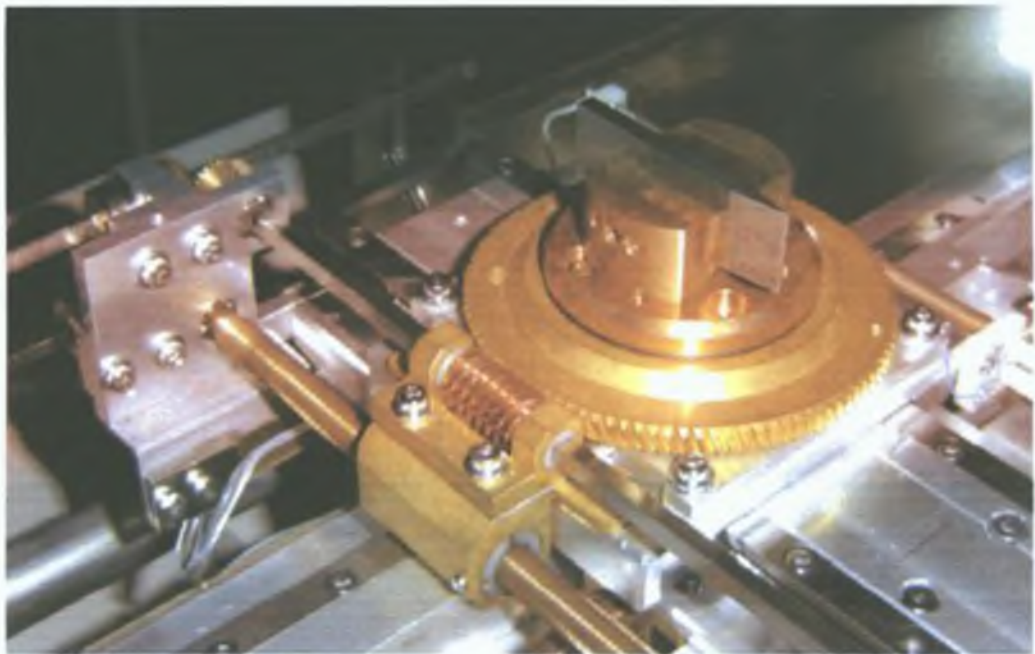


Figure 3.15 Blade set-up in Scanning Electron Microscope

Results

Results from the SEM are high definition, with all the details of the blade being presented. The image shown in Figure 3.16 shows the tip radius of a sample blade as well as the blade flanks.

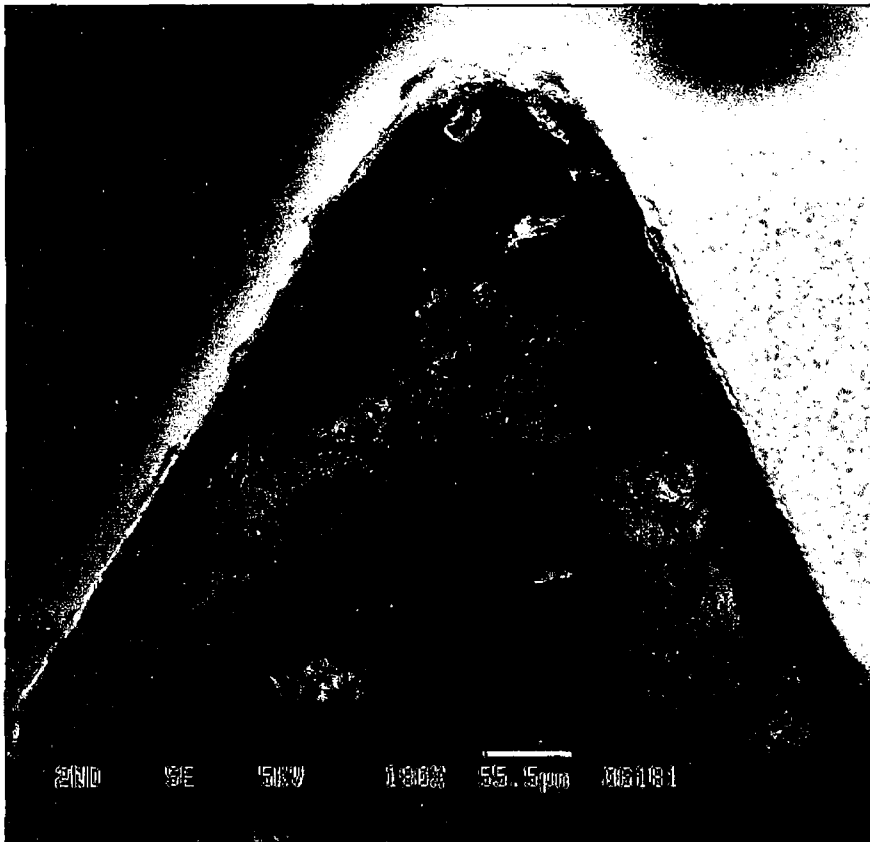


Figure 3.16 Image generated by Scanning Electron Microscope

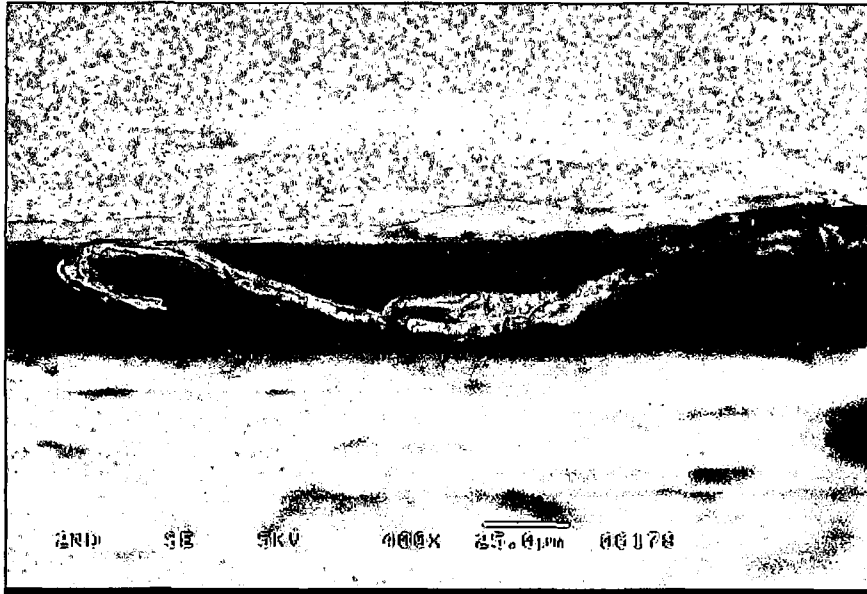


Figure 3.17 Image of top of blade using Scanning Electron Microscope

Figure 3.17 illustrates the detail on the top of a blade, showing a broken wire edge caused by the sharpening process.

3.3.6 Dynamic force microscope

Technology background

The dynamic force microscope evaluated was the BT01000 easyScan DFM. Marketed by Winsor Scientific UK. (Figure 3.18)



Figure 3.18 Dynamic Force Microscope (DFM)

The operation of the DFM is based upon a cantilever which is vibrated by means of a pizo at 160kHz. The 10 μ m stylus tip is vibrated a distance of 10 μ m above the surface to be scanned. Movement of the cantilever is detected by means of a laser. (Figure 3.19)

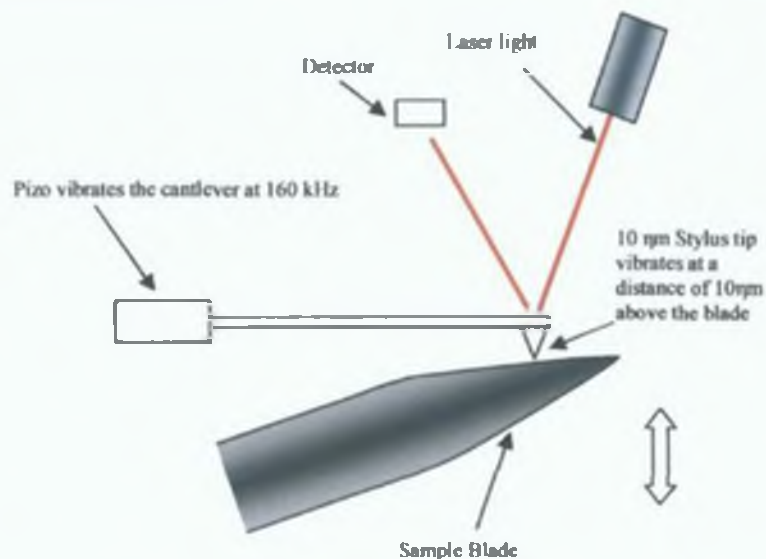


Figure 3.19 Operation of Dynamic Force microscope

Test Setup

The dynamic force was evaluated using the sample blades, however it was found that setting up the equipment was difficult even for a trained technician.

To scan the tip radius of the blade, the blades were orientated in a vertical direction, (Figure 3.20). It proved extremely difficult to place the 10nm stylus tip over the blade edge, even with the use of a microscope.

Attempts at scanning the blade tip edge radius resulted in breaking the stylus tip on many occasions during the tests.

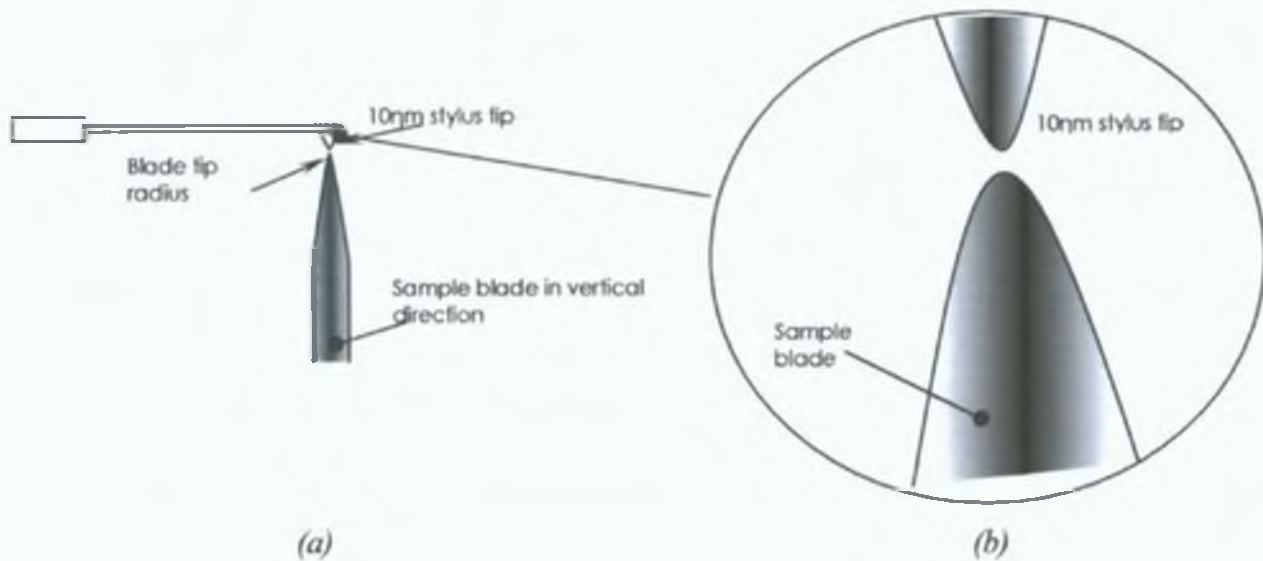


Figure 3.20 (a) Sample blade in vertical direction being scanned with Dynamic Force Microscope (b) detail of scanning blade with 10nm stylus tip, illustrating difficulty in alignment of stylus tip and blade edge.

Results

Results on the flanks of the blade were of a high resolution as shown (Figure 3.21). It was found that no details could be obtained on the tip radius of the blade.

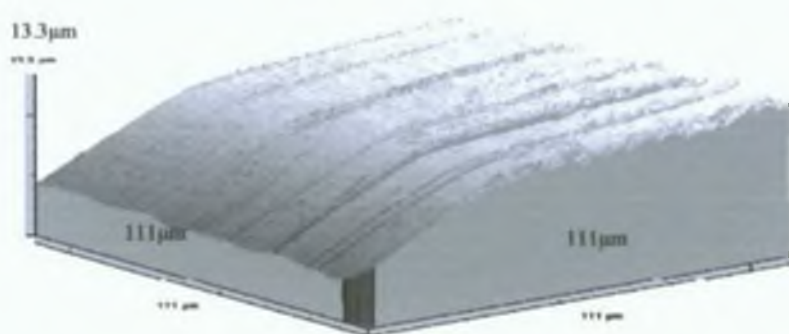


Figure 3.21 Image of scalpel generated by Dynamic Force Microscope.

3.4 Conclusions

Throughout the evaluations it became clear that no single technology was capable of measuring all the geometric parameters of a blade, this is illustrated by the diagram (Figure 3.22). The measurement technologies varied from coordinate measurement machines to dynamic force microscopes.

Each technology had its own strengths and weakness, devices with a high resolution lacked the depth of field to give any detail on the flanks of the blade, while those with low resolution could measure blade flanks but could not collect detail near the blade tip.

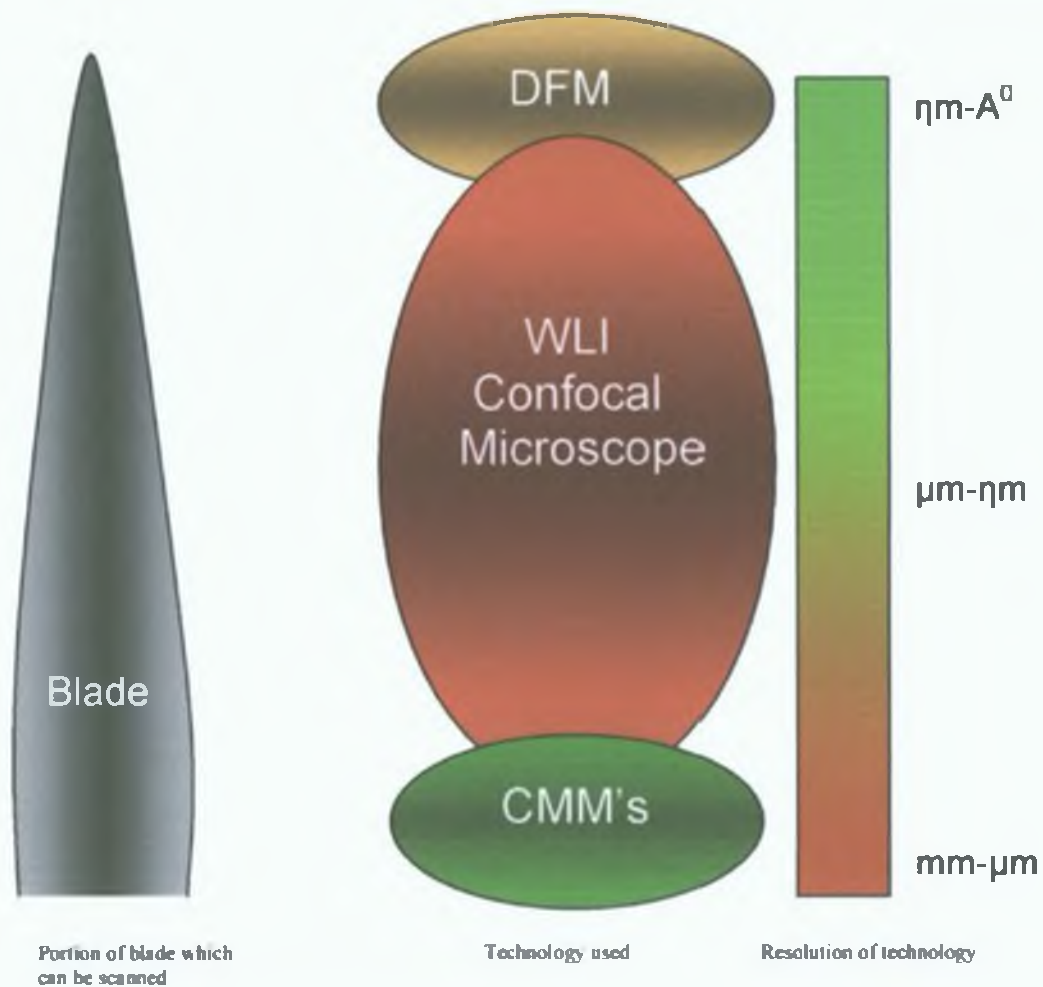


Figure 3.22 Comparisons of various measurement technologies, showing the ability of various devices to measure the geometric parameters of a blade

Table 3.1 shows a summary of the operating specifications, test results and key observations on all technologies reviewed. From this study and the literature review it was concluded that scope existed for development of a prototype device for simultaneous measurement of blade geometry of both sides of the cutting blade and in the region of the cutting edge.

Table 3.1 Summary of operating specifications

Technology	System	Specifications								
		Vendor/ Manufacturer	Ease of set up	Resolution flat surface	Accuracy	Range (z)	vibration proof table required	Scan on both sides	Could software be modified?	Spot Size
White light Interometry										
Zygo	NewView 5000 10X	Requires clamp	200X		1.18mm.	Yes	Yes		N/A	2D
Zygo	NewView 5000 50X	Requires clamp	1000X		0.64mm.	Yes	Yes		N/A	2D
Zygo	NewView 100	Requires clamp	0.1ηm.		100μm.	Yes	No			3D
Veeco	Wyko NT1100	Requires clamp	0.01ηm.		1mm.	Yes	No	Yes		3D
Confocal Microscopy										
Nanofocus	μscan CF 2001	Requires clamp	0.1μm		1mm.		No		1.5μm	3D
Contact Profilometer										
Mitutoyo	Formtracer CS3000	Requires clamp	0.08μm	3μm/5mm	5.0mm.	No	Yes		N/A	2D
Mitutoyo	Formtracer CS3000	Requires clamp	0.008μm.		0.5mm	No	Yes		N/A	2D
Mitutoyo	Formtracer CS3000	Requires clamp	0.0008μm.		0.05mm	No	Yes		N/A	2D
Optical Profile projector										
Aberlink	Axiom B89	No special jig	N/A		N/A	No	Yes	Export into excel	N/A	2D
Starrett	HD 400	No special jig	N/A		N/A	No	Yes	N/A	N/A	2D
OGP	Smartscope Flash	Requires clamp	0.5μm		N/A	No	Yes	Yes	N/A	2D
Dynamic Force Microscope										
Winsor Scientific	Easyscan DFM.	No special jig	0.027ηm.		10μm.	No	No	SMP software	N/A	3D
Laser Profilometer										
OGP	Cobra	No special jig	0.125μm.		300μm.	No	Yes	Export into excel	N/A	3D
OGP	Cobra	No special jig	1.0μm.		2.0mm.	No		Export into excel	N/A	3D
OGP	Cobra	No special jig	4.0μm.		8.0mm.	No		Export into excel	N/A	3D
Scantron	Proscan 2000/laser	No special jig	0.1μm		2.8mm.	No	No	Export into excel	30μm	3D
Chromatic white light										
Scantron	Proscan 2000	Requires clamp	0.01μm.		0.3mm.	No	No	Export into excel	4μm.	3D

Chapter 4.0 Design of measurement device

4.1 The Design Process

This chapter deals with the design of a prototype measurement device to measure blade profiles. In order to design this prototype standard design processes were used as outlined in (Figure 4.1).

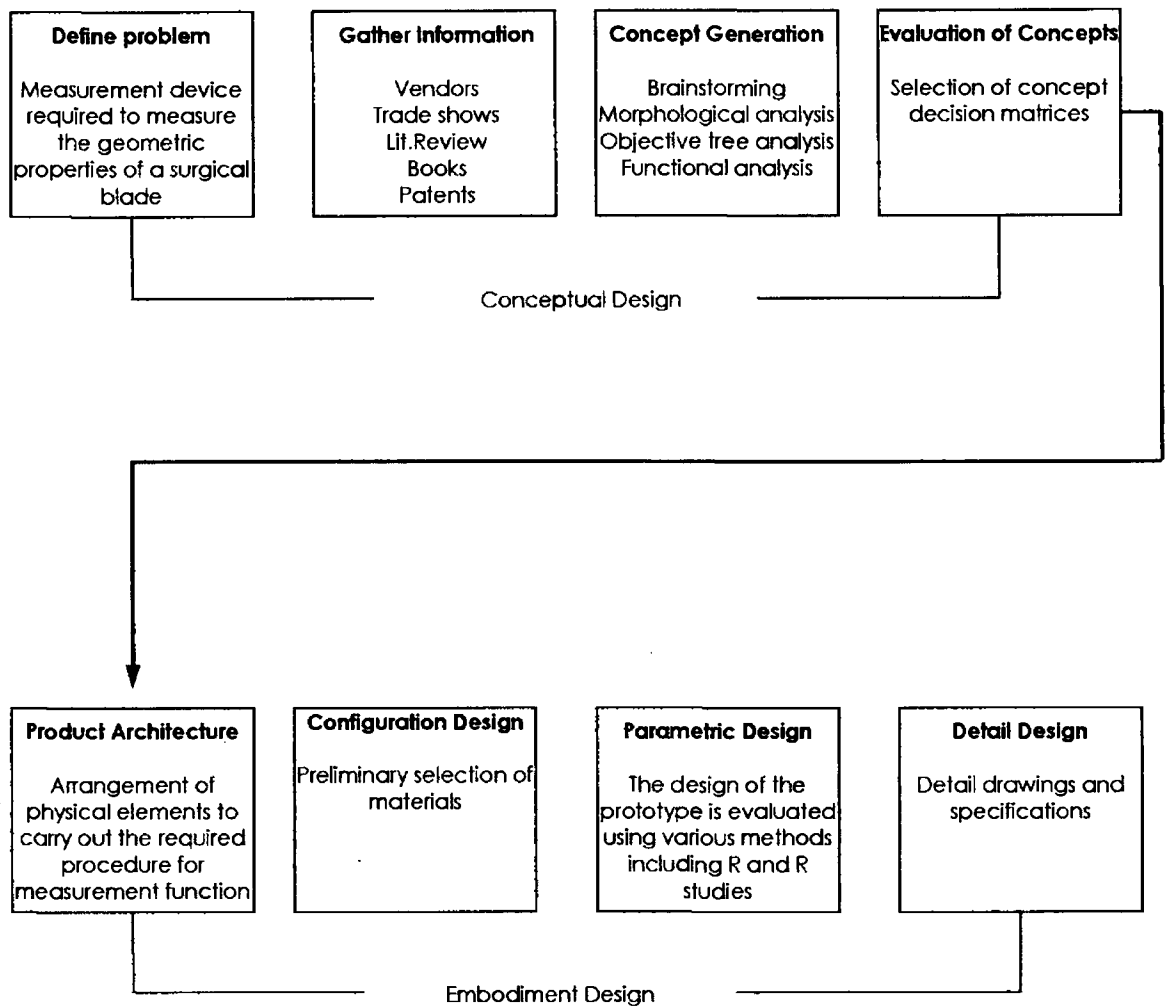


Figure 4.1 The design process outlining the stages during the design of the prototype

4.2 Phase I Conceptual Design

4.2.1 Design Brief

The design brief was to design and prototype a method of measuring the profile of a straight edged surgical cutting blade called an osteotome. The device should be capable of measuring the blade in a non-contact manner. The blade chosen for this research was a surgical osteotome, this instrument was chosen because it is a reusable surgical instrument, these instruments are periodically taken out of service and re-sharpened.

In parallel with the design of this measurement device other research is ongoing within the SUB³ group on the characterisation of the cutting process and relationship between the blades edge parameters, the type of material being cut and the cutting process. This research data will be used to determine the optimum blade geometry required to cut a particular material, and ongoing work focus on the effect of blade wedge angle.

This extends the design brief to use the gathered geometric data on the blade and compare this to the research data. This comparison will determine if a blade has been re-sharpened to the optimum angle to cut a particular material.

The proposed measurement device will scan a surgical cutting instrument (osteotome) determine the wedge angle and display this information in a manner that can be understood by an operator, and subsequently used in conjunction with experimental results to calculate blade cutting efficiency.

4.2.2. Information Gathering

In order to assemble information on the current state of the art technology that is used for profile measurement, it was decided to visit various manufactures and vendors of measurement devices. This has been described in detail in Chapters 2 and 3. This research was coupled with a review of research literature to provide a basis for devising the design brief (Figure 4.2).

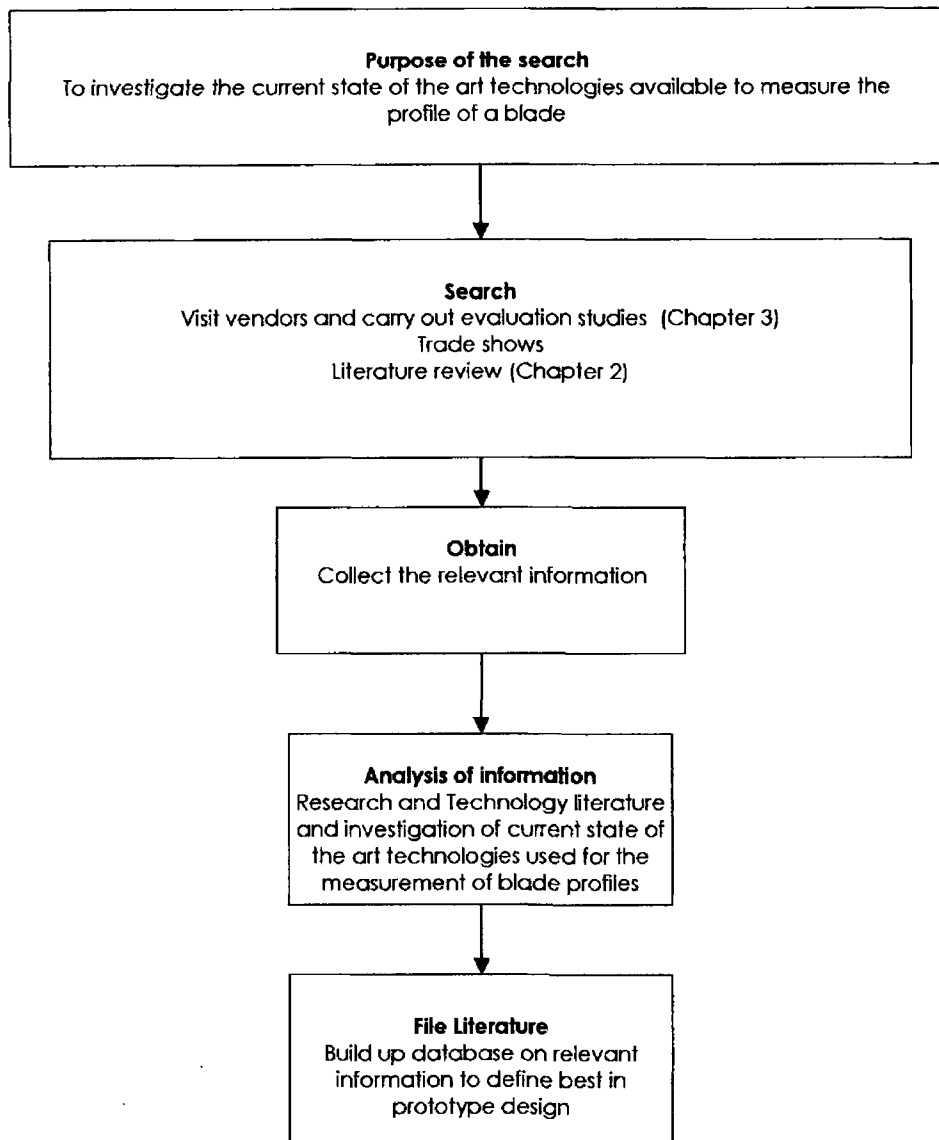


Figure 4.2 Methods used to gather information

4.2.3 Objective Tree Analysis

In the objective tree analysis the objectives of the measurement device are laid out (Figure 4.3). This determines what the device is required to do, it does not state how these operations are to be performed. The main objective of the measurement device is to measure a blade wedge angle in a non-contact manner and return the measured angle.

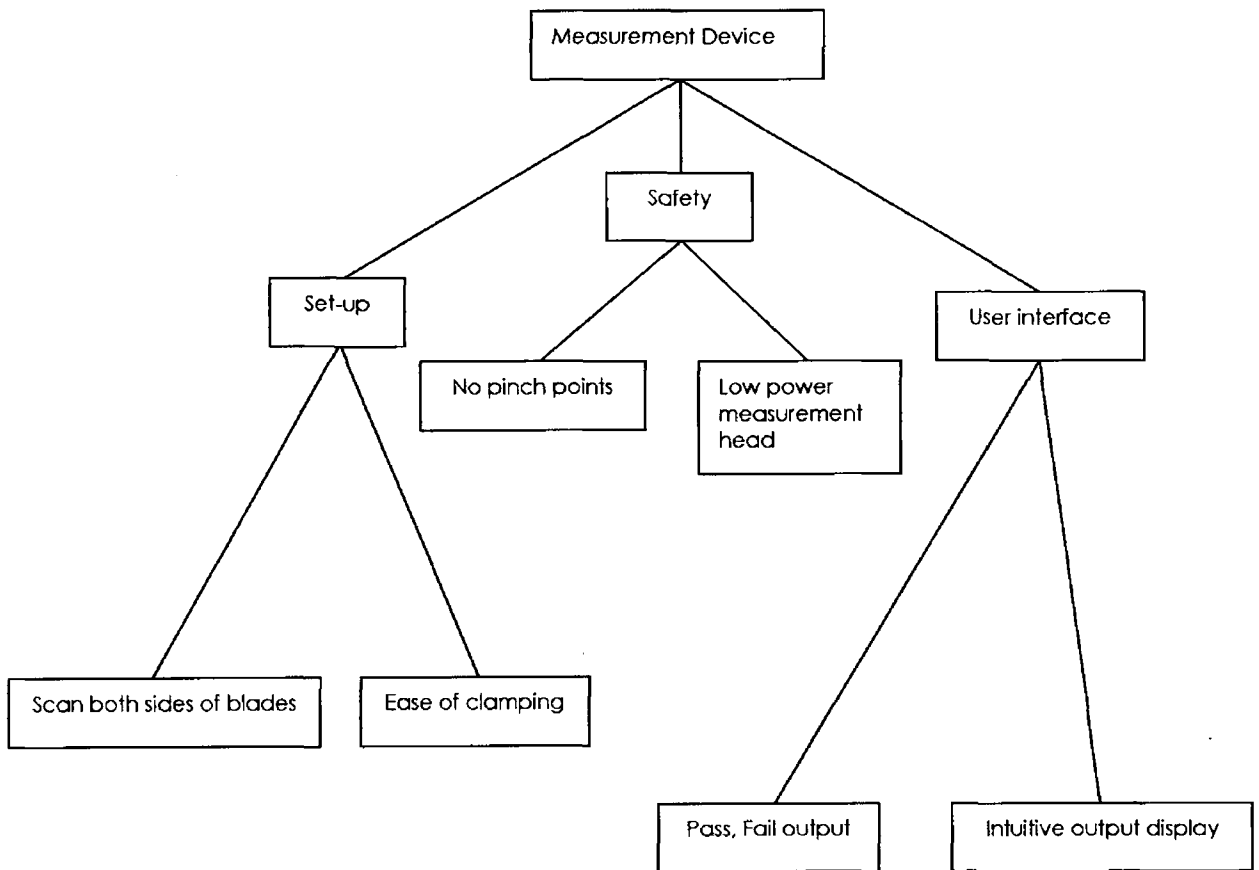


Figure 4.3 Objective tree analysis

4.2.4 Functional Analysis

As a method to further define the design brief a functional analysis was used to determine the required functionality of the device. This determines how the device will perform the required functions (Figure 4.4).

In this case the functions required of the measurement device were well defined, it is required to:

- Scan the blade in one operation.
- Scan both sides of the blade.
- Measure the wedge angle of the blade.
- Display the angle following the test.

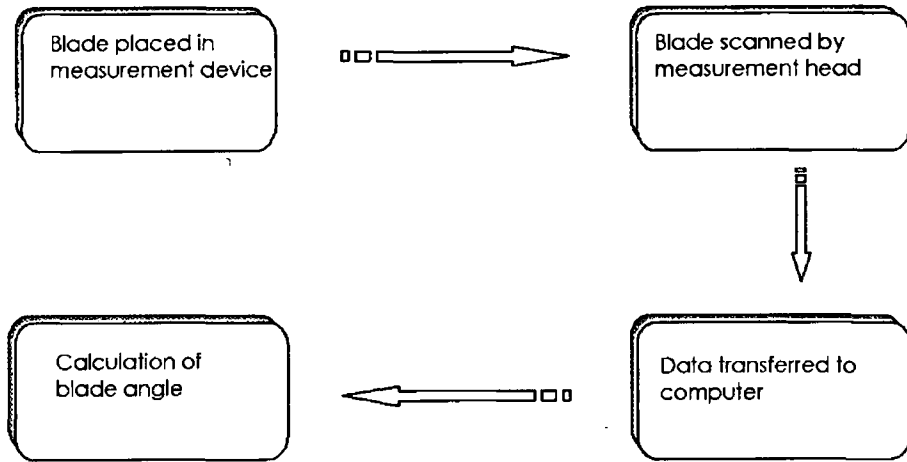


Figure 4.4 Functional analysis showing the outline functions required of the measurement device

The aim of the overall research project requires that the calculated blade's wedge angle is compared to research data gathered by on-going investigations by the SUB³ research group. This comparison should determine if the blade is suitable for a particular cutting application, the measurement instrument output would display a pass/fail output. (Figure 4.5), however in its current form the prototype will present a wedge angle to be used in conjunction with ongoing research work external to this specific project conducted by the author.

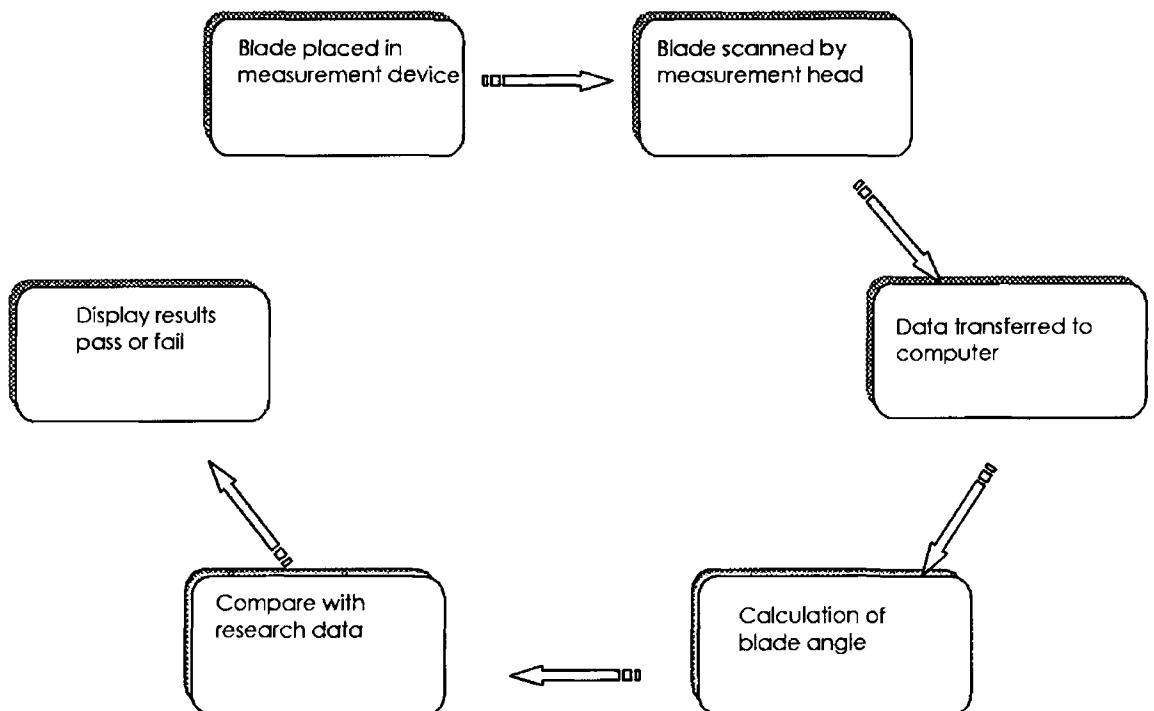


Figure 4.5 Functional analysis showing final functions required of the measurement device

This functional analysis (Figure 4.5) shows the required functionality of the measurement device, the device is required to clamp or hold the blade as it is scanned, by moving the blade under the sensor or the sensor over the blade. The data gathered is analysed and the wedge angle of the blade calculated.

4.2.5 Product Design Specification

The product design specification is a document which outlines the specifications required of the product, in this case the PDS stems from the literature review, patent searches and competition analysis, this PDS was used as the reference for the design process (Figure 4.6).

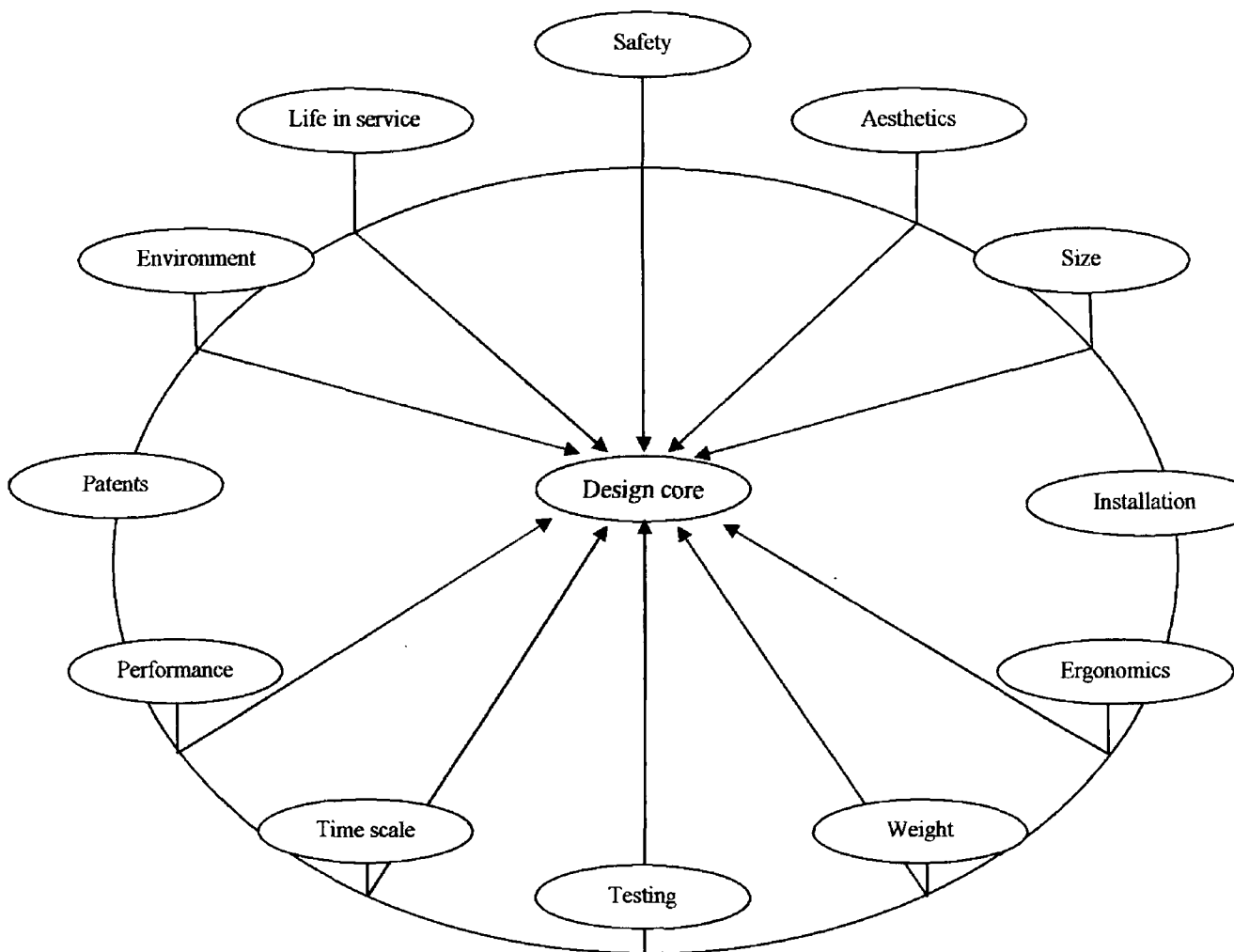


Figure 4.6 Product design specification

Table 4.1 Product Design Specification

Safety	Must meet all relevant safety standards
Performance	Must perform its basic function of measuring a surgical blade in a non-contact manner
Quality	Must meet all relevant quality standards
Ergonomics	Easy to use, user friendly blade restraint system Ease of set up
Testing	At each stage of development the measurement device tests are carried out to ensure that the design meets requirements, tests include machine evaluation, measurement head evaluation tests and gauge R and R tests.
Environment	The measurement device is designed to operate indoors
Materials	Materials selection must be appropriate to function
Patents	Device should be uninhibited by existing patents
Aesthetics	The device is a prototype, aesthetics is not a major factor
Size	Unit to be portable, either desktop, or provided with rolling castors
Installation	Unit must be portable as its location may vary
Weight	N/A
Time scale	Development under 3 years
Life in service	N/A this is a first stage prototype.

4.3 Phase II Concept generation

Concept generation for the measurement device looked at various aspects of profile measurement. The brief stated a device for the non-contact measurement of a cutting blade.

4.3.1 Concept (a)

The first concept was to use an existing profilometer and rotate the blade using a specially designed jig (Figure 4.7) the blade is scanned on one side, the location pin is raised and the blade is rotated 180 degrees, the location pin is inserted and the other side of the blade is scanned (Figure 4.8).

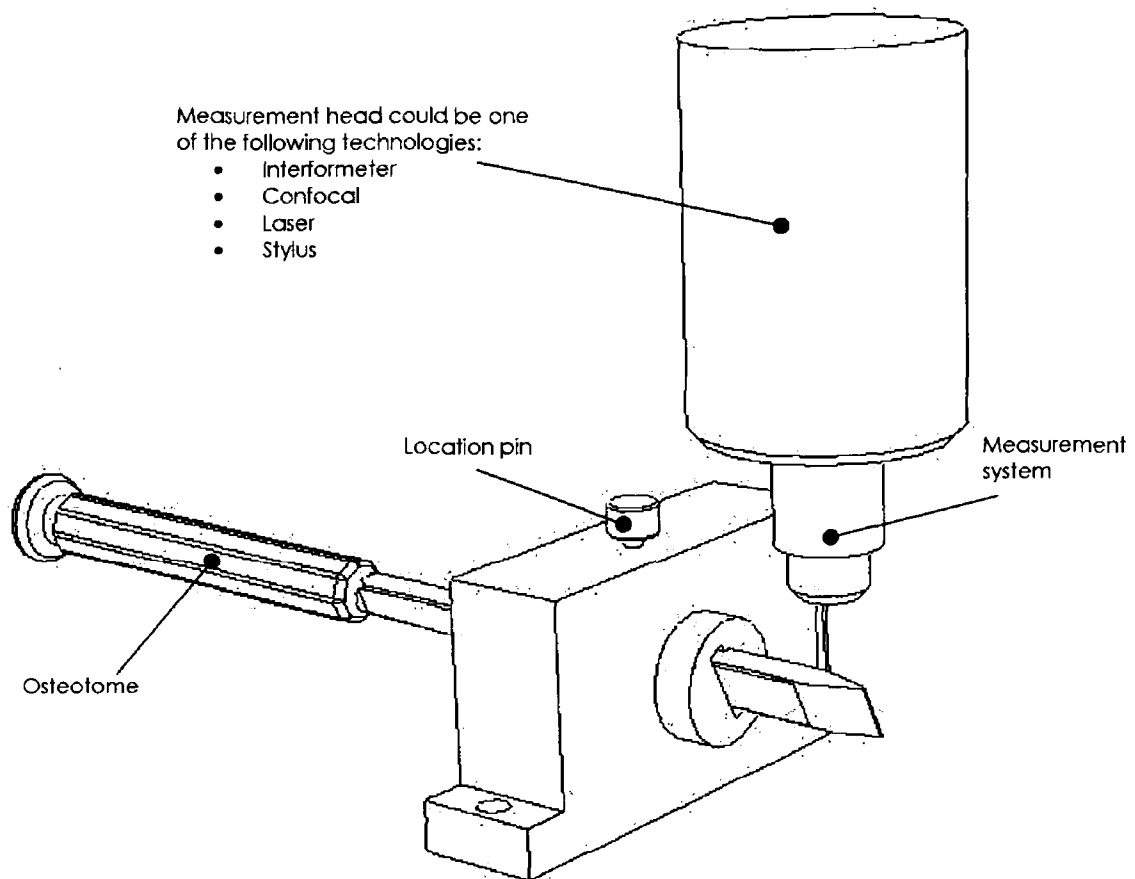


Figure 4.7 Device designed to rotate blade 180 degrees to allow a scan on both sides of the blade

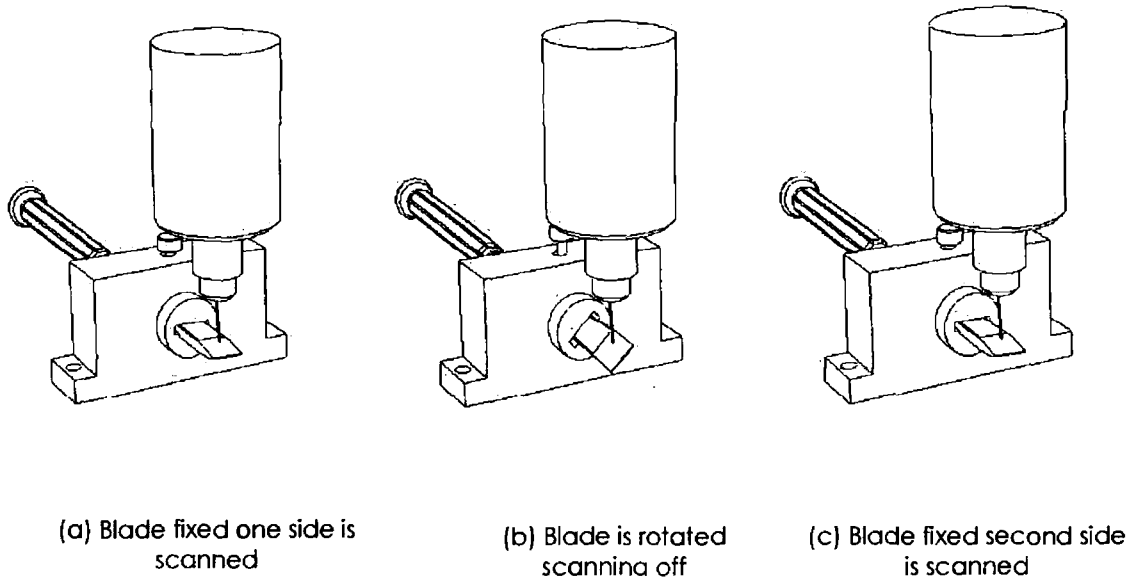


Figure 4.8 Sequence of operation of the blade clamp device used to scan both sides of the blade

4.3.2 Concept (b)

A goniometer was designed and built this system measures the wedge angle of a blade by splitting the incidental laser beam with the wedge angle of the blade (Figure 4.9).

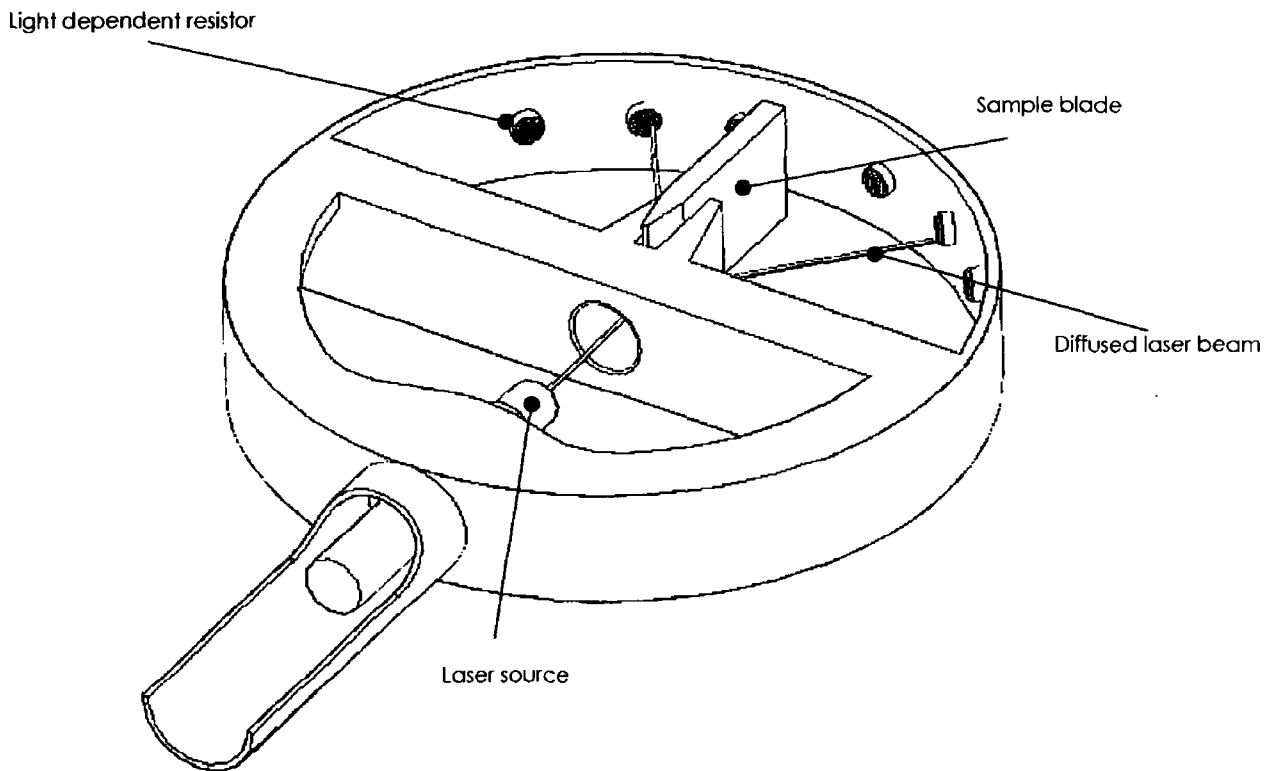


Figure 4.9 Goniometer concept showing the laser light source and position of the light dependent resistors

The laser light hits the tip of the blade and is diffused by the flanks of the blade, the light is detected by means of the light dependent resistors this gives an indication of the wedge angle of the sample blade. This particular Gonometer was designed based on the Gonometer supplied by CATRA, extra features included the automatic angle detection features.

4.3.3 Concept (c)

In this concept two laser displacement sensors are used to measure the blade flanks simultaneously. The laser heads are diametrically placed to measure both the top and bottom of the blade as it is passed between the laser heads. (Figure 4.10)

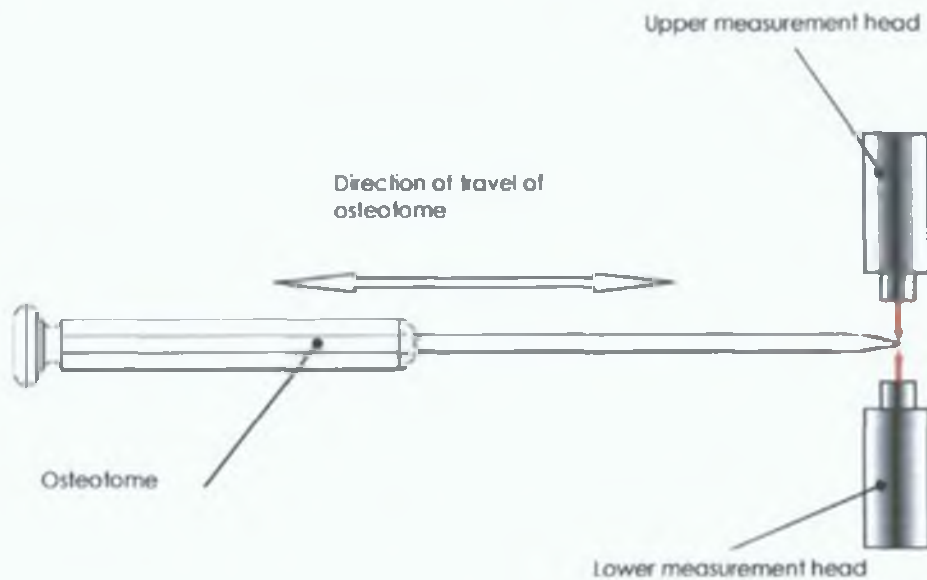


Figure 4.10 Concept of device to scan both sides of a blade simultaneously

4.4 Evaluation of Concepts

The various concepts that were devised to measure the profile of the blade were evaluated using appropriate selected factors from the PDS and a weighted objective method. Concepts were rated on a scale of 0-5 on how they satisfied the various factors. The scale gives a value of 0 if the feature is not suitable to a

value of 5 for a feature which is suitable for the application. A weighting factor was applied subsequent to the analysis.

Table 4.2 Weighted analysis matrix for measurement device

Objective	Weight factor	Rating			Weight factor X Rating		
		Concept (a)	Concept (b)	Concept (c)	Concept (a)	Concept (b)	Concept (c)
Scan both sides of blade without resetting	6	0	5	5	0	30	30
Non-contact scanning method	5	5	5	5	25	25	25
Ease of set up	3	3	3	5	9	9	15
Portable	2	4	4	3	8	8	6
Resolution of scan	4	5	2	4	20	8	16
Speed of operation	1	3	4	4	3	4	4
Total					65	84	96

From the results of the weighted analysis (Table 4.2) Concept C scored the highest, and this concept was taken to the detail design stage. The weight factor was determined by the various requirements of the measurement device as agreed by members of the SUB³ group. The rating applied to each concept was based on a judgement of the ability of the various concepts to perform the various tasks.

4.4.1 Morphological analysis

A morphological analysis was used to determine the best combination of features to develop a device to measure a blade.

Table 4.3 Morphological Chart

Feature	Solutions			
Measurement head	Interferometer	Stylus	Laser	confocal
Blade Clamp	magnetic	Screw clamp	Spring Loaded clamp	Solenoid clamp
XY Slide	D.C. motor with servo control	Servo motor	Stepper motor	Manual slide
Software for control and data analysis	C++	Visual basic	Java	LabView

From the morphological chart it was possible to identify the combination of features best suited to construct the measurement device.

All components for functions of the measurement system were evaluated based on pass/fail criteria with the exception of cost which was used on the basis of providing a cost effective solution. These evaluations are presented in the ensuing tables.

It was decided to use a triangulation displacement laser, as opposed to tactile profilers, as measurement with laser profilometers is a non-contact method and for that reason non-destructive. For clarity of reading the chosen solution is highlighted in bold in each table

Table 4.4 Component selection for measurement head

Feature	Interferometer	Stylus	Laser	confocal
Cost		√	√	
Resolution	√	√	√	√
Contact non-contact	√		√	√

Table 4.5 Component selection for blade clamp				
Feature	Magnetic	Screw clamp	Spring loaded clamp	Solenoid clamp
Cost		√	√	
Ease of use	√	√	√	√
Clamping ability		√	√	√
Simplicity of design		√		

The blade will be clamped using a thumbscrew clamp this solution was felt to be the most straightforward and practical.

Table 4.6 Component selection for XY slide drive				
Feature	D.C. motor	Dc motor with servo control	Stepper motor	Manual slide
Cost				√
Resolution	√	√	√	
Feedback control		√		√
Interface with Labview software		√	√	

The blade will be traversed under the lasers using a motorised XY slide, motion is provided by a DC motor with servo control. This option was chosen because of the feedback control provided with the servo system, the ability of the system to integrate with the Labview data acquisition software and the resolution associated with a servo system. The manual slide unit would not provide feedback control, the stepper motor unit would require a separate feedback control system.

4.5 Component selection

From the morphological analysis the specifications for the components required for the measurement device were established, the selection criteria for each of the components was as shown in (Table 4.7)

Measurement head (Laser)	Capable of measurement to micron resolution, can integrate with the slide system. Range of greater than 3mm to accommodate the measurement of a surgical osteotome
XY Slide	Capable of moving the osteotome in an XY raster to facilitate a complete scan of the blade. Must have a travel range of 10-20mm to allow for a full scan of the flanks of a surgical blade. Resolution of movement must be micron resolution.
Blade clamp	Capable of restraining the blade for scanning, Simple to operate, robust, consistent clamping force
Software	The software must be capable of being used in conjunction with a data acquisition system, must be capable of integrating the slide units and measurement head, must be able to analyse the resulting data and display a result of the scan.

4.5.1 Lasers

Following the result of the research carried out on the state of the art measurement devices, it was decided to use triangulation laser technology.

Laser triangulation comprises of several different technologies, namely Scattering Laser Triangulation and Reflective Laser Triangulation. There are two light position detecting technologies used by laser triangulation sensors, PSD (position sensitive device) and CCD (charged coupled device). The light reflected by a target passes through the receiver lens used to focus the light on the PSD or CCD.

The position sensitive detector uses the light quality distribution over the entire beam spot on the PSD to determine the beam spot centre and identifies this as the target position. If the distribution of light is affected by the surface finish of the target material, this causes variations in the measured values (Figure 4.11).

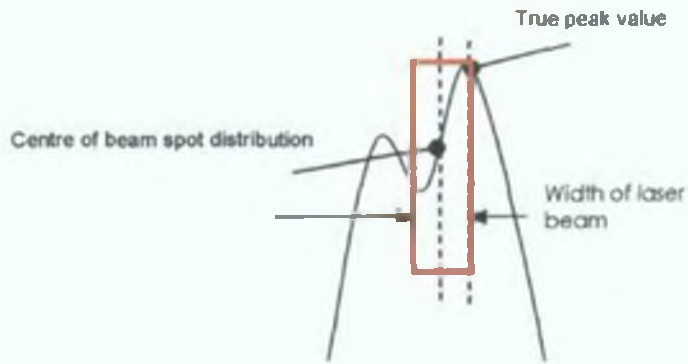


Figure 4.11 PSD the entire beam spot is used to determine the beam spot centre, the quality of the surface finish affects the distribution of light

The CCD detects the light intensity distribution for each pixel and identifies this as the target position. This means that the CCD will give highly accurate displacement values regardless of the quality of the beam spot, therefore the surface finish of the target material has less effect on the variability of the laser head measurements, this was considered of importance in selecting the type of laser head, as the surface finish of the scanned blades may vary (Figure 4.12).

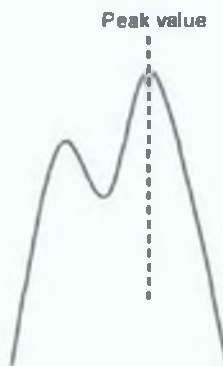


Figure 4.12 CCD detects the peak value of the distribution of the beam spot for each pixel, allows for variations in surface finish of target material

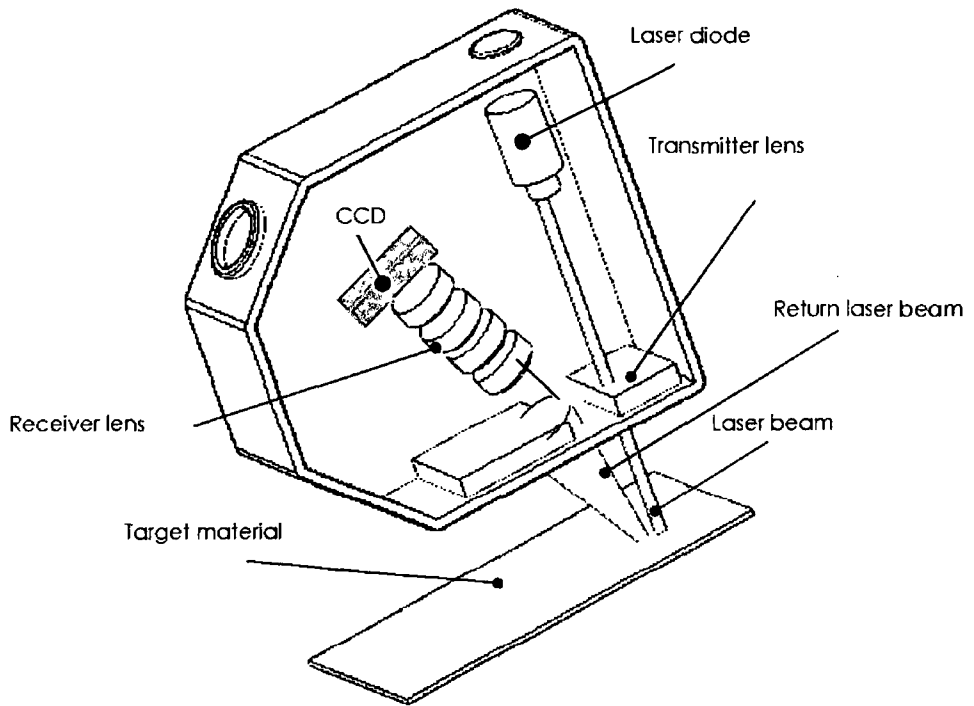


Figure 4.13 Principle of operation of laser triangulation (Charge Coupled Device)

The possible arrangement for a laser scanning head relative to a blade is as shown in (Figure 4.14). The emitter and receiver are located at different positions. Scattering laser sensors shine the laser light directly down onto the surface. When the light impacts the surface it scatters in many directions. As long as some of this light shines into the detector it will form an image. This allows the laser sensor to measure surfaces which diffuse light in different directions.

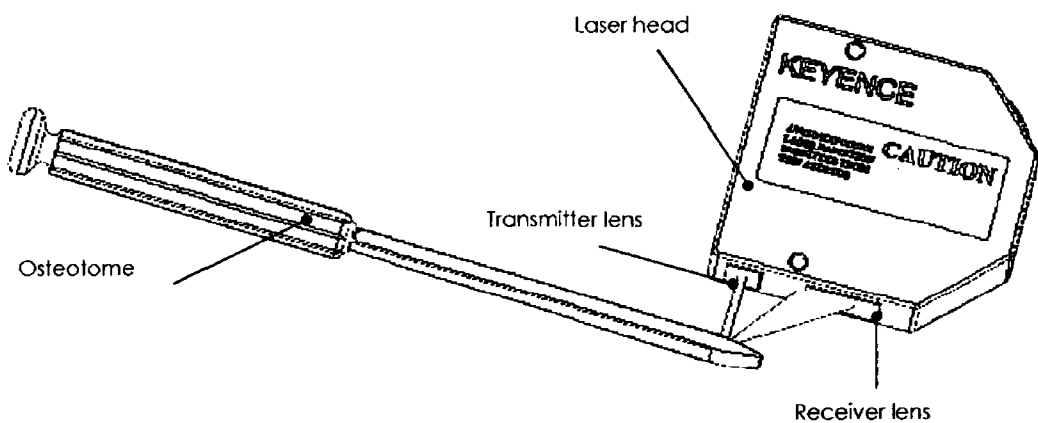


Figure 4.14 Arrangement of laser triangulation head relative to blade

The laser heads are controlled by the Keyence LK-2001 laser controller unit (Figure 4.15), this gives an analogue output of ± 5 volts. When measurement is outside the range then +12 volts is output.



Figure 4.15 Keyence LK-31 laser head controller

The output from the LK-2001 is fed to a 68-pin shielded connector block (SCB-68), (Figure 4.16) with the connection configuration in the differential mode, then the data is transferred to a Dell Latitude D800 Pentium 1.6 GHz laptop computer through a NI PCI-6036E multifunction 200ks/s 16 bit I/O data acquisition card supplied by National Instruments.



Figure 4.16 68-pin shielded connector block supplied by National Instruments

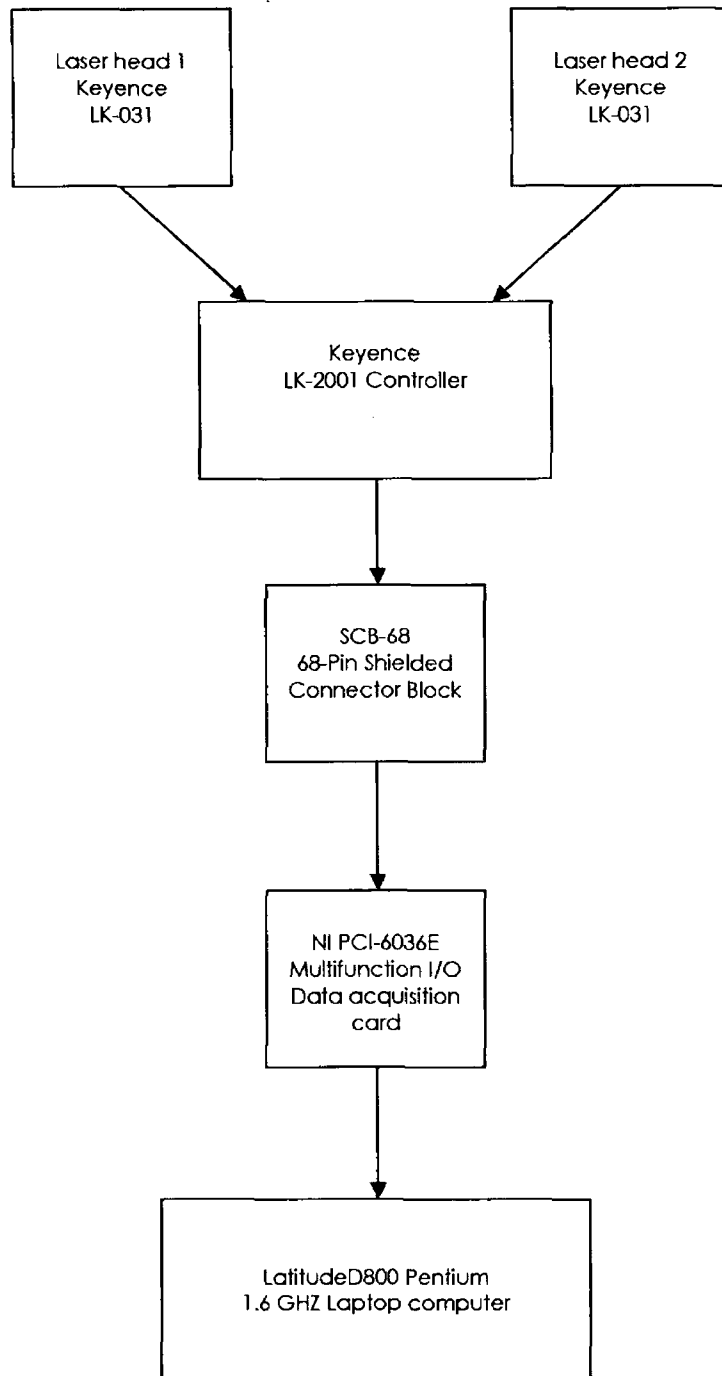


Figure 4.17 Data flow from laser heads to laptop

4.5.2. XY Slides

As the laser technology selected for the scanning device is a point source, it is a requirement to move the blade relative to the lasers or the lasers relative to the blade. Through research into the state of the art measurement devices (Chapter 3) it was found that the best option was to move the blade relative to lasers, In order to move the blade, it was required to use a slide device. The options were to build a slide device or purchase an off the shelf unit.

It was decided to purchase a slide unit to achieve the resolution and precision required for the positioning of the blade in the measurement system.

The design constraints for the slide were:

Travel range:	10-20 mm.
Resolution of slide:	Micron range.
Size of slide:	Compact (less than 150mm X150mm).
Operation:	Electrical.
Drive software:	Software must integrate with laser heads, control positioning and provide feedback.

Vendors were short listed based on the above criteria, vendors evaluated included I.A.I. Industrieroboter GmbH, Automation (automation and motion control products), Tusk, Rodriguez (UK) Ltd, Newmark Systems inc, Physik Instrumente GmbH.

The vendors finally selected to supply the micro-slides were Physik Instrumente GmbH supplied through the vendors (Lambda Photometrics Ltd. UK.). They fitted all the selection criteria, as well as providing support for integration of the slides with the laser heads and controlling software. The slides had an envelope of just 62mm X 70mm which allowed scope for the design of the prototype measurement instrument.

Evaluations were carried at the vendor's premises to ensure that the slides suited the requirements. The slides were then tested in house to ensure that the slides would integrate with the laser scanning heads. The slide model finally selected are the P.I.M-111DG high resolution motorized translation stages.

Travel range is 15mm, which is adequate for the type of blade being tested in the experiments. The resolution of the slides is $0.05\mu\text{m}$ with a unidirectional repeatability of $0.1\mu\text{m}$. the velocity is up to 2.0 mm/sec (Figure 4.18)



Figure 4.18 Slide unit M-111.1DG. Travel range 15mm. resolution $0.05\mu\text{m}$ supplied by Physik Instrumente (Image courtesy of Physik Instrumente GmbH).

To provide for future scanning over the entire blade it was necessary to produce a XY raster of the blade surface, the micro-slides selected were configured in a "piggy back" arrangement to give a XY slide configuration as shown in (Figure 4-19).The design of the slide units allows multiple slides to be easily mounted one on top of the other.

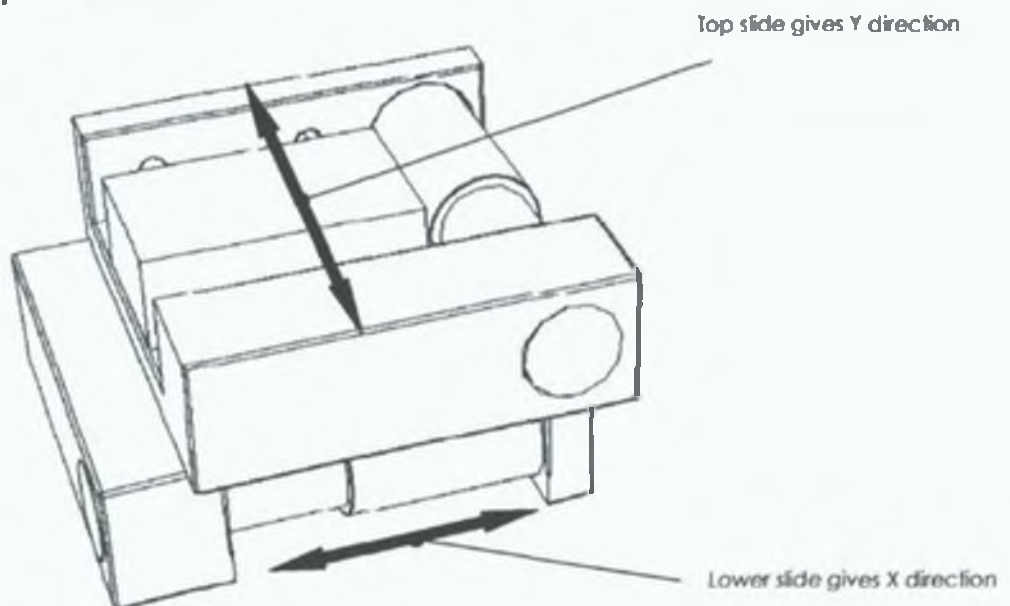


Figure 4.19 XY slide configured from two PI. M-111 high resolution motorized translation stages

To ensure that the slide units were set up properly it was necessary to align them using a dial gauge (Figure 4.20). The alignment procedure used a calibrated square block (Browne and Sharpe) the block was set parallel to the lower slide using the dial gauge on "Front" face, then the top slide was set perpendicular to the lower slide using "Side" face of the block



Figure 4.20 Aligning the slides using dial gauge

The clamp unit was set up using a parallel which was adjusted using a dial gauge to ensure that the clamp runs parallel to the direction of the slide



Figure 4.21 Aligning the clamp unit using dial gauge

4.5.3 Control of XY Slides

Control of the slide units is achieved using the Mercury II DC-Motor Controller (Supplied by Lambda Photometrics Ltd. UK.). This controller provides PID servo-control of position, velocity, and acceleration.

The mercury controller comes with its own built-in commands and features, however it was decided to use independent software which would control both the slide units and the laser heads simultaneously. Each slide unit requires a controller (Figure 4.22) and up to 16 controllers can be connected to one RS-232 port in a daisy chain.



Figure 4.22 Mercury II C-862 single-axis DC-motor controller

4.5.4 Blade clamp design

To restrain the blade during scanning it was required to hold the blade in a manner which was easy to operate and would not damage the blade. The design constraints for the clamp were that it must be fixed to the XY slide and must not interfere with the scanning process. The blade clamp device was custom designed and built to suit the type of blade being scanned (Figure 4.23) and (Figure 4.24).

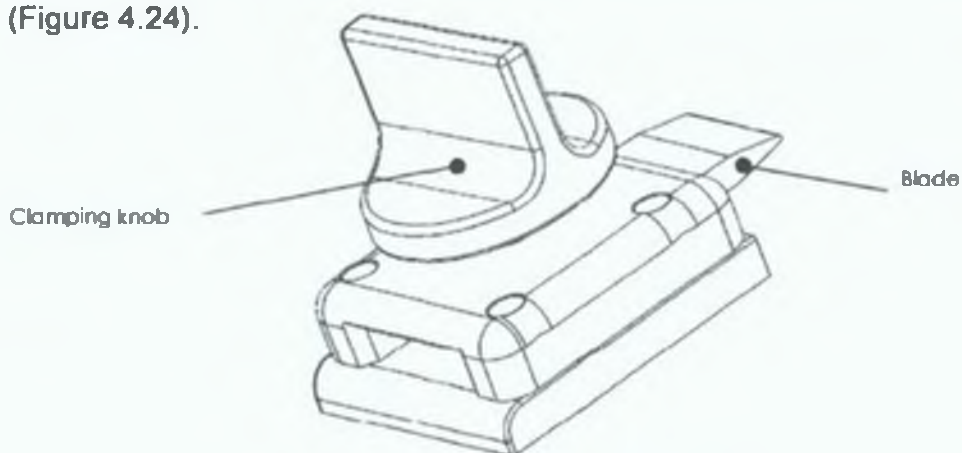


Figure 4.23 Design for blade clamping unit

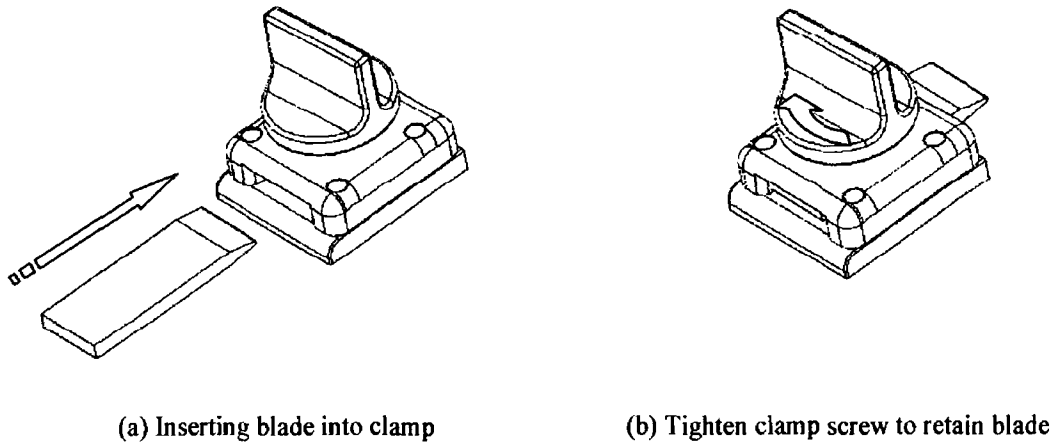


Figure 4.24 Operation of clamp unit

The blade clamping device was fixed directly to the XY slide. The unit was designed so that it could be easily removed to allow a different clamping system to be installed, a separate clamping system might be required to clamp oversize blades (Figure 4.25).

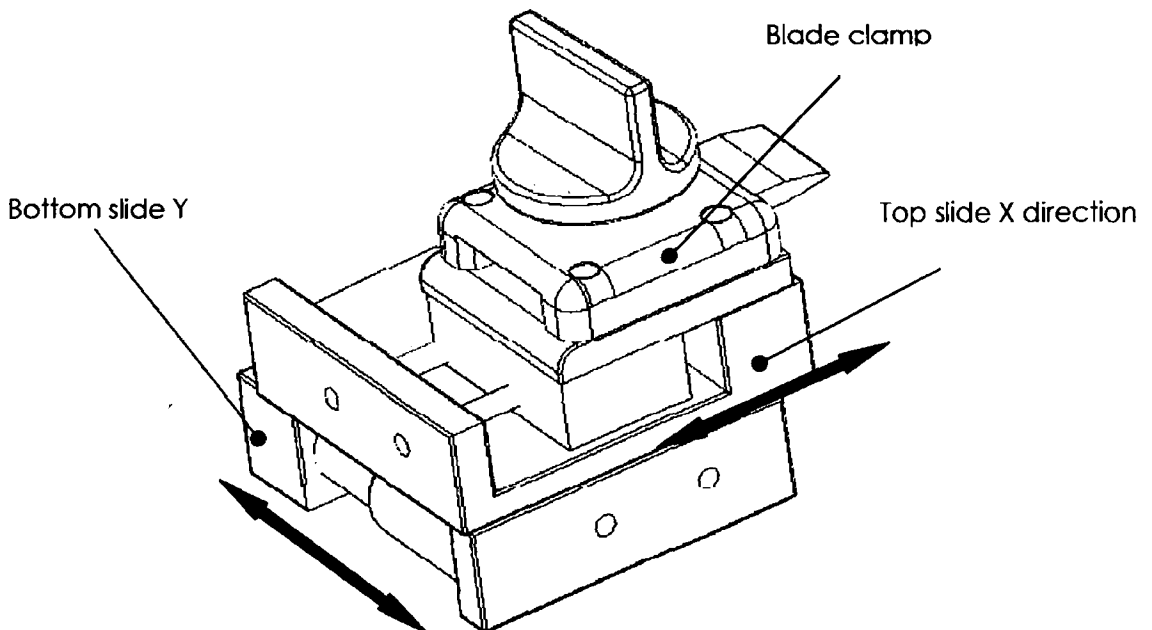


Figure 4.25 Clamp unit fitted to XY slide

4.5.5. Software Design.

To integrate the various components of the measurement device it was decided to use Labview Software Version 7.1. This is an object based programming language, developed by National Instruments. LabView programs are also known as virtual instruments, because their appearance and operation imitate actual physical instruments using a set of tools for analysing and displaying

To test the laser heads a Labview program was written as shown in the schematic (Figure 4.26) this program takes in the raw data from the lasers through a data acquisition virtual instrument (VI), this data is fed to zero offset compensator and then to a span multiplier the output is sent to an output display. This zero and span compensator allows for calibration of the laser heads through the software.

This program evaluated was written to test the ability of the laser heads to measure a stepheight. Slip gauges were used in the initial tests, (serial No.16724, traceability No. 48412 NAMAS).

Zero sets the datum; in the case of the measurement device the datum would be set on the centre line of the blade (Figure 4.27).

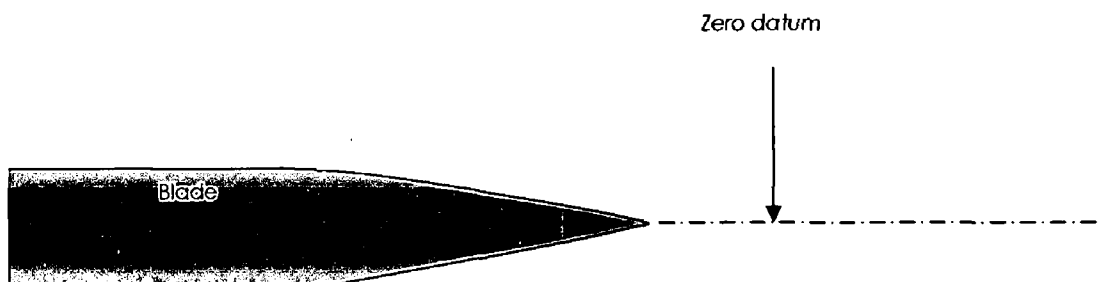


Figure 4.27 Zero datum for blade

Span relates to the linearity of the measurement over the range of the measurement (Figure 4.28).



Figure 4. 28 Span setting for blade

Calibration was carried out to test the operation of the laser head. The procedure for the test was to set a parallel in the blade clamping device (Figure 4.29) the Keyence LK – 2001 laser head controller was powered up and allowed to settle for 30 mins as specified by Keyence. A parallel was set up in

the blade clamp this gives the zero setting. A 3mm slip gauge¹ was placed on the parallel to set the span. The initial reading of 0.29mm was adjusted to give a reading of 0.00 then a reading of the span (with the 3mm slip gauge in place) was taken. This gave a reading of 2.81mm, the span was set to 3.00mm then the zero was checked again the results are as shown in (Table 4.8). This

Table 4.8 Calibration of laser head

		Test 1	Test 2	Test 3	Test 4	Check
Zero	Reading	0.29	0.04	0.01	0.03	0.00
	Adjustment	0.00	0.00	0.00	0.00	N/A
Span	Reading	2.81	2.94	2.99	3.00	3.00
	Adjustment	3.00	3.00	3.00	N/A	N/A

procedure was repeated until a null variation between the required and measured values was achieved

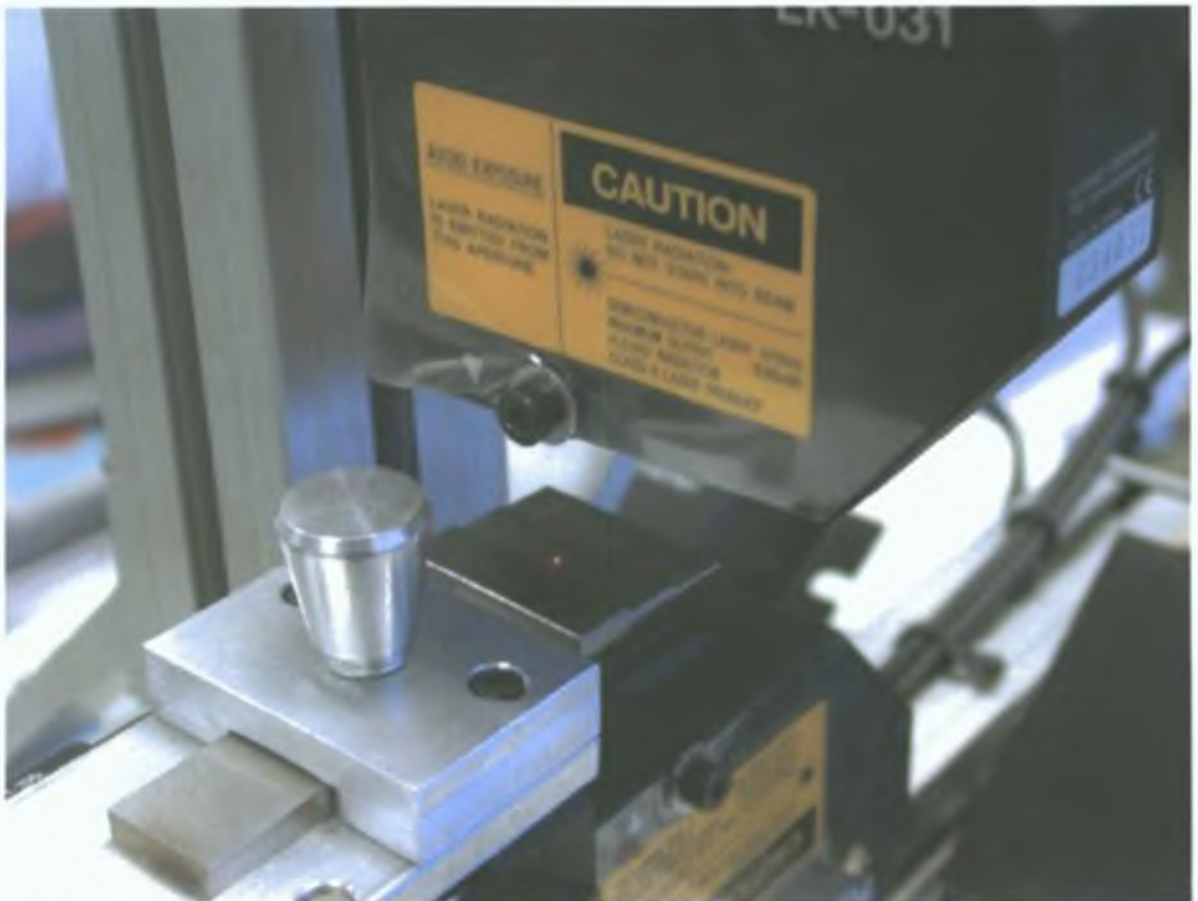


Figure 4.29 Using slip gauges to calibrate laser heads

¹ Slip gauges traceability No 48412

Table 4.9 Results of scans on slip gauges

Gauge block	Reading	Deviation
0.5	0.5	0
1.0	1.0	0
1.5	1.49	.01
2.0	1.98	.02
2.5	2.49	.01
3.0	2.98	.02

After the calibration of the laser head a series of tests were carried out using slip gauges, the gauges used were 0.5mm,1.5mm,2.0mm,2.5mm,3.0mm the results were as shown in (Table 4.9).

Some variation in the measurements were evident at the larger end of the span, therefore it was necessary to re-calibrate the laser head. The calibration scans of the slip gauges were repeated again this time the results were more consistent (Table 4.10).

Table 4.10 Results of second series of tests using slip gauge

Gauge block	Reading	Deviation
0.5	0.5	0
1.0	1.0	0
1.5	1.5	0
2.0	2.0	0
2.5	2.5	0
3.0	3.0	0

4.5.7 Program Design – Slide and laser interoperability

The next stage was to move the slide relative to the laser, the parallel was also used for this test. The program was designed as outlined in (Figure 4.30). The reader should refer to Figure 4.47 for schematic of device layout and component notation.

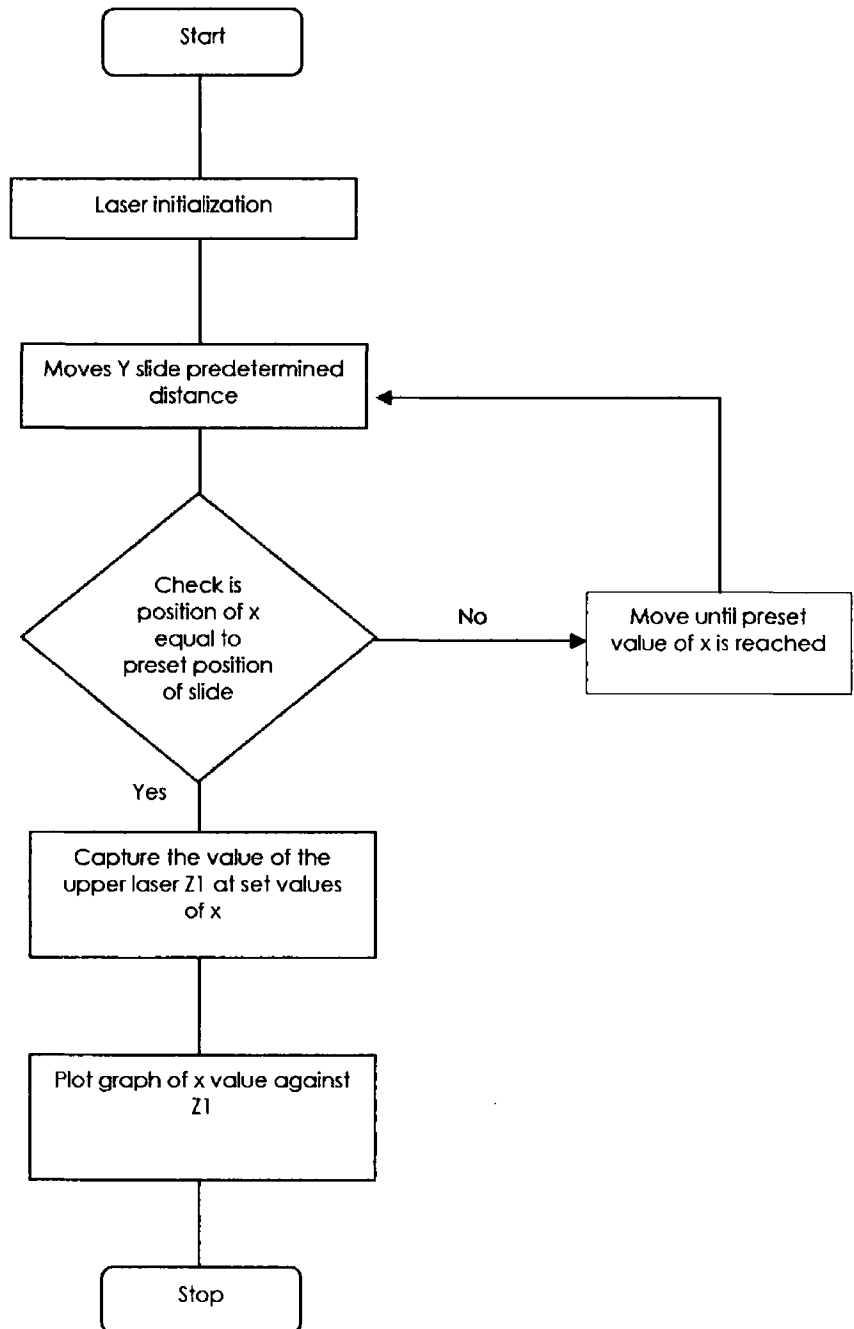


Figure 4.30 Outline of program to scan blade using one laser

Microsoft Excel was used to carry out the calculations on the wedge angle of the blade. The data points were exported from Labview to a text file, this data was then read into Excel to analyze the data (Figure 4.31) using a macro. A basic trigonometric formula was used to calculate the wedge angle, by taking two scanned points on the blade, at distinct positions.

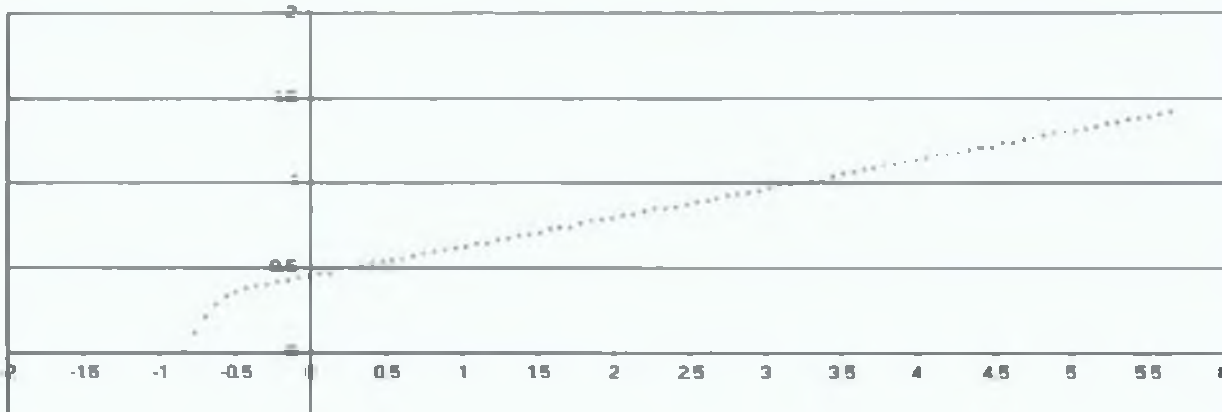


Figure 4.31 Data as displayed in excel

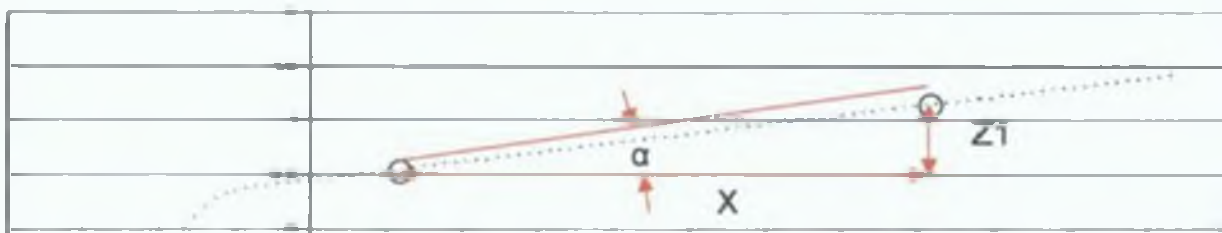


Figure 4.32 Calculation of wedge angle

The calculation of the wedge angle consists of picking two actual data points (Figure 4.32) along the wedge angle and the values of X and Z are calculated and from this the value for α is found.

Figure 4.33 outlines the program for scanning operation using two laser heads.

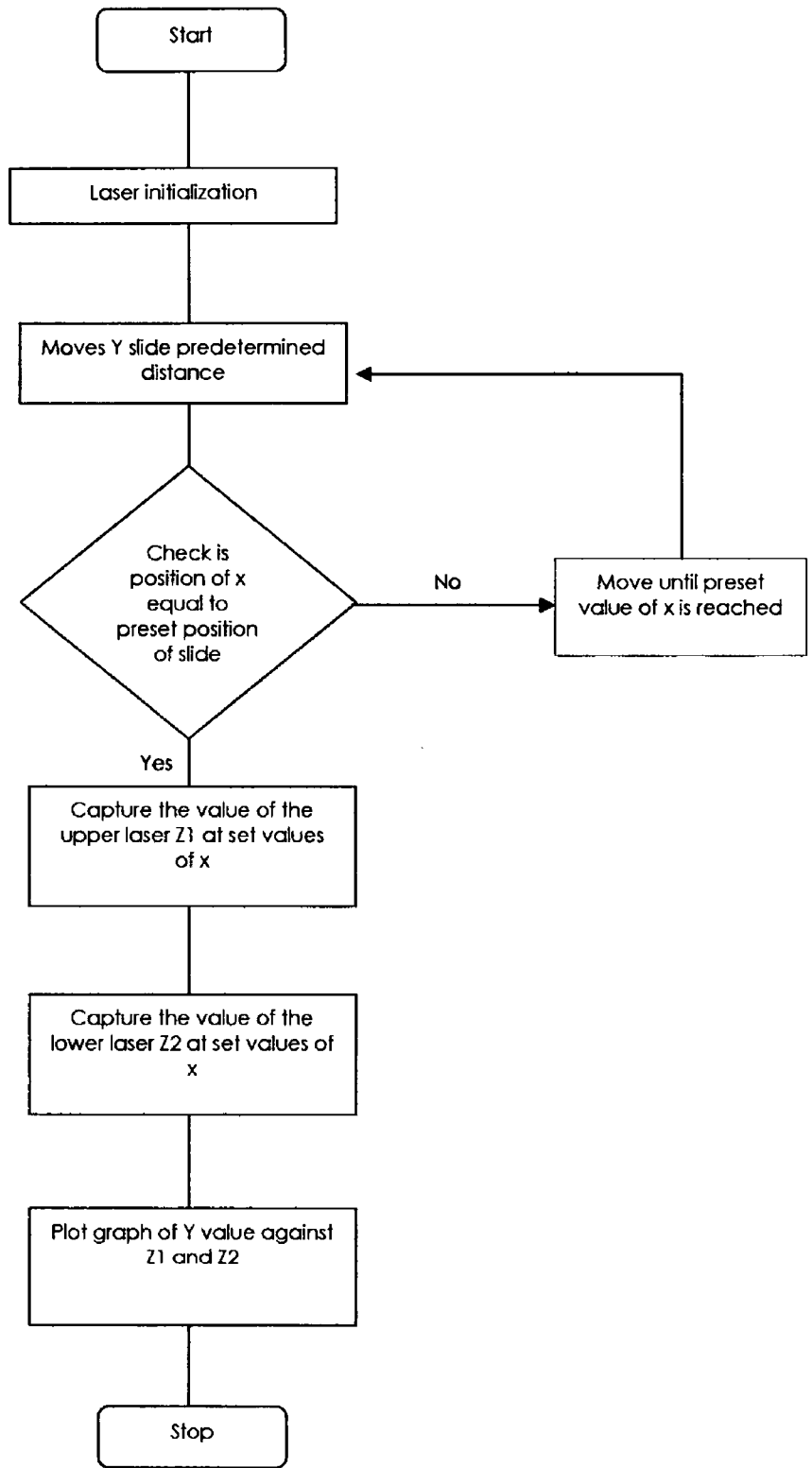


Figure 4.33 Outline of program to scan blade using two lasers

The acquired data points were exported to Microsoft Excel as in the original program however this time a scan was obtained on both sides of the blade the data as displayed in Excel (Figure 4.34) shows the complete profile of the blade. The formula was modified to take into account the full profile of the blade. it may be observed that data points are collected by the device at fixed intervals which affects the resolution of the scan on the blade radius.

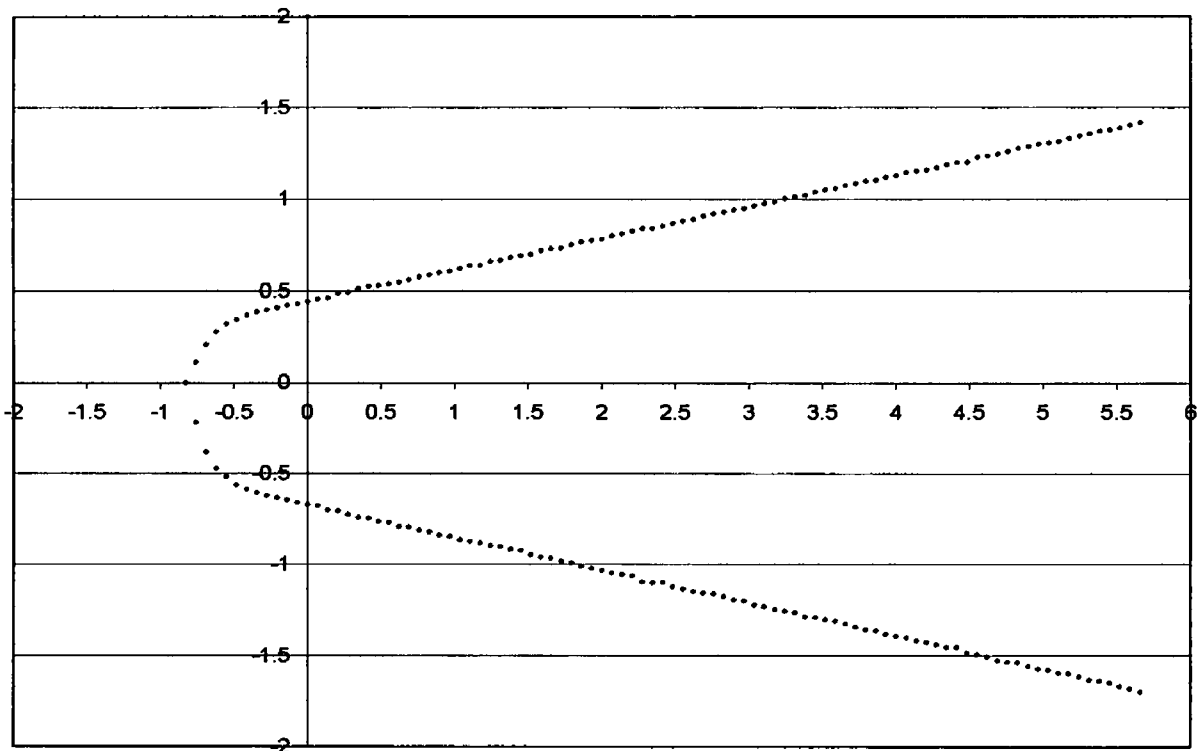


Figure 4.34 Graph of data points scanned into excel

Each side of the blade wedge angle was calculated separately and the angles then added to obtain the total wedge angle, this procedure was used to allow for any variations in the symmetry of the blade.

The total wedge angle θ was calculated by the sum of $\alpha_1 + \alpha_2$. (Figure 4.35) Tests were carried out to ensure that the calculation was capable of determining the wedge angle as described in a later section. To test the operation of the program the lasers and XY slides were assembled, components were clamped

in a temporary jig, as the final arrangement of the components was not determined at this time.

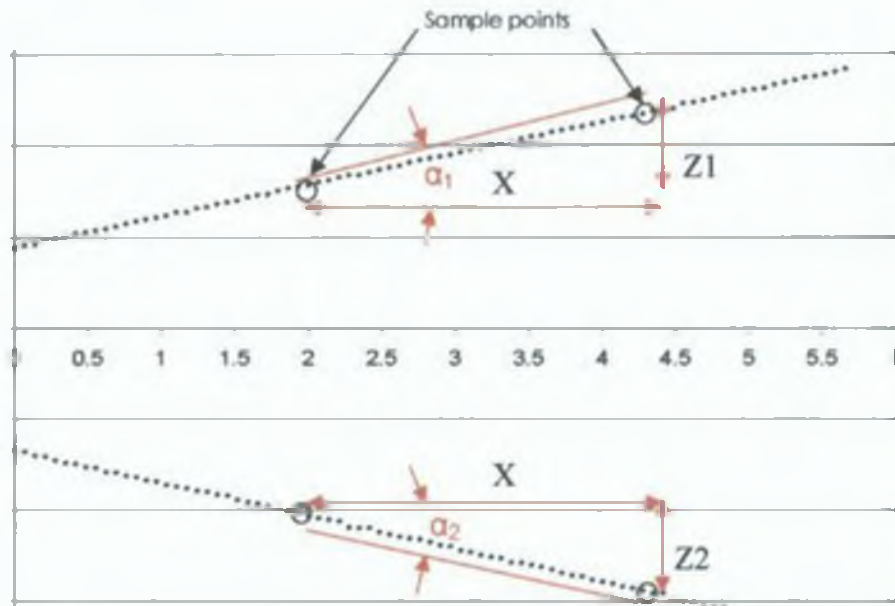


Figure 4.35 Calculation of wedge angle of blade

4.6 Phase III Detail Instrument Build

The product design specification was cross-checked to ensure that the detail design met with the original P.D.S. requirements. The layout of the components was determined to allow the measurement instrument to perform the task required.

4.6.1 Component configuration

This section of the design process, deals with the configuration of the design of the measurement device, the component layout requires the lasers to be positioned to acquire a scan of the blade on both sides simultaneously. The blade must be positioned between the laser heads to scan the blade.

(Figure 4.36)

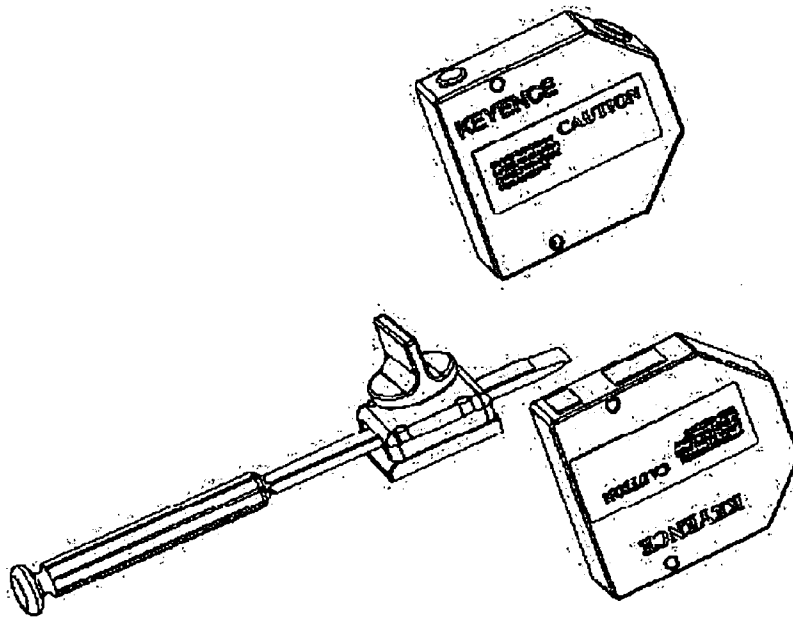


Figure 4.36 Proposed layout of Laser heads relative to blade clamp device

Support frame selection

The support frame was constructed from aluminium profile, this decision was taken to allow modifications to the overall frame structure before a final decision was made on layout and dimensions of the measurement instrument. Components were positioned to give the optimum layout for the measurement device (Figure 4.37). This format allowed for the adjustment of the laser heads

to give the correct standoff distance between the lasers and the blade being measured.

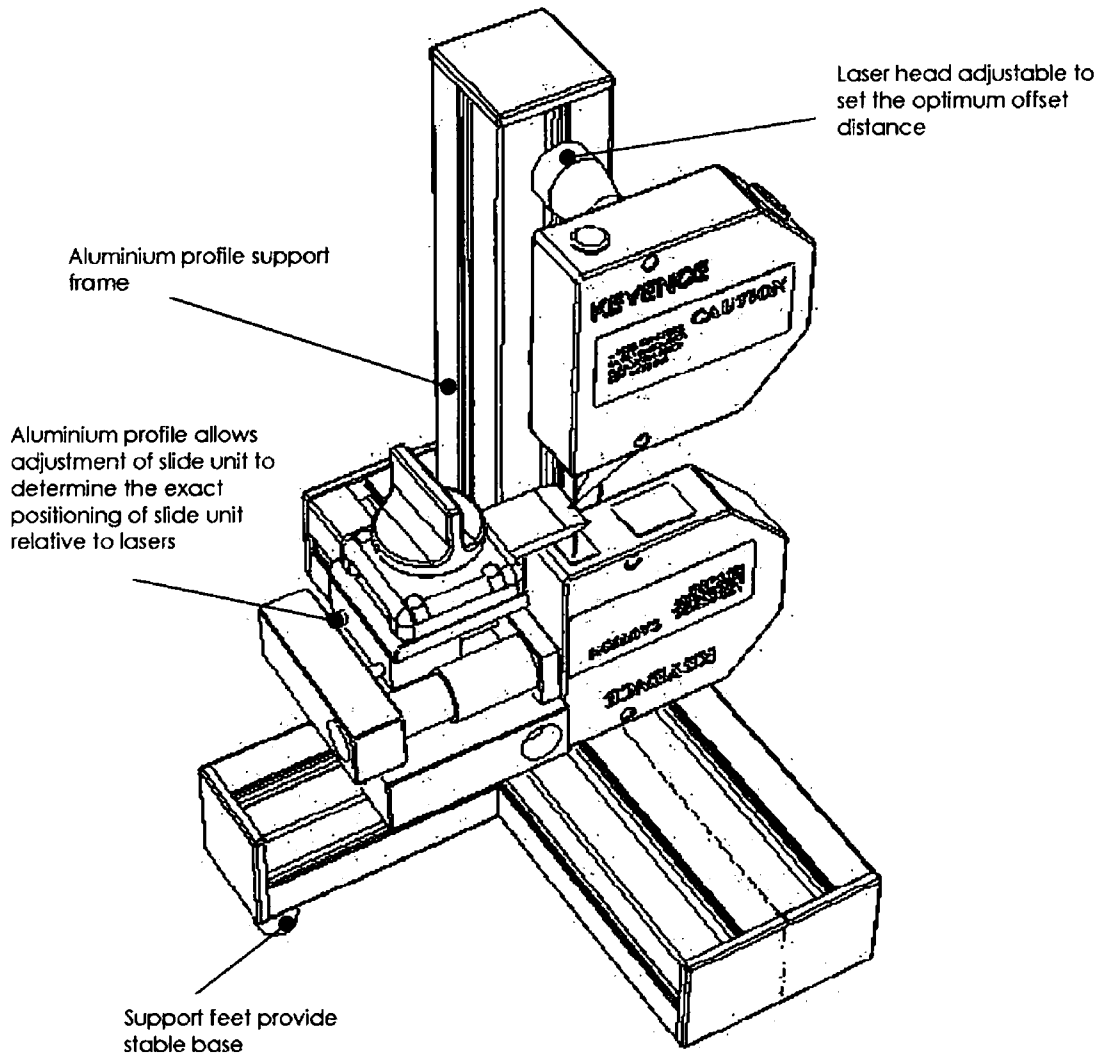


Figure 4.37 Support frame

To ensure an accurate scan the laser heads must be aligned to each other, a procedure was devised to ensure that the laser heads were aligned correctly. A calibration plate was used (Figure 4.38). The calibration, uses a plate with a series of precision holes of varying in diameter from 2mm to 0.5mm the procedure is as follows: A piece of paper is placed under the calibration plate as shown in the top laser (Z_1) is powered up, the calibration plate is adjusted to give a clear image on the paper. Then the top laser is switched off and the lower laser (Z_2) is powered up the piece of paper is placed over the calibration plate the laser head is adjusted to give a clear image, this procedure is repeated for the smaller holes.



Figure 4.38 Aligning laser head

Figure 4.39 shows the result of laser misalignment, the laser light is diffused as it impacts on the sides of the hole indicating that the laser head is out of line.

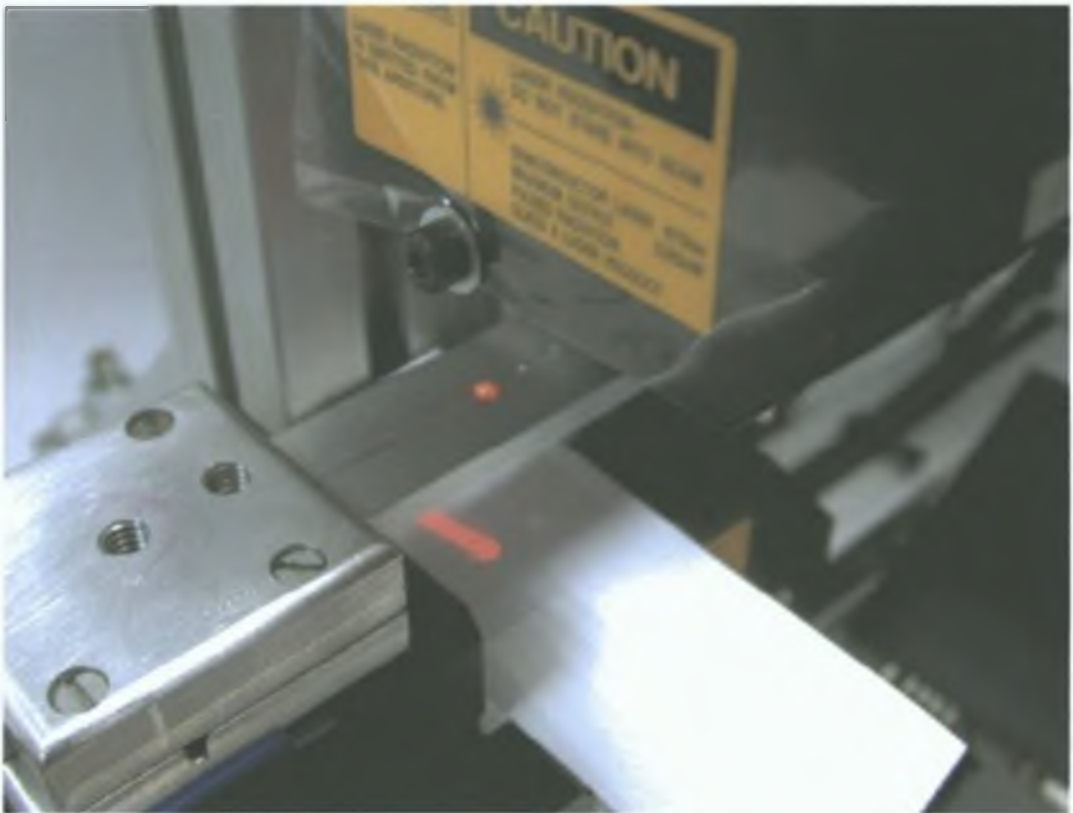


Figure 4.39 Effect of laser head misalignment

Then the device was examined for design robustness. To establish the performance of the measurement device, various tests were carried out, this included evaluation of the laser head orientation leading to the;

(1) Laser head orientation modification as outlined in (Section 4.4.1) detail design.

(2) Blade clamping device modification (Section 5.3) this modification was the direct result of the repeatability and reproducibility study carried out and detailed in the results Section 5.0.

4.7 Instrument Testing

This section outlines the stages in the detail testing of the prototype non-contact measurement device. This section will also describe modifications carried out as the result of tests carried out on the device.

4.7.1 Laser interference study

Initial tests of the machine revealed problems with diffused light interference from the laser heads. Initial arrangement of the measuring device is demonstrated in (Figure 4.40). In this arrangement it was found that laser light diffused from one laser as the blade finished its scan and was picked up by the second laser, causing interference. (Figure 4.41).

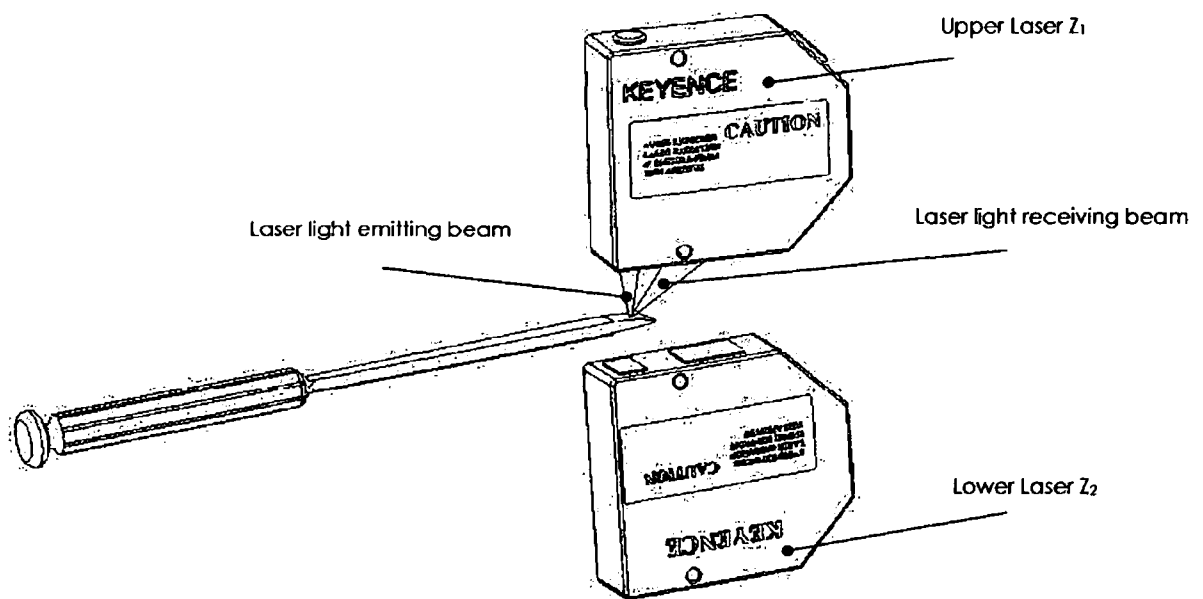


Figure 4.40 As blade flanks are scanned no interference is experienced by the lower laser

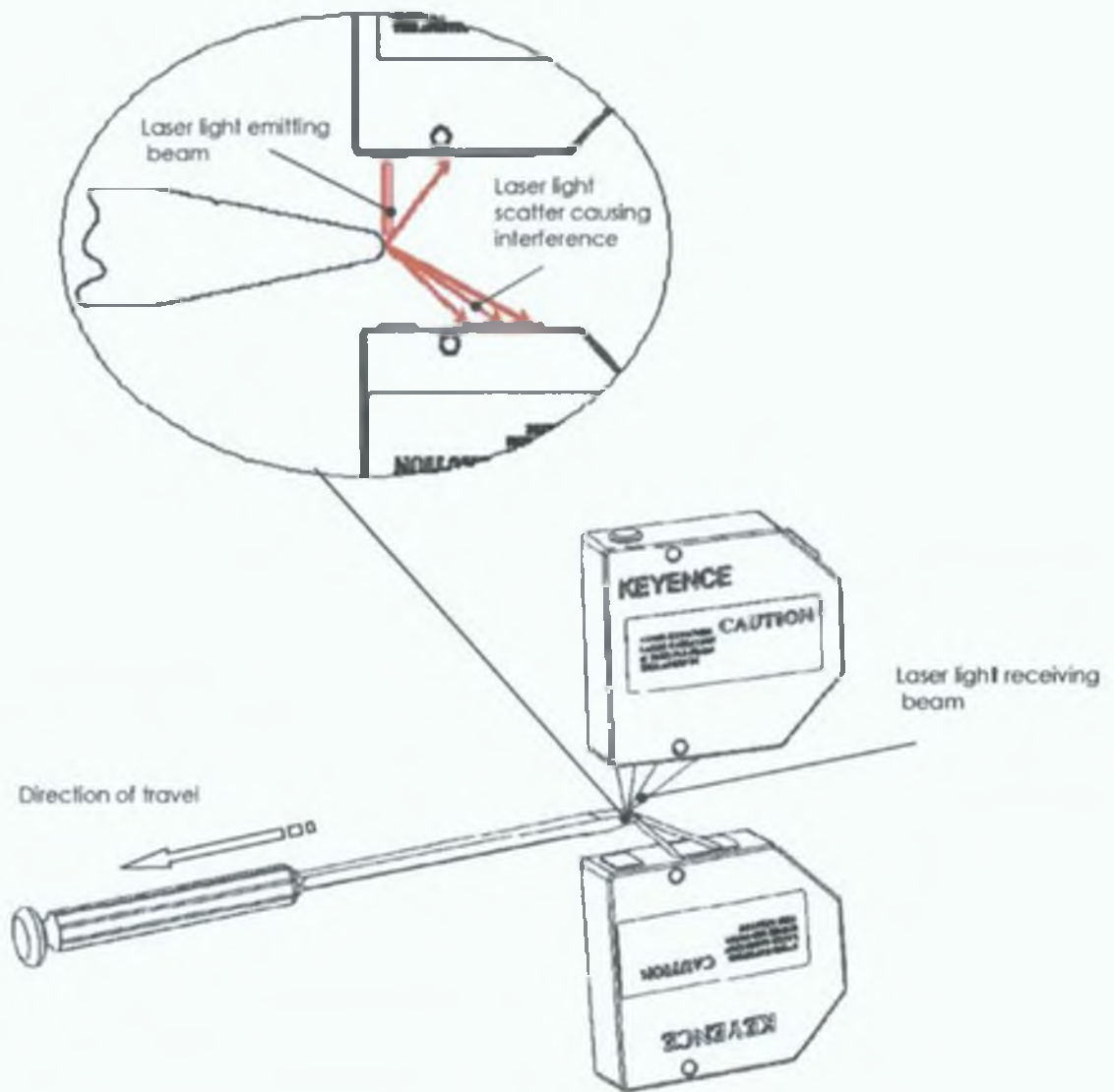


Figure 4.41 As blade is scanned some diffused from the top laser is picked up by the lower laser

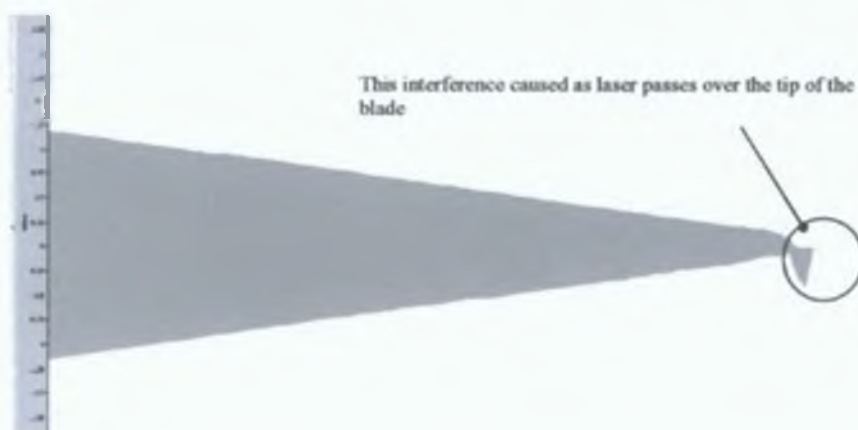


Figure 4.42 Measurement errors as a result of diffused light from laser

The result of the problem caused by the orientation of the laser heads is illustrated in Figure 4.42, the interference caused is apparent as the laser light passes over the tip of the blade. To reduce this interference the laser orientation was changed, it was established that an arrangement with the lasers aligned at 90° gave the best results. The receivers on both lasers in this arrangement are in different positions, therefore the diffused light from one laser will not be picked up by the receiving sensor on the other laser (Figure 4.43).

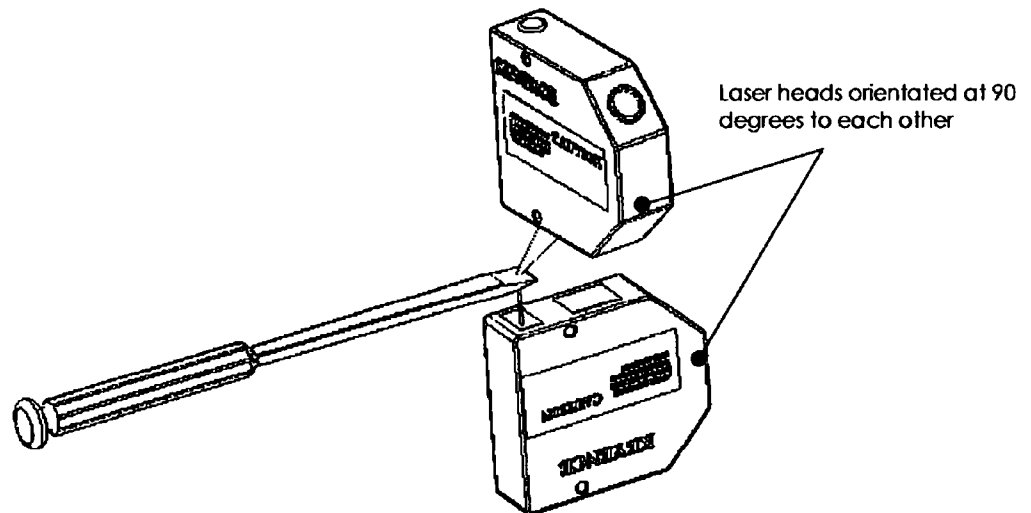


Figure 4.43 Laser head reorientation changed to eliminate the problem associated with laser light scatter.

Results of the scans of the same sample blade which were carried out after the modifications to the laser head orientation are outlined Section 5.6.

4.8 User interface

The front panel was designed to allow for easy user interface, As stated in the product design specification the measurement device must be user friendly, therefore the front panel should reflect this by being simple and easy to read, it is not a requirement to display the actual profile of the blade, the wedge angle of the blade should be displayed following the test. To achieve this, the front panel only provides this measured result (Figure 4.44).

27.5 Degrees Wedge Angle

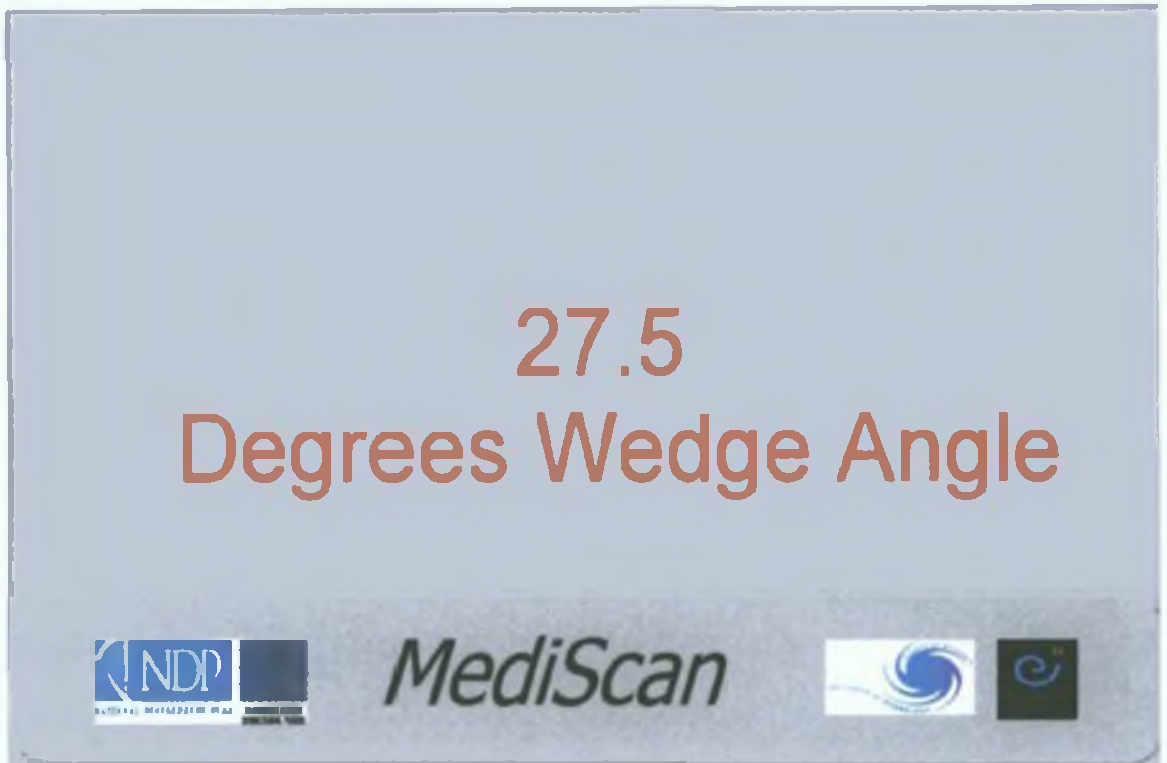


Figure 4.44 User interface screen

It should be noted that the wedge angle calculated at the time of writing is for display purposes only, completed data were not available from within the larger project group to determine the optimum cutting wedge angle for cutting various types of bone. However Figure 4.45 shows the typical result from ongoing experiments by other researchers to measure the effect of blade wedge angle and tip radius on the cutting forces using high density polyurethane foam. The charts clearly show that the force increases with wedge angle, and illustrate that when wedge angle is known, the cutting efficiency of a blade for a defined material can be determined, and can be done in conjunction with the wedge angle generated by this chart

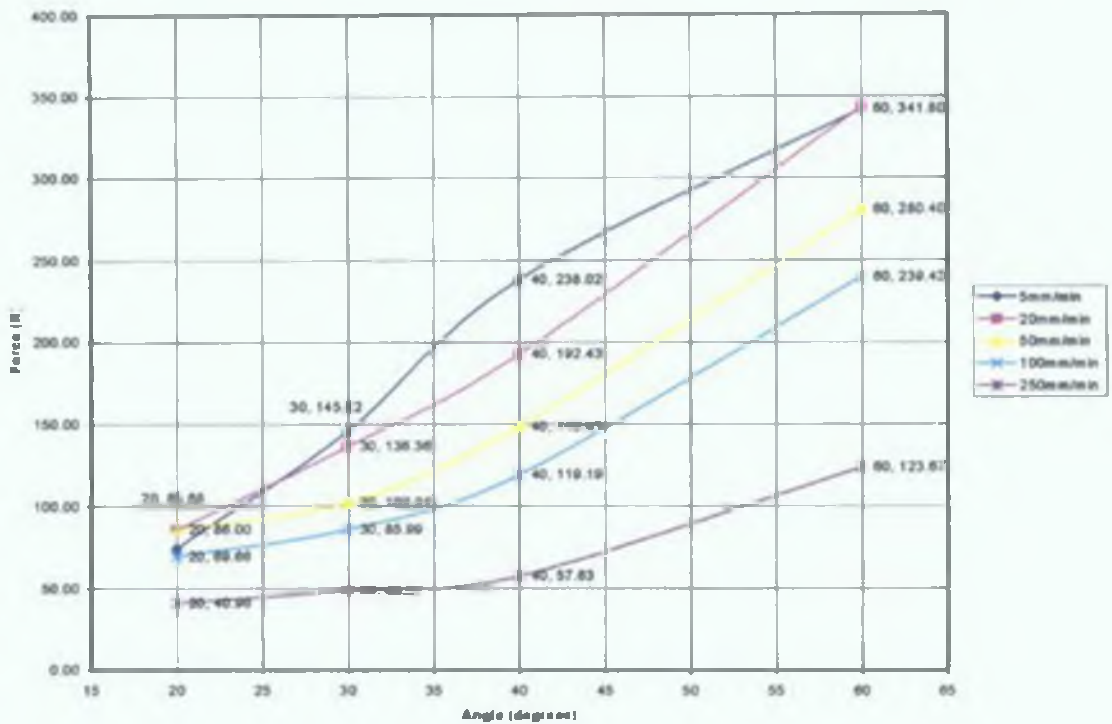


Figure 4.45 Maximum force/wedge angle for HDRPF 40PCF

The experimental result shown in Figure 4.46 was conducted to evaluate the effect of the wedge angle on cutting force using HDRPF 40PCF. The experiment was conducted at a range of cutting speeds. For each experimental cutting speed there was an increase in the cutting force with increase in wedge angle.

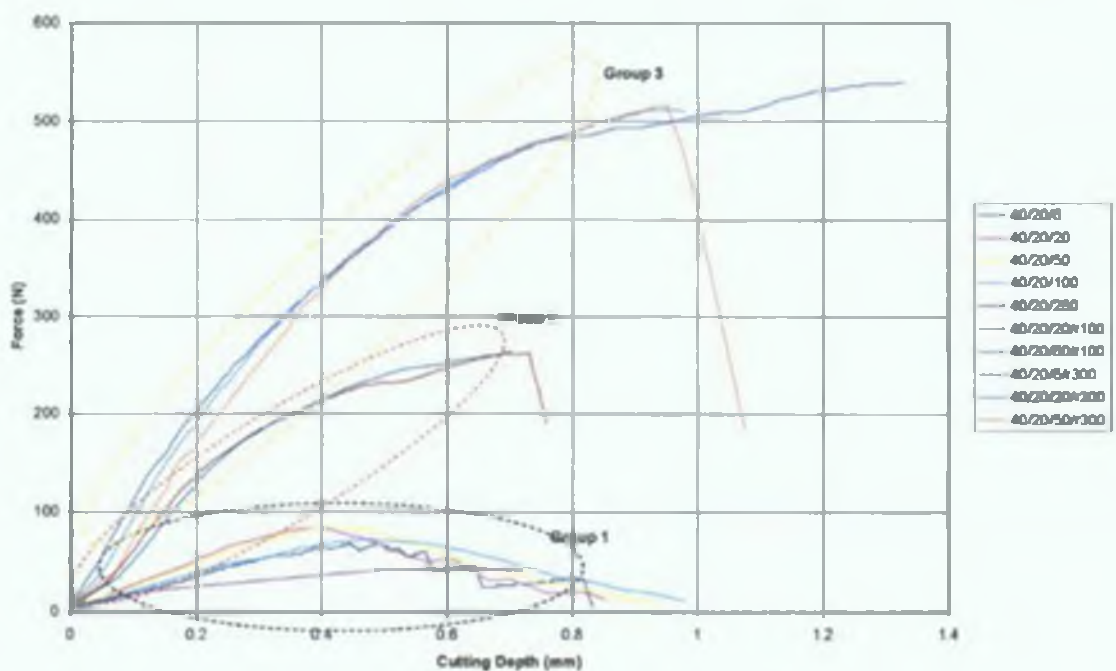


Figure 4.46 Maximum force/cutting edge radius for HDRPF of varying densities

Figure 4.46 illustrates the effect of edge rounding on the cutting force. All tests were carried out on HDRPF 40PCF with a test blade having an internal wedge angle of 20degree test speeds ranged from 5mm/min to 250mm/min.

4.9 Final layout of components

The configuration of the measurement instrument with consideration for the orientation of the laser heads is shown in Figure 4.47

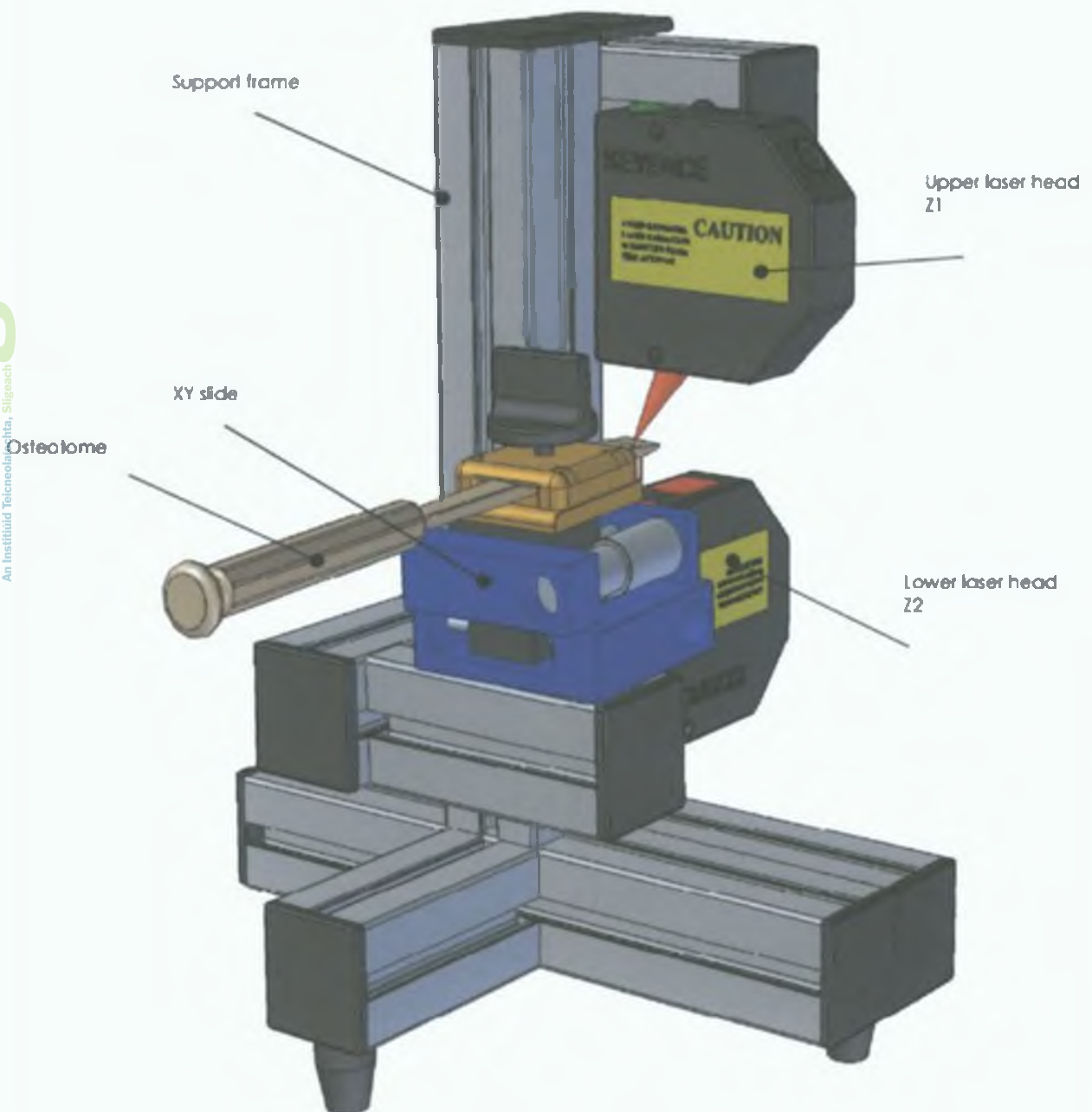


Figure 4.47 Layout of components

Chapter 5.0 Instrument Testing

To ensure that the measurement instrument performed as designed a series of tests were carried out;

- 1) To test the performance of the measurement instrument an instrument evaluation study was carried out
- 2) To test the operation of the measurement instrument with regard to human interoperability a Repeatability and Reproducibility study was carried out.

5.1 Instrument Evaluation Study

Repeatability reflects the inherent precision of the measurement device. This study was carried out to evaluate the consistency of the measurements which the prototype measurement device was capable of achieving. In this study one blade was used (Sample blade number 3). The blade remains in the holder throughout the test, 50 data points on each side of the blade were sampled (50 X 2) with the test being repeated 20 times. Only one operator is used. The results of this test are as shown in (Table 5.1).

Procedure

In this study the blade is inserted into the holder, the program is executed which scans the blade between the laser heads, each measurement interval was 69 μ m and at each interval a reading from the lasers was taken, this information was fed into an array which was exported into Excel and analysed and the wedge angle of the blade calculated, the results of the 20 scans were plotted to a graph of wedge angle versus scan number (Figure 5.1).

Instrument Evaluation Study

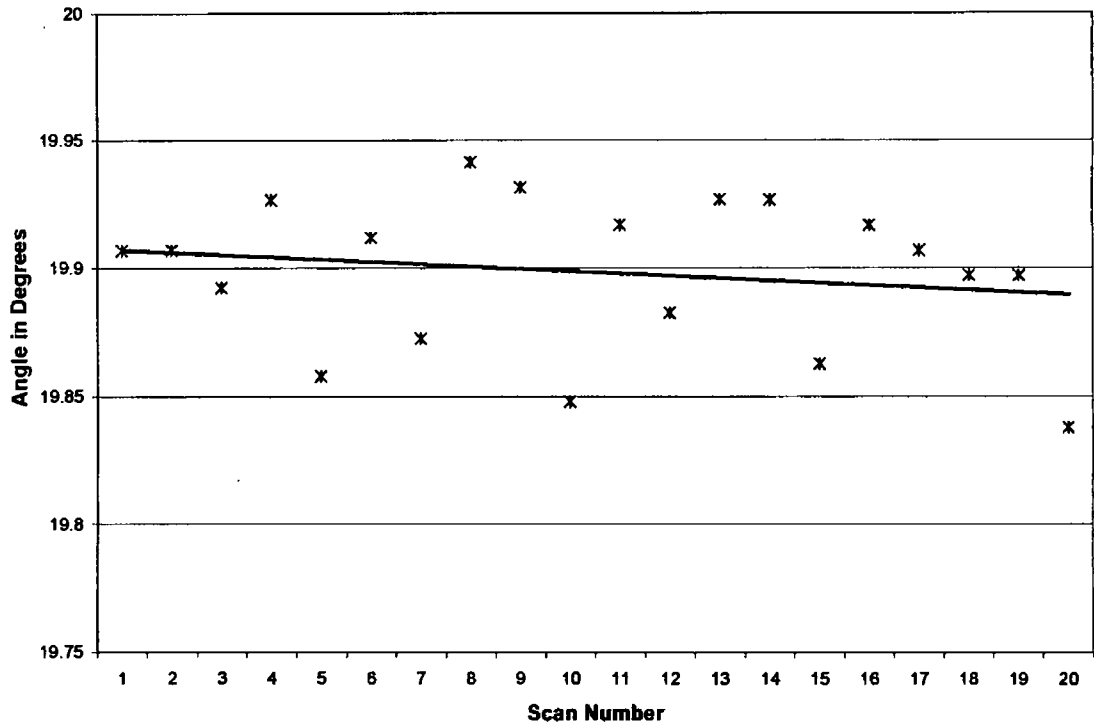


Figure 5.1 Results of Instrument evaluation study

Table 5. 1 Table of results for Machine evaluation study

Scan No.	Angle in Degrees		
0	19.907		
1	19.907		
2	19.892		
3	19.926	Average =	19.899
4	19.858		
5	19.912	Max =	19.941
6	19.872		
7	19.941	Min =	19.838
8	19.941		
9	19.848	Range =	0.103
10	19.917		
11	19.882		
12	19.927		
13	19.926		
14	19.862		
15	19.917		
16	19.907		
17	19.897		
18	19.897		
19	19.838		

5.2 Gauge R and R Study

The purpose of this study was to determine the affect of human interoperability on the operating performance of the measurement instrument. This study determines the precision of the measurement not the accuracy, (accuracy of the instrument is determined in Section 5.7)

Figure 5.2 illustrates the concept of precision and accuracy.

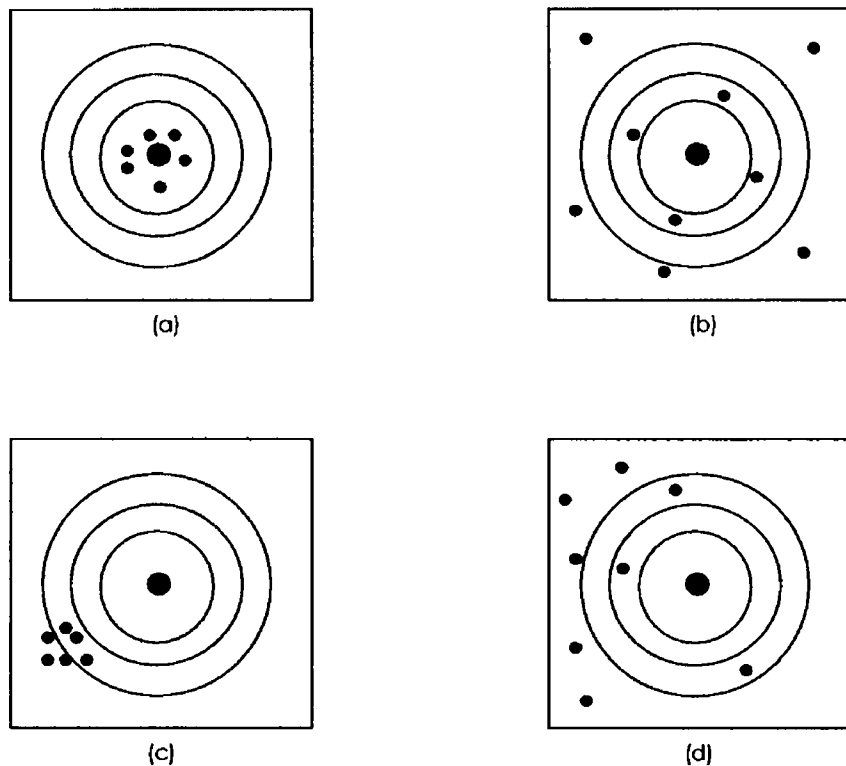


Figure 5. 2 Concepts of precision and accuracy. (a) The gauge is accurate and precise. (b) The gauge is accurate but not precise. (c) The gauge is not accurate but is precise. (d) The gauge is neither accurate nor precise.

The study carried out consisted of three operators each performing a scanning operation on the blade. The test set-up procedure sheet (Appendix B) was followed. Each operator had to insert the blade into the holder tighten the blade retaining clamp and perform the scan. The operator was then instructed to fully remove the blade from the holder and re-insert the blade tightening the clamp again, this procedure was repeated 20 times for each operator. The scan of the blade consisted of the blade being moved between the laser heads in increments of $69\mu\text{m}$, at each incremental position a reading was obtained from both laser heads. This information was fed into an array and exported to Excel

as a text file, a formula was used to extract the wedge angle as described in (Chapter 4.5.3.3.)

The results for each of the 20 scans for each operator were compared to give a max, min, average and range of the scans. (Table 5.1) it was observed that the range of the measurements from each operator had increased from that range which was observed for the machine evaluation study.

The range of the twenty measurements taken in the machine evaluation study was 0.103 degrees (Table 5.1). The range in the gauge R and R study varied from 0.7 degrees to 1.18 degrees (Table 5.2) this variation could be attributed to (a) the repeatability of the measurement device, (b) the effect of the human interface on the consistency of the measurements. Factors affecting the repeatability of the measurement instrument include the rigidity of the instrument frame, the step size of the scan movement, the speed of the scan, the acceleration of the slide units, settling of the instrument after clamping of blade. Factors affecting the reproducibility of the scans (human interface) include setting the blade up in the blade clamping device and the amount of force applied to the thumbscrew on the blade clamping device. The results from the R and R gauge study are presented in Table 5.2.

Table 5.2 Summary of results for R and R study

	Operator 1	Operator 2	Operator 3
	19.898 deg	20.075 deg	20.234 deg
	19.557 deg	19.988 deg	19.910 deg
	19.714 deg	19.881 deg	19.936 deg
	20.109 deg	20.106 deg	19.926 deg
	19.886 deg	19.988 deg	20.198 deg
	19.830 deg	19.794 deg	20.172 deg
	19.624 deg	19.625 deg	19.977 deg
	19.770 deg	19.788 deg	19.655 deg
	19.903 deg	20.028 deg	19.685 deg
	19.785 deg	19.767 deg	20.351 deg
	19.936 deg	20.213 deg	19.870 deg
	19.987 deg	20.106 deg	19.773 deg
	19.847 deg	20.065 deg	20.110 deg
	19.837 deg	20.510 deg	19.972 deg
	20.696 deg	20.070 deg	19.823 deg
	20.031 deg	19.865 deg	19.818 deg
	19.920 deg	20.014 deg	20.019 deg
	19.624 deg	19.968 deg	20.008 deg
	19.511 deg	20.029 deg	19.891 deg
	19.798 deg	20.029 deg	19.983 deg
	19.863 deg	19.995 deg	19.966 deg
Average	19.863 deg	19.995 deg	19.966 deg
Max	20.696 deg	20.510 deg	20.351 deg
Min	19.511 deg	19.625 deg	19.655 deg
Range	1.184 deg	0.885 deg	0.696 deg

In R and R studies two components of measurement error are investigated that of *repeatability* (the inherent precision of the measurement instrument) and *reproducibility* (the variability which may be due to different operators)

$$\sigma_{\text{measurement error}}^2 = \sigma_{\text{gauge}}^2 = \sigma_{\text{repeatability}}^2 + \sigma_{\text{reproducibility}}^2$$

The above formula shows that the gauge variability is the sum of the variance due to the measurement instrument plus the variability due to the operator.

Gauge reproducibility is the variability that arises because of differences among the three operators

$$\bar{x}_{\text{max}} = \max(\bar{x}_1, \bar{x}_2, \bar{x}_3)$$

Average of operator values

$$\bar{x}_{\text{max}} = 19.995$$

$$\bar{x}_{\text{min}} = \min(\bar{x}_1, \bar{x}_2, \bar{x}_3)$$

$$\bar{x}_{\min} = 19.863$$

$$R_{\bar{x}} = \bar{x}_{\max} - \bar{x}_{\min}$$

$$\sigma_{\text{reproducibility}} = \frac{R_{\bar{x}}}{d2}$$

In this case a value of 1.693 is used for d because $R_{\bar{x}}$ is the range of a sample size of three. (three operators)

$$\text{In this case } \bar{x}_{\max} = 19.995 \quad \bar{x}_{\min} = 19.863 \quad R_{\bar{x}} = 0.132$$

$$\sigma_{\text{reproducibility}} = \frac{0.132}{1.693}$$

$$\sigma_{\text{reproducibility}} = 0.0779 \quad (sol_1)$$

Gauge repeatability is obtained from the average of the three average ranges. Since in this experiment one blade was measured twenty times by each of the three operators, it was required to obtain the moving range of each of the scans from this was calculated the average moving range.(Table 5.3)

Table 5. 3 Results of calculation of moving range for R and R study

Operator 1			Operator 2			Operator 3		
Scan	Angle	Moving Range	Scan	Angle	Moving Range	Scan	Angle	Moving Range
1 =	19.898		21 =	20.075	0.278	41 =	20.234	0.204
2 =	19.557	0.341	22 =	19.988	0.087	42 =	19.910	0.324
3 =	19.714	0.157	23 =	19.881	0.108	43 =	19.936	0.026
4 =	20.109	0.395	24 =	20.106	0.225	44 =	19.926	0.009
5 =	19.886	0.223	25 =	19.988	0.118	45 =	20.198	0.271
6 =	19.830	0.055	26 =	19.794	0.194	46 =	20.172	0.026
7 =	19.624	0.206	27 =	19.625	0.169	47 =	19.977	0.195
8 =	19.770	0.146	28 =	19.788	0.163	48 =	19.655	0.323
9 =	19.903	0.133	29 =	20.028	0.240	49 =	19.685	0.030
10 =	19.785	0.118	30 =	19.767	0.261	50 =	20.351	0.666
11 =	19.936	0.151	31 =	20.213	0.446	51 =	19.870	0.481
12 =	19.987	0.051	32 =	20.106	0.107	52 =	19.773	0.097
13 =	19.847	0.140	33 =	20.065	0.041	53 =	20.110	0.338
14 =	19.837	0.011	34 =	20.510	0.445	54 =	19.972	0.138
15 =	20.696	0.859	35 =	20.070	0.440	55 =	19.823	0.150
16 =	20.031	0.665	36 =	19.865	0.205	56 =	19.818	0.005
17 =	19.920	0.111	37 =	20.014	0.149	57 =	20.019	0.201
18 =	19.624	0.296	38 =	19.968	0.046	58 =	20.008	0.011
19 =	19.511	0.112	39 =	20.029	0.061	59 =	19.891	0.117
20 =	19.798	0.286	40 =	20.029	0.000	60 =	19.983	0.092
$\bar{x}_1 = 19.863$	$\overline{MR}_1 = 0.235$		$\bar{x}_2 = 19.995$	$\overline{MR}_2 = 0.199$		$\bar{x}_3 = 19.966$	$\overline{MR}_3 = 0.195$	

The calculation of gauge repeatability as obtained from the average of the three average ranges are

$$\bar{R} = \frac{1}{3}(\overline{MR}_1 + \overline{MR}_2 + \overline{MR}_3)$$

$$\bar{R} = \frac{1}{3}(0.235 + 0.199 + 0.195)$$

$$\bar{R} = 0.209$$

$$\sigma_{\text{repeatability}} = \frac{\bar{R}}{d_2}$$

$$\sigma_{\text{repeatability}} = \frac{0.209}{1.128} \quad (\text{note : } d = 1.128 \text{ for sample size of two})$$

$$\sigma_{\text{repeatability}} = 0.185 \quad (\text{sol}_2)$$

Both components of the measurement error are calculated (sol₁) and (sol₂) these are used to calculate $\hat{\sigma}_{\text{gauge}}$

$$\hat{\sigma}_{\text{gauge}}^2 = \hat{\sigma}_{\text{repeatability}}^2 + \hat{\sigma}_{\text{reproducibility}}^2$$

$$\hat{\sigma}_{\text{gauge}}^2 = 0.185^2 + 0.078^2$$

$$\hat{\sigma}_{\text{gauge}}^2 = \sqrt{0.04}$$

$$\hat{\sigma}_{\text{gauge}} = 0.2$$

$$\text{as } P/T = \frac{6\sigma_{\text{total}}}{\text{total tolerance}}$$

$$\text{Total Tolerance} = \frac{6\sigma_{\text{total}}}{P/T} = \frac{1.2}{0.1} = 12 \text{degrees} \quad (\text{sol}_3)$$

From the results of the R and R study (sol₃) a value of 12 degrees was calculated, this was the specification limit of the measurement instrument this indicates the blade may be measured with a tolerance band of 6 degrees. This tolerance band includes the variation in the measurement instrument and the human interface, as it was observed that some variation occurred between the three operators, it was felt that this variation may be caused by the setting up of the blade in the clamp (Figure 5.1). Since total variation was much larger than that incurred in machine evaluation study. To reduce this variation a new system of blade clamping was designed (Section 5.3 clamp modification design).

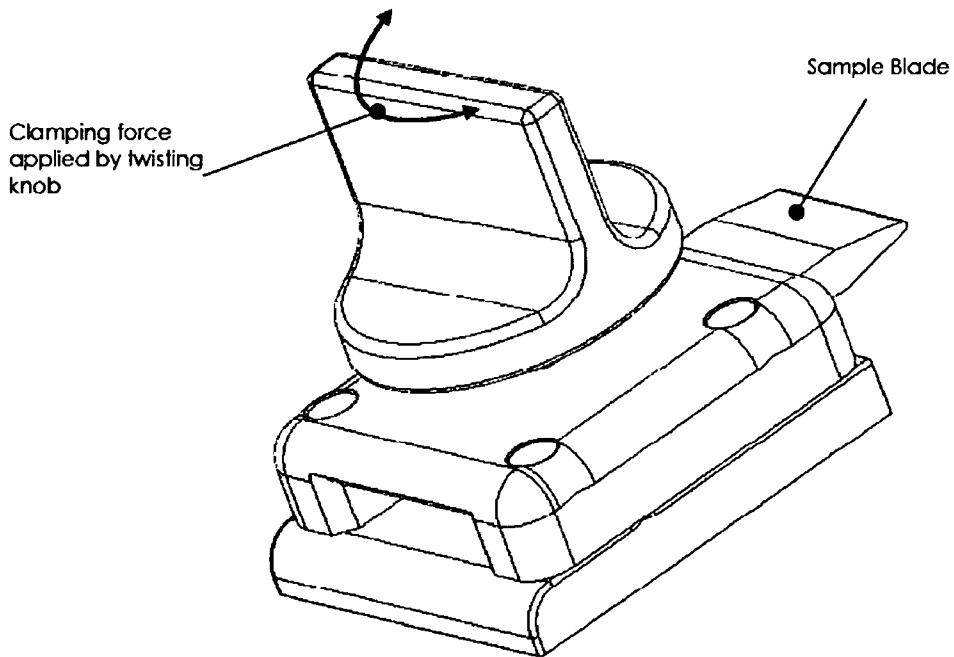


Figure 5.3 Original design for blade clamping unit

5.3 Clamp Modification Design

In order to accurately and consistently scan the blade a modified clamp was designed, this design uses a spring loaded pin to clamp the blade (Figure 5.4) This modification resulted from the repeatability and reproducibility study carried out. This repeatability and reproducibility study illustrated that some variation occurred between operators. To eliminate some of this variability, the human

factor was reduced. This was achieved by using a spring loaded clamp in place of the screw clamp. To insert the blade the spring loaded clamp is lifted, the blade is inserted and the plunger is released, this arrangement ensures that the same pressure is applied each time the blade is clamped.

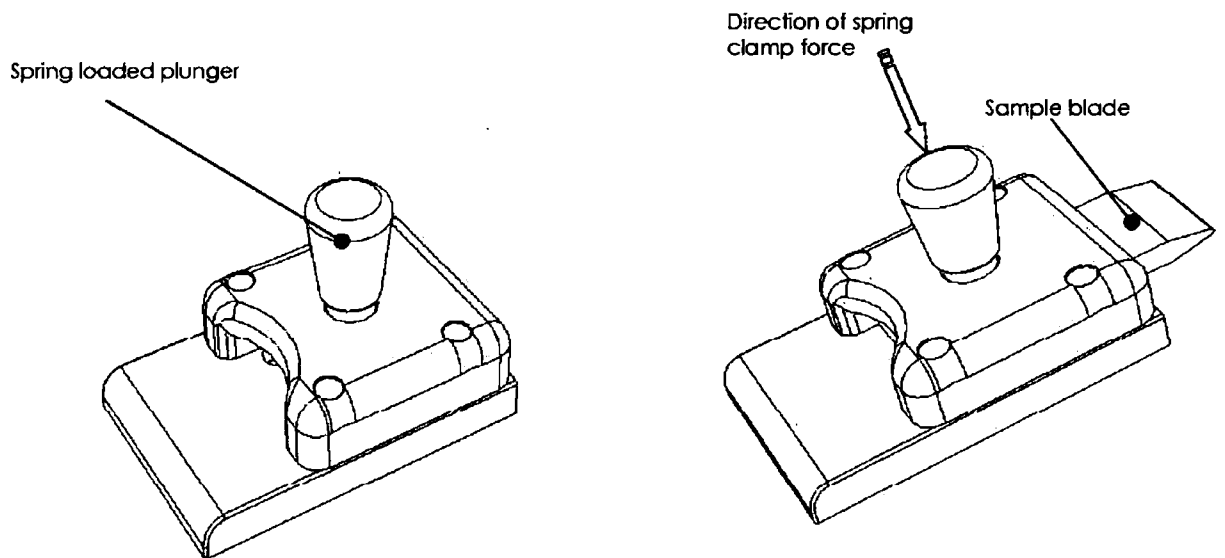


Figure 5.4 Modified blade holder

To test the operation of the modified blade clamp a second gauge R and R study was carried out, in this study the same three operators were used the same sample blade was used and the same scanning program was used Procedure 2 R and R study (Appendix B) A new set of results are presented in Table 5.4

Table 5.4 Summary of results for R and R study (2)

	Operator 1	Operator 2	Operator 3
	19.345 deg	19.135 deg	19.591 deg
	18.825 deg	19.418 deg	19.637 deg
	18.834 deg	19.427 deg	19.746 deg
	18.852 deg	19.309 deg	19.691 deg
	18.770 deg	19.344 deg	19.774 deg
	18.806 deg	18.852 deg	19.436 deg
	18.852 deg	19.336 deg	19.755 deg
	18.798 deg	19.035 deg	19.692 deg
	19.062 deg	19.545 deg	19.409 deg
	19.663 deg	19.171 deg	19.756 deg
	19.080 deg	19.272 deg	19.372 deg
	19.154 deg	19.299 deg	19.354 deg
	19.572 deg	19.454 deg	19.336 deg
	19.472 deg	19.254 deg	19.391 deg
	19.490 deg	19.327 deg	19.263 deg
	19.454 deg	19.208 deg	19.436 deg
	19.518 deg	19.226 deg	19.108 deg
	19.536 deg	19.710 deg	19.646 deg
	19.636 deg	19.611 deg	19.783 deg
	19.384 deg	19.783 deg	19.345 deg
Average	19.205 deg	19.336 deg	19.526 deg
Max	19.663 deg	19.783 deg	19.783 deg
Min	18.770 deg	18.852 deg	19.108 deg
Range	0.893 deg	0.931 deg	0.675 deg

Results for the gauge R and R study were recalculated using formula and procedures previously described.

$$\bar{x}_{\max} = \max(\bar{x}_1, \bar{x}_2, \bar{x}_3)$$

$$\bar{x}_{\max} = 19.526$$

$$\bar{x}_{\min} = \min(\bar{x}_1, \bar{x}_2, \bar{x}_3)$$

$$\bar{x}_{\min} = 19.205$$

$$R_{\bar{x}} = \bar{x}_{\max} - \bar{x}_{\min}$$

$$\sigma_{\text{reproducibility}} = \frac{R_{\bar{x}}}{d2}$$

In this case a value of 1.693 is used for d because $R_{\bar{x}}$ is the range of a sample size of three.

$$\text{In this case } \bar{x}_{\max} = 19.526 \quad \bar{x}_{\min} = 19.205 \quad R_{\bar{x}} = 0.321$$

$$\sigma_{\text{reproducibility}} = \frac{0.321}{1.693}$$

$$\sigma_{\text{reproducibility}} = 0.1896 \quad (\text{sol}_1)$$

The calculation of gauge repeatability as obtained from the average of the three average ranges are

$$\bar{R} = \frac{1}{3}(\overline{MR}_1 + \overline{MR}_2 + \overline{MR}_3)$$

$$\bar{R} = \frac{1}{3}(0.174 + 0.227 + 0.205)$$

$$\bar{R} = 0.202$$

$$\sigma_{\text{repeatability}} = \frac{\bar{R}}{d_2}$$

$$\sigma_{\text{repeatability}} = \frac{0.202}{1.128} \quad (\text{note : } d = 1.128 \text{ for sample size of two})$$

$$\sigma_{\text{repeatability}} = 0.179 \quad (\text{sol}_2)$$

Both components of the measurement error are calculated (sol₁) and (sol₂) these are used to calculate $\hat{\sigma}_{\text{gauge}}$

$$\hat{\sigma}_{\text{gauge}}^2 = \hat{\sigma}_{\text{repeatability}}^2 + \hat{\sigma}_{\text{reproducibility}}^2$$

$$\hat{\sigma}_{\text{gauge}}^2 = 0.179^2 + 0.1896^2$$

$$\hat{\sigma}_{\text{gauge}}^2 = \sqrt{0.04}$$

$$\hat{\sigma}_{\text{gauge}} = 0.26$$

$$\text{as } P/T = \frac{6\sigma_{\text{total}}}{\text{total tolerance}}$$

$$\text{Total Tolerance} = \frac{6\sigma_{\text{total}}}{P/T} = \frac{1.56}{0.1} = 15.6 \text{ degrees} \quad (\text{sol}_3)$$

From the results of the second gauge R and R study the repeatability value decreased from 0.185 to 0.179 however the reproducibility increased from 0.0779 to 0.1896. This indicates that the operators still have an influence on the scanning operation. The total deviation therefore increased from 12 degrees to 15.6 degrees. This suggests that the clamp modification is not the only factor affecting measured results.

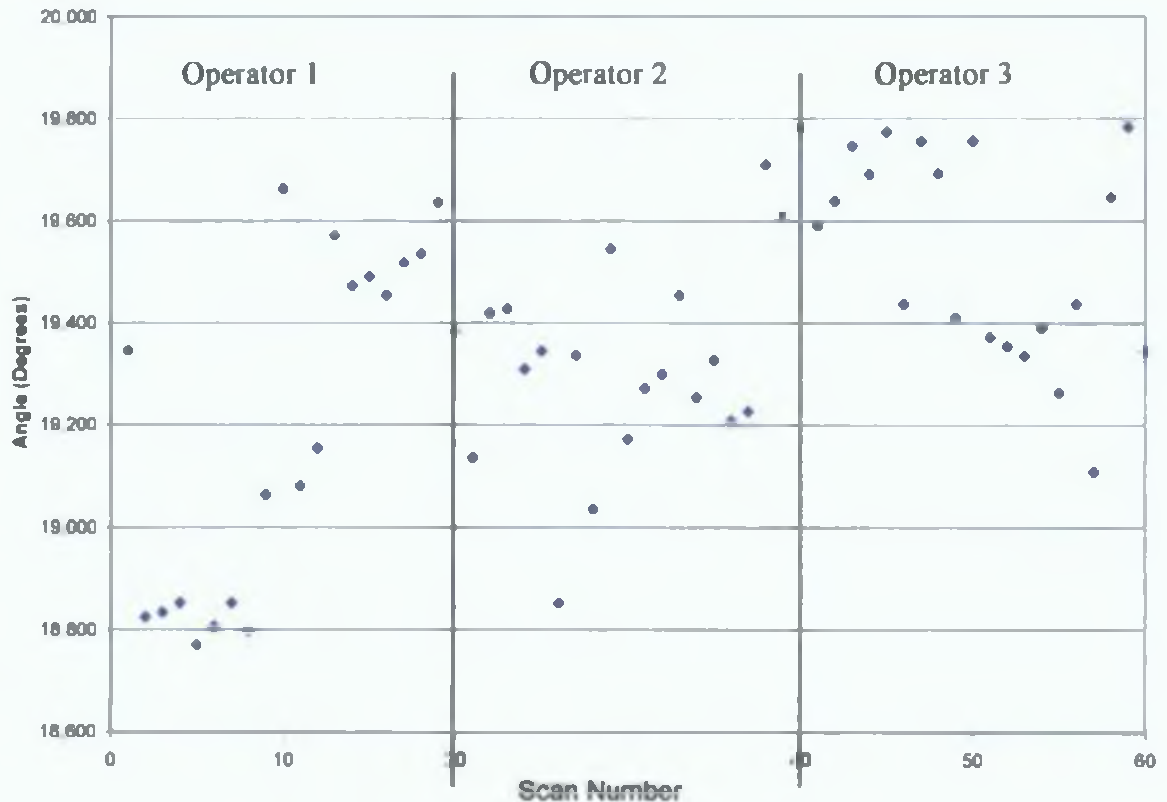


Figure 5.5 Reproducibility and Repeatability study

Table 5.5 shows the variation in the three operators it illustrated that a pattern has developed, operator 1 returned values with a wide scatter, operator 2 returned values concentrated at the mid to low end while operator 3 returned values at the high end. From these results it was decided to analyse the scanning program (Section 5.4 program modification)

5.4 Program Modification Design

The scanning program used in the gauge R and R studies collects 50 X 2 data points, however the calculation of the wedge angle only considers four data points to perform its calculation. (Figure 5.5)

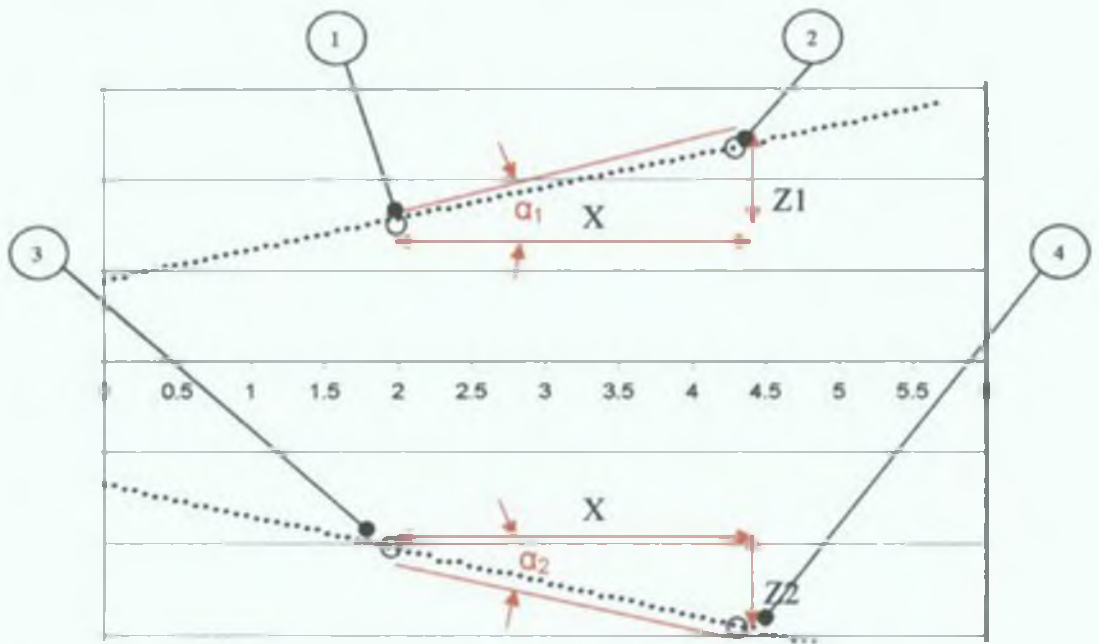


Figure 5.6 Original calculation of wedge angle of blade

It was concluded that this type of calculation method could introduce errors if all measured data points were not considered each time (Figure 5.6).

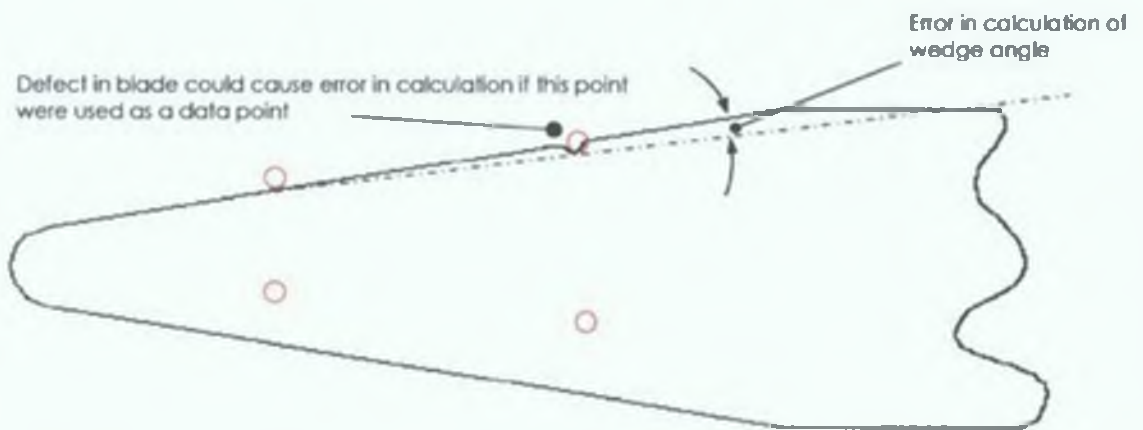


Figure 5.7 Effect of using just four data points to calculate the wedge angle of blade

To overcome this problem a linear regression formula is used, this method calculates the best fit straight line for a set of data points (Figure 5.7).

$$m = \frac{n \sum XZ - \sum X \sum Z}{n \sum X^2 - (\sum x)^2}$$

$$c = \bar{Z} - m\bar{X}$$

Where

m = Slope coefficient

c = Intercept value

n = Number of data points

x = Horizontal axis values in this case the horizontal travel of the slide

\bar{X} = Average of X values

Z = vertical readings from the lasers

\bar{Z} = Average of Z readings

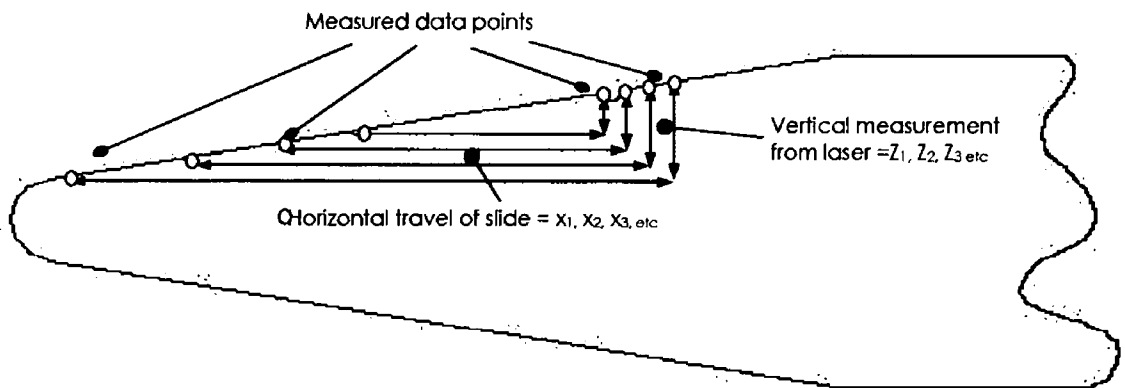


Figure 5.8 Schematic of point parameters for regression calculation.

To test the effectiveness of the regression formula a second instrument evaluation study was carried out, this study consisted of twenty scans, the results of the scans are shown in Figure 5.8 a moving average line is displayed to show the variation of the measured values.

Instrument Evaluation Study (Without regression formula)

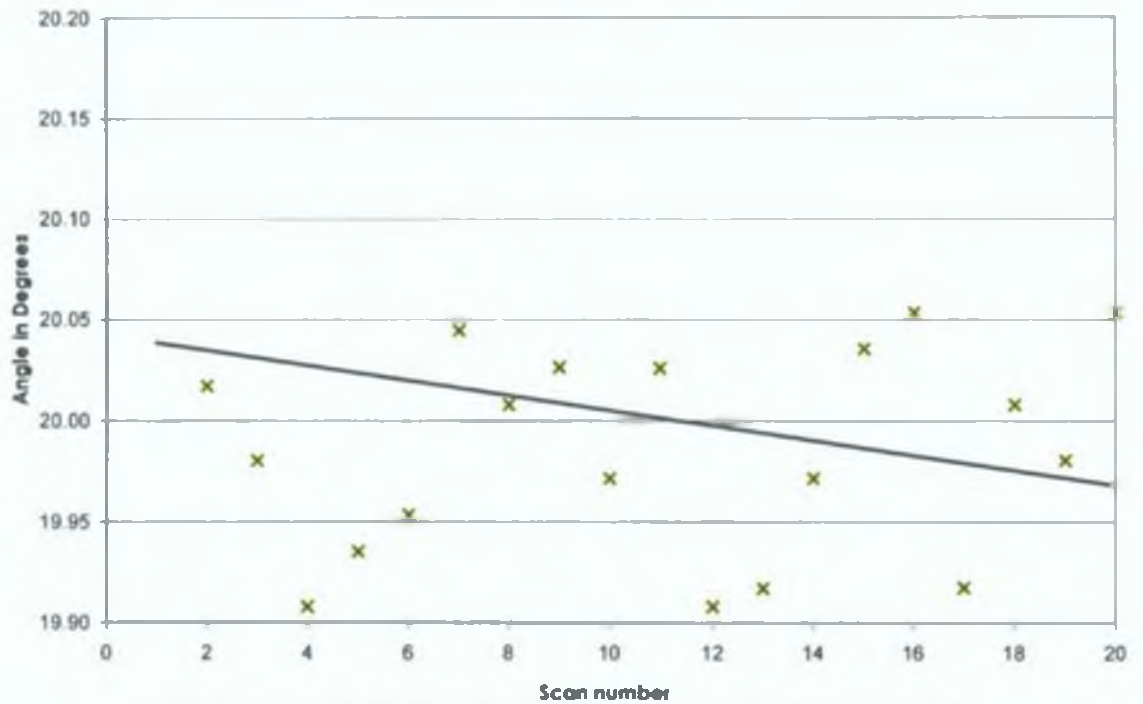


Figure 5.9 Instrument evaluation study without regression formula

The same scans were calculated using the regression formula, the results are shown Figure 5.9 it was observed that the spread of the measured angles was reduced when using the regression formula.

Instrument Evaluation Study (using regression formula)

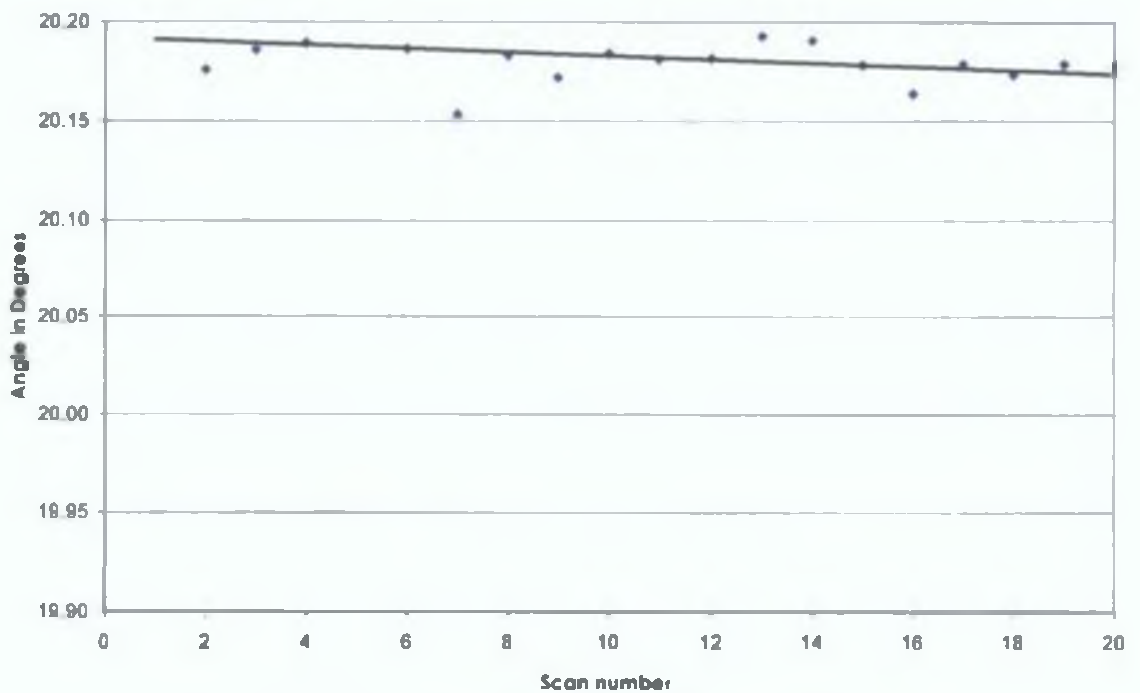


Figure 5.10 Instrument evaluation study with regression formula

Both set of results are shown Figure 5.10 this clearly illustrates the differences in the results of both methods of calculation of the wedge angle, the first difference is the spread of the values which is greatly reduced from a range of 0.441 degrees for the results without the regression formula to a range of 0.06 degrees for the results using the regression formula. Also illustrated is the difference in average measured value the average for the measured angle without the regression formula is 20.003 degrees while the average for the measured angle using the regression formula is 20.18 degrees. As shown in the results section (Table 5.5) the value 20.18 degrees as measured using the regression formula compares favourably with the other methods of profile measurement.

Instrument Evaluation Study (comparison of formula)

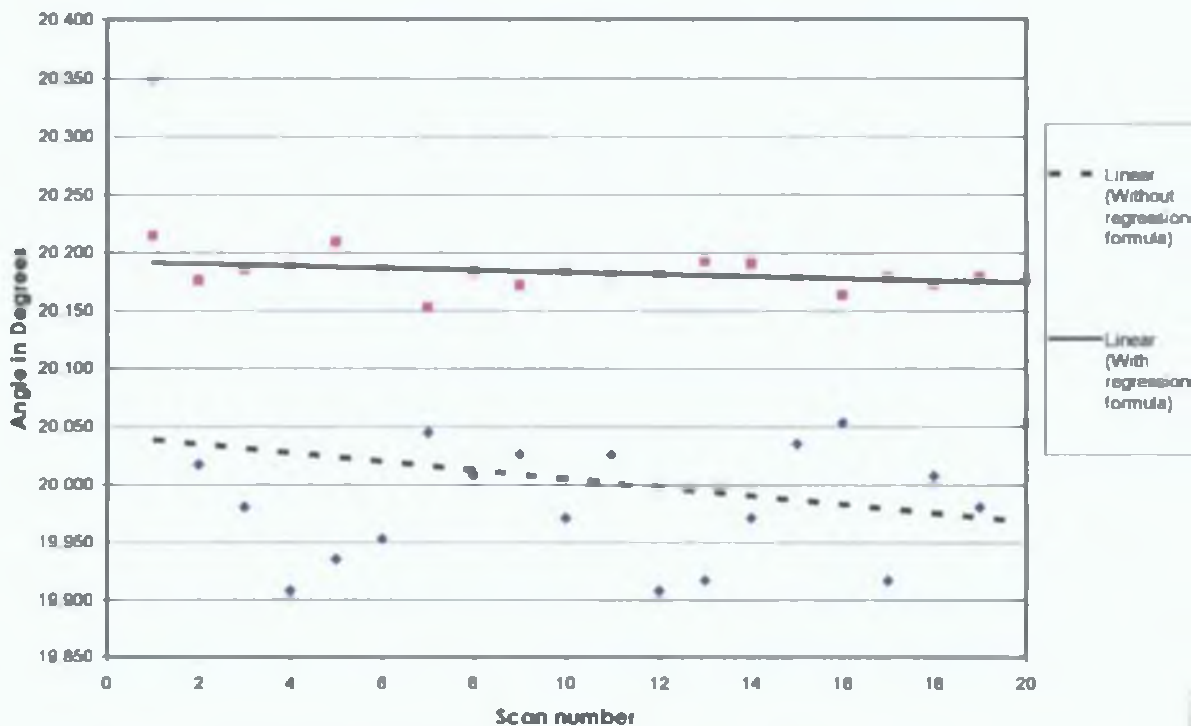


Figure 5.11 Comparison of results using regression formula V's without regression formula

5.5 Results single side scans

In this section the results are outlined. As described in the materials and methods section each component of the measurement device was tested at each stage of development.

Each laser was tested individually to determine the resolution of the scan. To achieve this, first laser number one (top laser) was used, the laser was calibrated to set the zero and span (as described in Section 4). The number of data scan points used was 50 per scan. First results from the lasers gave a single side of the blade profile, (Figure 5.11), (Figure.5.12) and (Figure.5.13).

It may be seen that surface roughness appears on the wedge angle of the blade, this is due to the graphics of the Labview software, higher resolution scans are obtained by using Microsoft Excel graphs. The three sample blades used in the tests were, 500 μm , 300 μm and 100 μm tip radius respectively with an included wedge angle of 20 degrees the results are presented in Figures 5.11 to 5.13. It may be seen that the data generated on the tip radius of the blade is adequate for display of tip geometry.

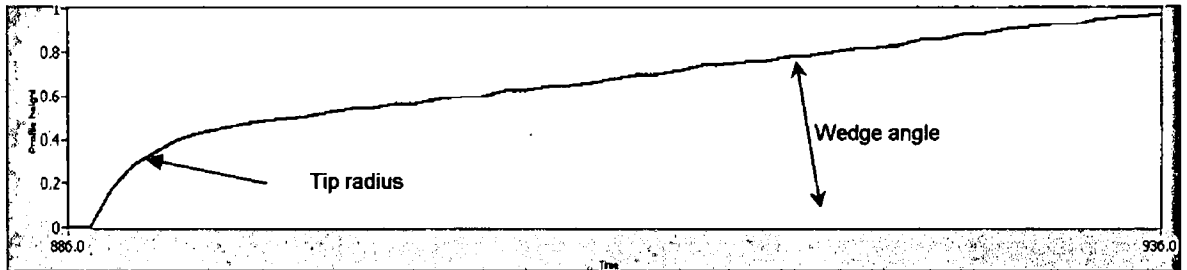


Figure 5.12 Single side of blade, tip radius 500 μm

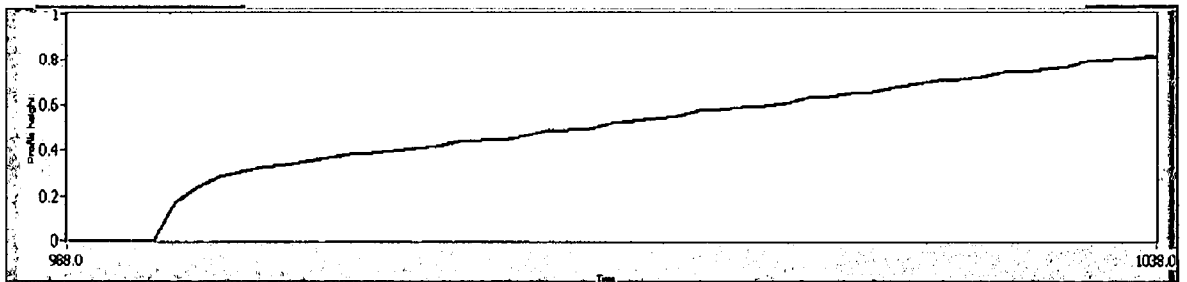


Figure 5.13 Single side of blade, tip radius 300 μm

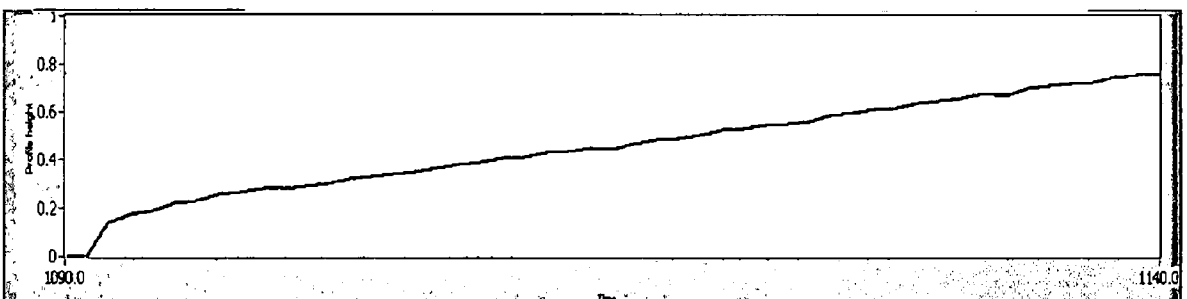


Figure 5.14 Single side of blade, tip radius 100 μm

5.6 Results double side scans

In these scans both lasers Z_1 and Z_2 were used, the lasers were calibrated and aligned previous to the scans as outlined in Chapter 4.

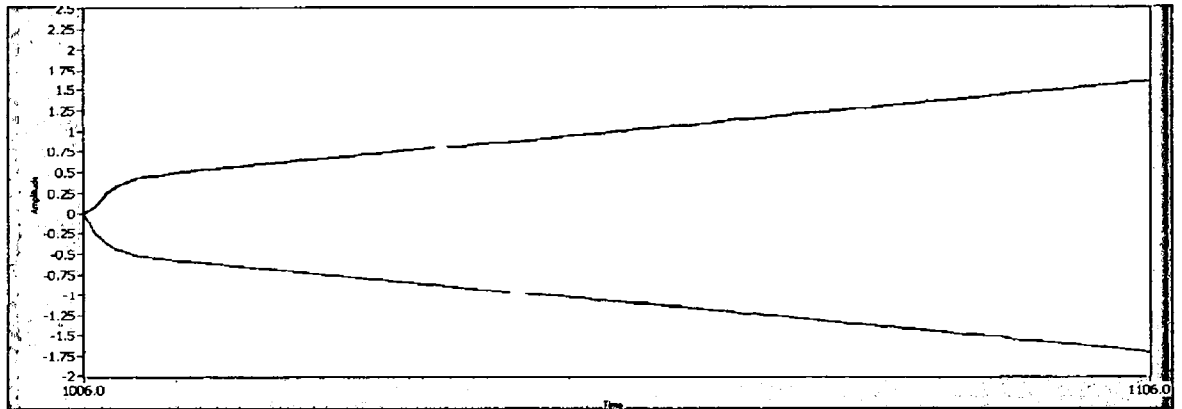


Figure 5.15 Double scan of sample blade radius 500µm.

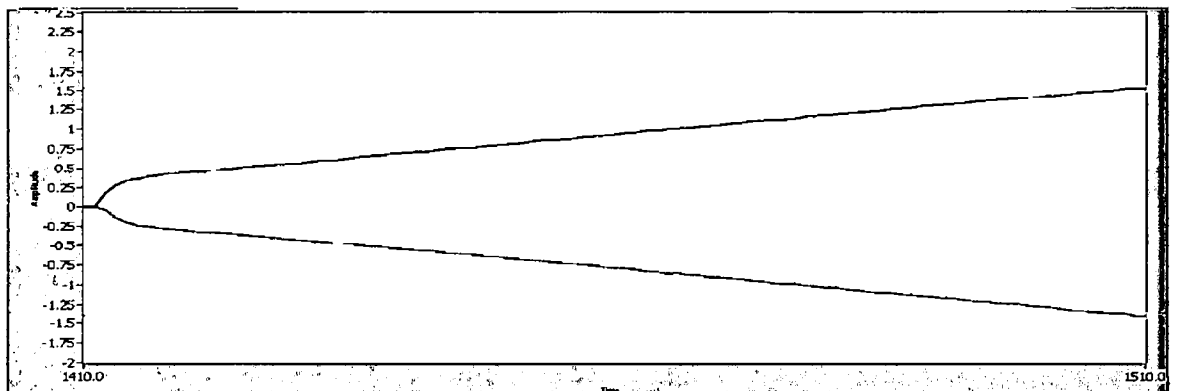


Figure 5.16 Double scan of sample blade radius 300µm.

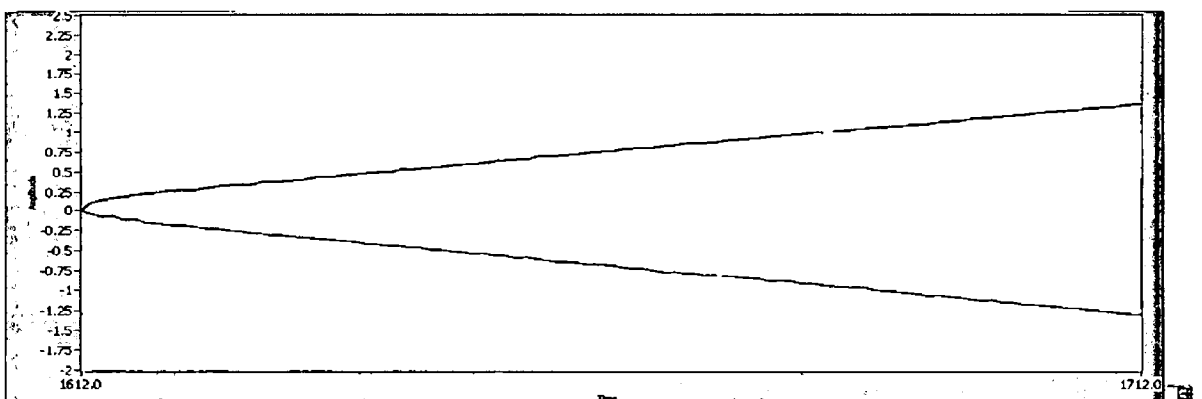


Figure 5.17 Double scan of sample blade radius 100µm.

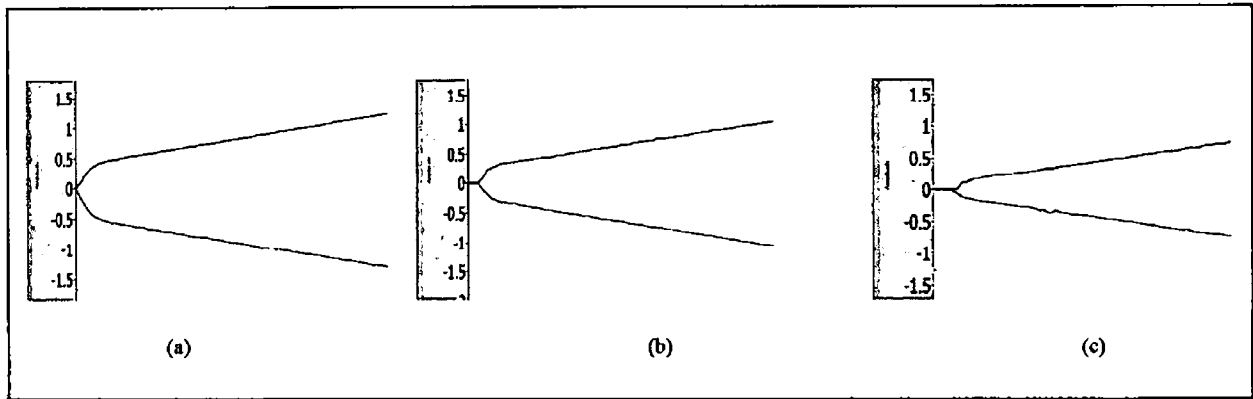


Figure 5.18 Results of scans on sample blades (a) 500µm radius blade (b) 300µm radius blade (c) 100µm radius blade

It may be seen that details on both the wedge angle and the tip radius are obtained from these scans (Figure 5.17). In order to analyze the results of the scans Excel software was used as described in Chapter 4.

5.7 Verification of Results

To gauge the effectiveness of the measurement instrument a comparison study was carried out between the measurement instrument and standard profile measuring equipment. The gauge R and R study carried out previously verifies the precision of the instrument (Section 5.2). The following tests were designed to test the accuracy of the measurement instrument. The standard measurement instrument used was a *Nikon Eclipse Metallurgical Microscope (ME600)* using a *JVC TK-C1381* video camera, the data analysis was carried out using *Omnimet Enterprise Software version 4.50 B021*

To ensure that no bias occurred the standard measurements were carried out independent of the author, the operator carrying out the verification measurements was not made aware of the results from the prototype measurement instrument, until all measurements were made.

Table 5.5 Verification of Results for prototype measurement Instrument

Blade wedge Angle (Nominal)	Prototype (MediScan)	Standard Measurement (Nikon ME600)	Deviation (Degrees)
20 Degrees	20.18 Degrees	20.47 Degrees	0.29 Degrees

From the results in Table 5.5 it may be seen that a good agreement exists between the wedge angle obtained from the prototype measurement instrument and the standard measurement device, some deviation will occur due to errors in the measurement instrument and due to the setting up of the blade in both the measurement devices, it is concluded that this deviation in measurement of the wedge angle is small. In studies carried out by (Duffy, 2003) it is shown that small differences of the magnitude of those recorded in wedge angle do not adversely affect the cutting performance of a blade when cutting solid rigid polyurethane foam.

5.8 Measurement of osteotome

During the testing and evaluation of the prototype measurement instrument sample blades were used to ensure consistency of comparisons. To ensure that the measurement instrument was capable of measurement of an osteotome scans were performed on a new osteotome. The blade used was a Bolton Surgical 12mm osteotome (Ref No 14/1453/4). The osteotome was set up in the measurement instrument as shown Figure 5.18



Figure 5.19 12mm osteotome set up for scanning

Figure 5.20 Results of scan on 12mm osteotome

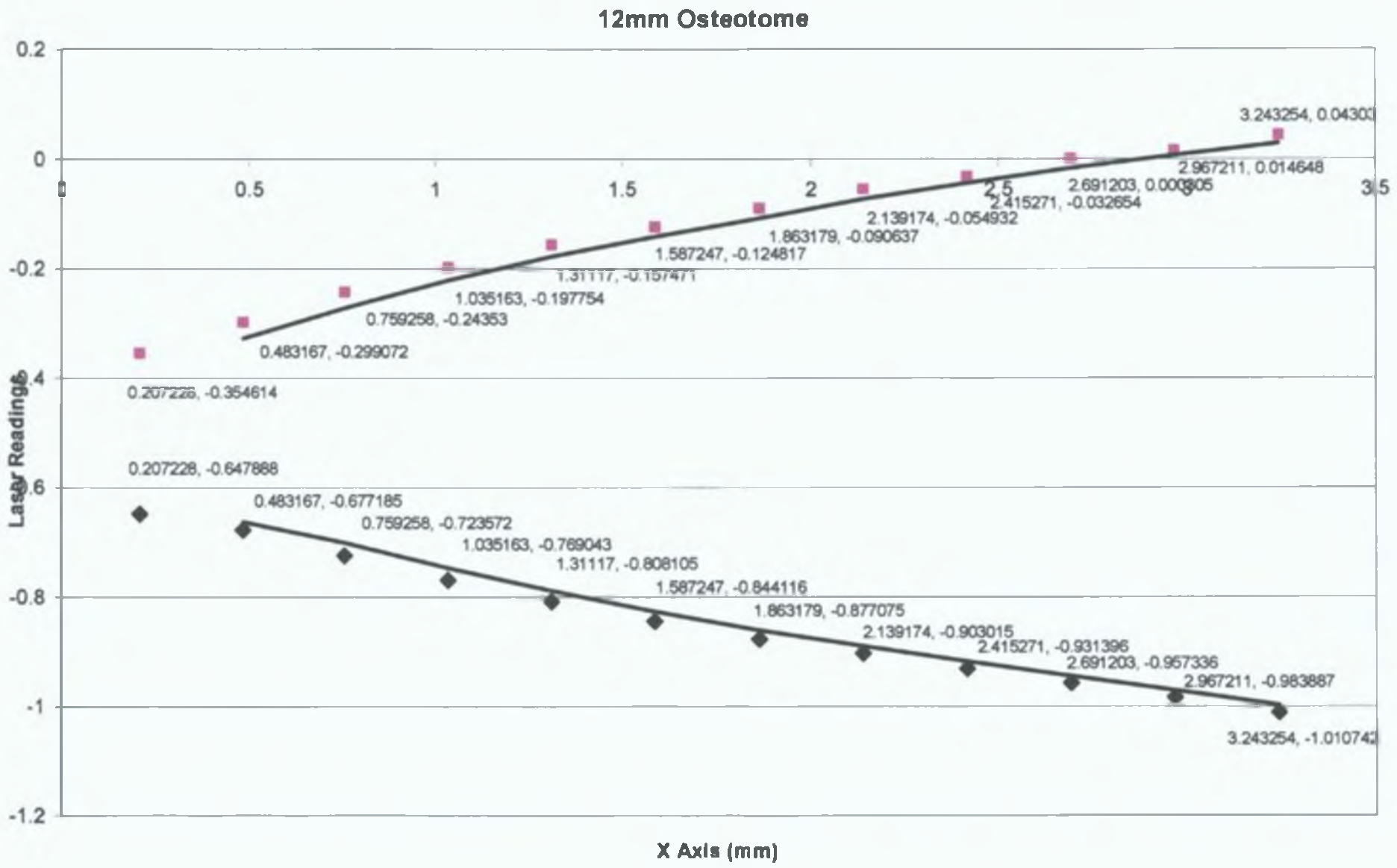


Figure 5.19 shows the result of the scan on the 12mm osteotome, this image is generated from Microsoft Excel and shows that the measurement instrument can also give the profile of an osteotome as well as its wedge angle osteotome is a curved profile rather than a simple wedge angle.

Chapter 6.0 Conclusions

6.1 Main conclusions and proposals for further work

In this thesis the author has investigated the various methods of profile measurement,

- From the literature review (Chapter 2) it is possible to conclude that no system exists for measurement of blade sharpness that provides the potential for relating the blade profile to a range of cutting materials. The system device prototyped by the author may be used in conjunction with appropriate cutting force curves for any material to provide a measurement of blade sharpness as shown by the data currently available from the larger project group (Chapter 4).
- The increment chosen for interval point measurement affects the resolution of the data on curved surfaces. Where the curved surface is small such as the radii on the blade cutting edge, this may likely lead to measurement error due to inadequate data on the profile. This can be controlled by variation in the interval step increment. The author proposes that in future work control of the step increment for the commencement of the scan be done on the basis of slope of the surface curvature or by definition of a small step increment in the first part of the scan in the region of the edge radius.
- From analysis of the operation of the device it is concluded that a variety of factors affect the ability of the device to measure the blade wedge angle in a reproducible and repeatable manner. These include the interaction of the operator with the device and the functionality of the device in terms of its scanning process and the evaluation of results.
- The author concluded from the preliminary testing and Gauge R & R tests that the device measurements are affected by the laser orientation, retention of the blade during scanning and the methodology for evaluation of the blade wedge angle. Modifications to these resulted in some minor improvements to the results recorded in Chapter 5.
- The author further concludes that other factors not considered for modifications such as device vibration, settling time for the device after

blade clamping, and consistent location and positioning as distinct to clamping of the blade may likely also affect results. The author proposes that these issues should be considered for evaluation in future work related to the device.

- The piggy back arrangement of the positioning slides permits positioning of the blade for scanning, or for scanning of a blade in a series of positions. The author proposes that in future work, consideration could be given to using this functionality for the development of a 3D geometry of the blade surface for detailed blade geometry evaluation.
- Scanning of the surgical osteotome shows that the device is capable of the evaluation of ground curved flanks known to exist on new osteotomes as supplied by the manufacturer. On resharpening it is common for the operator to grind these flanks as surfaces creating the wedge angle discussed, and the device is capable of accommodating both blade flanks.

References

References

- Akura, J., Funakoshi, T., Kadonosono, K., Saito, M., (2001). Differences in incision shape based on the keratome bevel. *Journal Of Cataract And Refractive Surgery* 27, 761-765.
- Al-Saidi, I. A., (2001). Using a simple method: conversion of a Gaussian laser beam into a uniform beam. *Optics & Laser Technology* 33, 75-79.
- Ampere A.Tseng, (2002). Laser-based internal profile measurement system, *Automation in Construction* 11, 667-679.
- Andersson, C., Andersson, M. T., Stahl, J.-E., (2001). Bandsawing. Part I: cutting force model including effects of positional errors, tool dynamics and wear. *International Journal of Machine Tools and Manufacture* 41, 227-236.
- Andersson, C., Stahl, J.-E., Hellbergh, H., (2001). Bandsawing. Part II: detecting positional errors, tool dynamics and wear by cutting force measurement. *International Journal of Machine Tools and Manufacture* 41, 237-253.
- Andersson, C., (2001). Bandsawing. Part III: stress analysis of saw tooth microgeometry. *International Journal of Machine Tools and Manufacture* 41, 255-263.
- Arcona, C., Dow, T., (1996). The role of knife sharpness in the slitting of plastic films. *Journal of Materials Science* 31, 1327-1334.
- Asai Shoichi, Taguchi Yoshio, Kasai Toshio, Kobayashi Akira, (1990). Measurement on cutting edge radius of single-point diamond tools ith newly developed SEM. *Science and Technology of New Diamond* 389-393.

Astakhov, (1998). A system concept in metal cutting. Journal of materials processing technology 79, 189-199.

Astakhov, V. P., Shvets, S. V., (1998). A system concept in metal cutting. Journal of materials processing technology 79, 189-199.

Balevi, B., (1996). Engineering specifics of the periodontal curet's cutting edge. Journal Of Periodontology 67, 374-378.

Breitmeier U., (1997). Lasercomp: A surface measurement system for forensic applications. Forensic Science International 89, 1-13.

Brodmann, R., Warrender, T., Weber, M., (2002). Application and limits of optical metrology by the confocal multi-pinhole-technique.

Budinski K.G., (1997). Needs and applications in precision measurement and monitoring of wear. journal of testing and evaluation 25, 226-232.

Cawley, J., (2003). Investigation of the effect of cutting edge radius on indentation cutting of solid rigid polyurethane foam. B.Eng. Thesis, Institute of Technology Sligo.

Chang, M., Lin, K. H., (1998). Non-contact scanning measurement utilizing a space mapping method. Optics and Lasers in Engineering 30, 503-512.

Chial Vanessa B., Greenish Stephanie, Okamura Alison M., (2002). On the display of haptic recording for cutting biological tissues. 10th International Symposium on Haptic Interfaces for Virtual Environment and Teleoperator Systems 1, 80-87.

Cho, M. W., Seo, T. i., Kwon, H. D., (2003). Integrated error compensation method using OMM system for profile milling operation. *Journal of materials processing technology* 136, 88-99.

Contet, P., Ville, J.-F., (1995). Surfscan 3D -- An industrial 3D surface texture characterisation instrument. *International Journal of Machine Tools and Manufacture* 35, 151-156.

Cutlery & Allied Trades Research Association, (2003). Personal communication.

Dawei, T. U., (1995). In-process sensor for surface profile measurement applying a common-mode rejection technique. *Optics & Laser Technology* 27, 351-353.

Drescher, J., (1993). Scanning electron microscopic technique for imaging a diamond tool edge. *Precision Engineering* 15, 112-114.

Drescher, J., (1993). Scanning electron microscopic technique for imaging a diamond tool edge. *Precision Engineering* 15, 112-114.

Duffy, S., (2003). Investigation of the effect of wedge angle on indentation cutting of solid rigid polyurethane foam. B.Eng. Thesis, Institute of Technology Sligo.

Endres William J., Kountanya Raja K., (2002). The effects of corner radius and edge radius on tool flank wear. *Journal of manufacturing processes* 4, 89-96.

Fallbohmer, P., Rodriguez, C. A., Ozel, T., Altan, T., (2000). High-speed machining of cast iron and alloy steels for die and mold manufacturing. *Journal of materials processing technology* 98, 104-115.

Fan, K. C., (1997). A non-contact automatic measurement for free-form surface profiles. *Computer Integrated Manufacturing Systems* 10, 277-285.

Fung, E. H. K., Yang, S. M., (2001). An approach to on-machine motion error measurement of a linear slide. *Measurement* 29, 51-62.

Giraud, J. Y., Villemin, S., Darmana, R., Cahuzac, J. P., Autefage, A., Morucci, J. P., (1991). Bone cutting. *Clinical Physics And Physiological Measurement: An Official Journal Of The Hospital Physicists' Association, Deutsche Gesellschaft Fur Medizinische Physik And The European Federation Of Organisations For Medical Physics* 12, 1-19.

Graff, E., Apparatus and method for non-contact measurement of the edge sharpness of a knife US Patent No 5196800, (1993).

Hall, R. M., (1965). The effect of high-speed bone cutting without the use of water water coolant. *Oral Surgery, Oral Medicine, And Oral Pathology* 20, 150-153.

Han, X. S., Lin, B., Yu, S. Y., Wang, S. X., (2002). Investigation of tool geometry in nanometric cutting by molecular dynamics simulation. *Journal of materials processing technology* 129, 105-108.

Hill, R., (1953). On the mechanics of cutting metal strips with knife-edged tools. *Journal of the Mechanics and Physics of Solids* 1, 265-270.

Huebscher, H. J., Goder, G. J., Lommatzsch, P. K., (1989). The sharpness of incision instruments in corneal tissue. *Ophthalmic Surgery* 20, 120-123.

Izmailov, G. A., Orenburov, P. I., Repin, V. A., Gorbunov, S. M., Izmailov, S. G., (1989). Evaluation of the healing of skin wounds inflicted by steel scalpels with various degrees of sharpness. *Khirurgiia* 6, 75-78.

Jacob, C. H., Berry, J. T., (1976). A study of the bone machining process--drilling. *Journal of Biomechanics* 9, 343-349.

Jacobs, C. H., Pope, M. H., Berry, J. T., Hoaglund, F., (1974). A study of the bone machining process-orthogonal cutting. *Journal of Biomechanics* 7, 131-136.

Jacobs, C. H., (1977). Fundamental investigations of the bone cutting process [proceedings. *Bulletin Of The Hospital For Joint Diseases* 38, 4.

Jiubin, T., Jie, Z., (2003). A small probe with a gradient index lens for confocal measurement. *Sensors and Actuators* 104, 121-126.

Johansson, T., Kleiner, M., (2000). Prediction of the scattering properties of surfaces by laser scanning of height profile. *Applied Acoustics* 60, 205-223.

Kaldor S., Venuvinod P.K., (1997). Macro-level optimization of cutting tool geometry. *Journal of manufacturing science and engineering* 119, 1-9.

Kataoka Hiroyuki, Washio Toshikatsu, Chinzei Kiyoyuki, Mizuhara Kazuyuki, Simone Chistina, Okamura Allison M., (2002). Measurement of the tip and friction force acting on a needle during penetration, Fifth International Conference on Medical Image Computing and Computer Assisted Intervention (MICCAI), Tokyo, Japan.

Kattan, I. A., Currie, K. R., (1996). Developing new trends of cutting tool geometry. *Journal of materials processing technology* 61, 231-237.

Kaulbach, H. C., Towler, M. A., McClelland, W. A., Povinelli, K. M., Becker, D. G., Cantrell, R. W., Edlich, R. F., (1990). A beveled, conventional cutting edge surgical needle: a new innovation in wound closure. *Journal of Emergency Medicine* 8, 253-263.

King, M. J., (1999). Slicing frozen meat with an oscillating knife. *Meat Science* 51, 261-269.

King, M. J., (1999). Knife and impact cutting of lamb bone. *Meat Science* 52, 29-38.

Komanduri, R., Chandrasekaran, N., Raff, L. M., (1998). Effect of tool geometry in nanometric cutting: a molecular dynamics simulation approach. *Wear* 219, 84-97.

Kountanya Raja J., Endres William J., (2001). A high-magnification experimental study of orthogonal cutting with edge-honed tools. 2001 ASME International Mechanical Engineering Congress and Exposition, New York.

Krause, W. R., (1987). Orthogonal bone cutting: saw design and operating characteristics. *Journal Of Biomechanical Engineering* 109, 263-271.

Kwok, S. K., Lee, W. B., (1995). The development of a machine vision system for adaptive bending of sheet metals. *Journal of materials processing technology* 48, 43-49.

Lawn Brian, Wilshaw Rodney, (1975). Review Indentation fracture: principles and applications. *Journal of Materials Science* 10, 1049-1081.

Le Bosse, J. C., Hansali, G., Lopez, J., Mathia, T., (1997). Characterisation of surface roughness by laser light scattering: Specularly scattered intensity measurement. *Wear* 209, 328-337.

Le Bosse, J. C., Hansali, G., Lopez, J., Dumas, J. C., (1999). Characterisation of surface roughness by laser light scattering: diffusely scattered intensity measurement. *Wear* 224, 236-244.

Li, B., Jiang Zhuangde, Luo Yiping, (2003). Measurement of three-dimensional profiles with multi structure linear lighting. *Robotics and integrated manufacturing* 19, 493-499.

Li, M., (2000). Micromechanisms of deformation and fracture in shearing aluminum alloy sheet. *International Journal of Mechanical Sciences* 42, 907-923.

Li, X. P., Rahman, M., Liu, K., Neo, K. S., Chan, C. C., (2003). Nano-precision measurement of diamond tool edge radius for wafer fabrication. *Journal of materials processing technology* 140, 358-362.

Liu, H., Su, W. H., Reichard, K., Yin, S., (2003). Calibration-based phase-shifting projected fringe profilometry for accurate absolute 3D surface profile measurement. *Optics Communications* 216, 65-80.

Lotze, W., (1996). ScanMax -- a novel 3D coordinate measuring machine for the shopfloor environment. *Measurement* 18, 17-25.

Lotze, W., (1996). ScanMax -- a novel 3D coordinate measuring machine for the shopfloor environment. *Measurement* 18, 17-25.

Lu, S., Gao, Y., Xie, T., Xie, F., Jiang, X. Q., Li, Z., Wang, F., (2001). A novel contact/non-contact hybrid measurement system for surface topography characterization. *International Journal of Machine Tools and Manufacture* 41, 2001-2009.

Maeda, Y., Uchida, H., Yamamoto, A., (1989). Measurement of the geometric features of a cutting tool edge with the aid of a digital image processing technique. *Precision Engineering* 11, 165-171.

Maeda, Y., Uchida, H., Yamamoto, A., (1989). Measurement of the geometric features of a cutting tool edge with the aid of a digital image processing technique. *Precision Engineering* 11, 165-171.

Mahvash Mohsen, H. V., (2001). Haptic rendering of cutting: A fracture mechanics approach. *Haptics_e 2*, 1-12.

Matzelle, T. R., Gnaegi, H., Ricker, A., Reichelt, R., (2003). Characterization of the cutting edge of glass and diamond knives for ultramicrotomy by scanning force microscopy using cantilevers with a defined tip geometry. Part II. *Journal Of Microscopy* 209, 113-117.

McGorry, R. W., Dowd, P. C., Dempsey, P. G., (2004). The effect of blade finish and blade edge angle on forces used in meat cutting operations. *Applied Ergonomics* 36, 71-77.

Meehan R.R., Burns S.J., (1998). Mechanics of slitting and cutting webs. *Experimental Mechanics* 38, 102-109.

Merchant M.E., (1944). Basic mechanics of the metal-cutting process. *Journal of Applied Mechanics* 11, A168-A175.

Merchant M.E., (1945). Mechanics of the metal cutting process.I. Orthogonal cutting and a type 2 chip. *Journal of applied physics* 16, 267-275.

Merchant M.E., (1945). Mechanics of the metal cutting process.II. Plasticity conditions in orthogonal cutting. *Journal of applied physics* 16, 318-324.

Mower, T. M., Argon, A. S., (1995). Experimental investigations of crack trapping in brittle heterogeneous solids. *Mechanics of Materials* 19, 343-364.

Muller, C., Rahn, B. A., Pfister, U., Weller, S., (1993). Extent of bluntness and damage to reamers from hospitals. *Injury* 24, S31-S35.

Novak Erik, Pasop Freek, Browne Trisha, (2003). Production metrology for MEMS characterization. Veeco literature.

O'Callaghan, P. T., Jones, M. D., James, D. S., Leadbeatter, S., Evans, S. L., Nokes, L. D., (2001). A biomechanical reconstruction of a wound caused by a glass shard--a case report. *Forensic Science International* 117, 221-231.

Oxley P.L.B., (1989). *The Mechanics of Machining: An Analytical Approach to Assessing Machinability*. Ellis Horwood Limited.

Ozel, T., Nadgir, A., (2002). Prediction of flank wear by using back propagation neural network modeling when cutting hardened H-13 steel with chamfered and honed CBN tools. *International Journal of Machine Tools and Manufacture* 42, 287-297.

Ozel, T., (2003). Modeling of hard part machining: effect of insert edge preparation in CBN cutting tools. *Journal of materials processing technology* 141, 284-293.

Pasquini, R., Clark, S. M., Baradaran, S., Adams, D. F., (1995). Periodontal files--a comparative study. *Journal Of Periodontology* 66, 1040-1046.

Ramamoorthy, B., Radhakrishnan, V., (1992). Computer-aided inspection of cutting tool geometry. *Precision Engineering* 14, 28-34.

Reilly, G. A., McCormack, B. A. O., Taylor, D., (2004). Cutting sharpness measurement: a critical review. *Journal of materials processing technology* 153-154, 261-267.

Robert Hobbs, (2005). Amputation saw 1600 Web search (2004) <http://antiquescientifica.com/articles%205.htm>.

Rossi, R., Smukler, H., (1995). A scanning electron microscope study comparing the effectiveness of different types of sharpening stones and curets. *Journal Of Periodontology* 66, 956-961.

Sajan, M. R., Tay, C. J., Shang, H. M., Asundi, A., (1998). TDI imaging--a tool for profilometry and automated visual inspection. *Optics and Lasers in Engineering* 29, 403-411.

Schimit Jonna, Krell Michael, Novak Erik, (2003). Calibration of high-speed optical profiler. Veeco literature.

Schimmel Roy J., Manjunathaiah Jairam, Endres William J., (2000). Edge radius variability and force measurement considerations. *Journal of engineering science and engineering* 122, 590-593.

Schimmel Roy J., Endres William J. Stevenson Robin, (2002). Application of internally consistent material model to determine the effect of tool edge geometry in orthogonal machining. *Journal of manufacturing science and engineering* 124, 536-543.

Shetty Devas, (1982). Laser evaluation of cutting angle and surface finish in scalpel blades. *Journal of Testing and Evaluation* 10, 25-27.

Sikdar, C., Paul, S., Chattopadhyay, A. B., (1992). Effect of variation in edge geometry on wear and life of coated carbide face milling inserts. *Wear* 157, 111-126.

Smith, G. E., Clark, N. P., (1989). Evaluation of hand instruments used in operative dentistry: hardness and sharpness. *Operative Dentistry* 14, 12-19.

Soares, S., (2003). Nanometer edge and surface imaging using optical scatter. Precision Engineering 27, 99-102.

Tal, H., Kozlovsky, A., Green, E., Gabbay, M., (1989). Scanning electron microscope evaluation of wear of stainless steel and high carbon steel cures. Journal Of Periodontology 60, 320-324.

Tan, J., Zhang, J., (2004). An optical system incorporating gradient-index lens for confocal inspection. Optics and Lasers in Engineering 42, 233-240.

Thacker, J. G., Rodeheaver, G. T., Towler, M. A., Edlich, R. F., (1989). Surgical needle sharpness. American Journal Of Surgery 157, 334-339.

Thiele, J. D., Melkote, N., (1999). Effect of cutting edge geometry and workpiece hardness on surface generation in the finish hard turning of AISI 52100 steel. Journal of materials processing technology 94, 216-226.

Thompson, e. al., (1986). In-process cutting tool condition compensation and part inspection, US Patent No 4620281.

Towness C.H., (2000). How the laser happened. Talanta 51, 831-832.

Wadsworth, J., Lesuer, D. R., (2000). The knives of Frank J. Richtig as featured in Ripley's Believe It or Not!(R). Materials Characterization 45, 315-326.

Wallace, A. M., Zhang, G., Gallaher, Y., (1998). Scan calibration or compensation in a depth imaging system. Pattern Recognition Letters 19, 605-612.

Wang, L. S., Lee, D. L., Nie, M. Y., Zheng, Z. W., (2002). A study of the precision factors of large-scale object surface profile laser scanning measurement. Journal of materials processing technology 129, 584-587.

Appendix A

- A1 Set up for machine evaluation study
- A2 Set up for R and R study
- A3 Results for CATRA sharpness test

Appendix A1

Set up for machine evaluation study

Machine Evaluation Set-up:

Calibration performed

Laser 1

Zero set:

Span set:

Laser 2

Zero set:

Span set:

Standards used: Slip Gauges Case Serial No: 16724,

Traceability No...48412.....NAMAS.....

Parameters

Scan Length: 3.45mm

Scan Time :22.37 seconds

Number of Steps:50

Runs

Number of runs performed: 20 runs performed per Operator

Number of runs performed:1 Operator used in study

Blade used

Sample Blade used: Sample Blade no. 3.

Signed.....

Date.....

Appendix A2

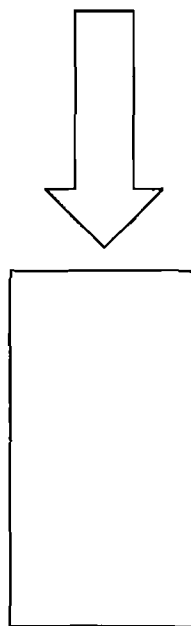
Set up for R and R study

Repeatability and Reproducibility study

Instructions for operators

- 1) Insert *blade* into holder.
- 2) Tighten clamp.
- 3) Press “Acquire button” on screen.
- 4) Remove blade from holder.
- 5) Place blade on area indicated.
- 6) Insert blade again and repeat process, 20 times.

Place blade here after each scan



Reproducibility Test Set-up:

Calibration performed

Laser 1

Zero set:

Span set:

Laser 2

Zero set:

Span set:

Standards used: Slip Gauges Case Serial No: 16724,

Traceability No...48412.....NAMAS.....

Parameters

Scan Length: 3.45mm

Scan Time : 22.37 seconds

Number of Steps:50

Runs

Number of runs performed: 20 runs performed per Operator

Number of runs performed: 3 Operators used in study

Blade used

Sample Blade used: Sample Blade no. 3.

Signed.....

Date.....

Appendix A3

Results for CATRA sharpness test

CATRA Sharpness Test Report to ISO 8442.5

Plain edge blades Type
A

Report number

Date 21st May 2003

Time 11:49:06

Blade description **Thick blade**

Edge angle

Edge Type

Test Number DUMMY.dat

	Sharpness ICP mm	Life TCC mm
knife tested	79.1	256.2
ISO limit mm	50	150
ISO Pass/ fail	pass	pass
CATRA comment	Average	Average

Test Speed mm/s 0

Test distance mm 50

Test load N 40

Test card available mm 50

mm 47

Blade offset mm 0

Test cycles 60

Test cycles completed 60

Test by machine Cutlery Research Association. [012]

Cycle number card cut mm Accumulative card cut

1	31.3	31.3
2	26.1	57.4
3	21.7	79.1
4	19.4	98.5
5	17.1	115.6
6	16.4	132
7	13.9	145.9
8	12.9	158.8
9	11.4	170.2
10	8.8	179
11	7.9	186.9
12	7.7	194.6
13	6.6	201.2
14	5.4	206.6
15	4.4	211
16	3.3	214.3
17	2.7	217
18	2.5	219.5
19	2.2	221.7
20	2.1	223.8
21	2	225.8
22	1.7	227.5
23	1.4	228.9
24	1.2	230.1
25	1.3	231.4
26	1.3	232.7
27	1.3	234
28	1.4	235.4

29	1.3	236.7
30	1.1	237.8
31	1.1	238.9
32	1	239.9
33	0.9	240.8
34	1	241.8
35	0.9	242.7
36	0.8	243.5
37	0.8	244.3
38	0.7	245
39	0.7	245.7
40	0.6	246.3
41	0.6	246.9
42	0.7	247.6
43	0.6	248.2
44	0.6	248.8
45	0.7	249.5
46	0.6	250.1
47	0.5	250.6
48	0.5	251.1
49	0.5	251.6
50	0.5	252.1
51	0.3	252.4
52	0.5	252.9
53	0.4	253.3
54	0.4	253.7
55	0.4	254.1
56	0.4	254.5
57	0.3	254.8
58	0.4	255.2
59	0.5	255.7
60	0.5	256.2

Appendix B

Calibration sheets

CERTIFICATE OF CALIBRATION

ISSUED BY TESA REFERENCE STANDARDS DIVISION

DATE OF ISSUE : 2nd October 1997

SERIAL NUMBER : 48545



CALIBRATION
No. 0001



Brown & Sharpe Ltd
Precision Measuring Instruments
Bradgate Street,
Leicester LE4 0AW
England.
Tel: INT'L +44 (0) 116 262 9012
Fax: INT'L +44 (0) 116 251 4762
e-mail: tesa@brownandsharpe.co.uk

PAGE 1 OF 2 PAGES

APPROVED SIGNATORIES

D. BARLOW
T. CREIGHTON
M. SINGH

Customer: J.E.D. Metrology, Ireland.
As Agents of: Sligo Regional Technical College, Ireland.

Order No: 9133


Description: A set comprising 14 angle gauges manufactured by TESA-RSD.

Serial No: 941

Report: These gauges have been examined at 20°C and the measured sizes found to be within the requirement of the N.P.L. Specification of Accuracy MOY/SCMI/18 Issue 5.

The measured deviation from nominal angles are given on page 2.

Date of Calibration: 2nd October 1997

Signature 



The uncertainties are for a confidence probability of not less than 95%

This certificate is issued in accordance with the conditions of accreditation granted by the National Measurement Accreditation Service, which has assessed the measurement capability of the laboratory and its traceability to recognised national standards and to the units of measurement realised at the corresponding national standards laboratory. Copyright of this certificate is owned jointly by the Crown and the issuing laboratory and may not be reproduced other than in full except with the prior written approval of the Head of NAMAS and the issuing laboratory.

CERTIFICATE OF CALIBRATION

DATE OF ISSUE

2nd October 1997

SERIAL NUMBER
48545

ISSUED BY TESA REFERENCE STANDARDS DIVISION
NAMAS ACCREDITED CALIBRATION LABORATORY No. 0001

PAGE 2 OF 2 PAGES

A set of 14 combination angle gauges.

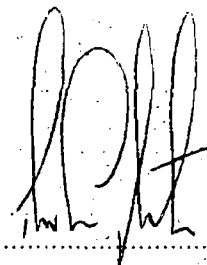
Case No. 941

ANGLE GAUGES

Nominal Angle Degrees	Measured error seconds of arc	Nominal Angle Minutes	Measured error seconds of arc
41	-0.7	27	-0.4
27	-0.1	9	-0.6
9	+0.2	3	-0.3
3	+0.2	1	-0.9
1	+0.3	0.5	-0.7
		0.3	+1.1
		0.1	+0.3
		0.05	-0.8

Uncertainty of Measurement \pm 2 seconds of arc.

Signature



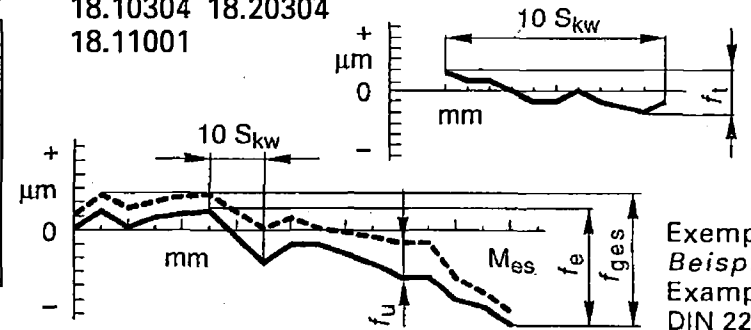
brown & sharpe

TESA CH-1020 Renens

**ATTESTATION DE CONFORMITÉ
ÜBEREINSTIMMUNGSATTEST
CONFORMITY SPECIFICATION**

18.10009 18.20011 18.18018 Comparateurs à levier
18.10010 18.20012 18.18019 Fühlhebelmessgeräte
18.10013 18.20015 Dial test indicators
18.10304 18.20304
18.11001

Champ de mesurage	Messspanne	Field of measurement	M_{es}	0,2 mm	.008 in
Valeur de l'échelon	Skalenteilungswert	Scale interval	S_{kw}	0,002 mm	100 μ in
Erreur d'indication	Abweichungsspanne	Span of error	f_e	2 μ m	100 μ in
Erreur d'indication locale	Abweichungsspanne in der Teilmessspanne	Local span of error	f_t	1 μ m	40 μ in
Erreur d'indication totale	Gesamtabweichungsspanne	Total span of error	f_{ges}	3,5 μ m	160 μ in
Hystérésis	Messwertumkehrspanne	Hysteresis band	f_u	1,5 μ m	60 μ in
Fidélité	Wiederholbarkeit	Repeatability	f_w	1 μ m	40 μ in

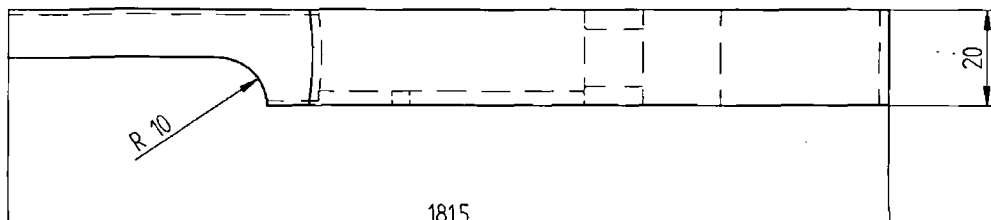
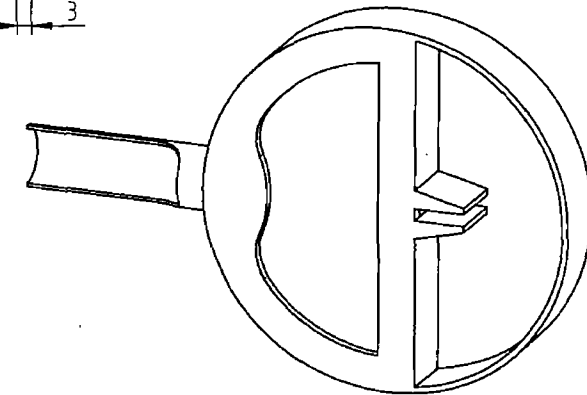
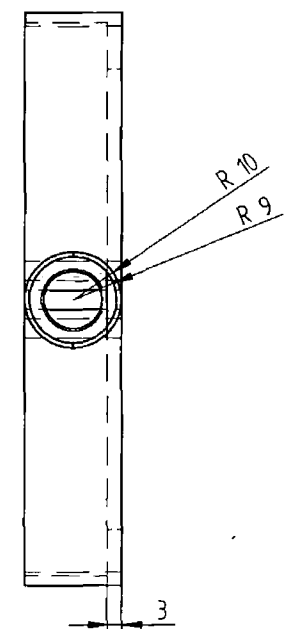
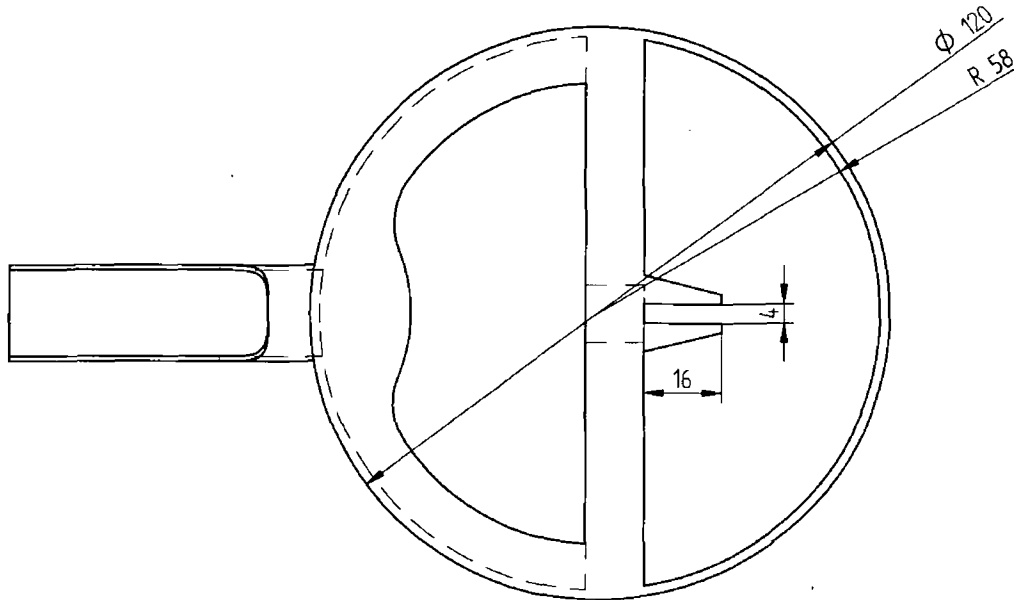


Exemple
Beispiel
Example
DIN 2270

Direction Assurance de la Qualité *[Signature]*

Appendix C

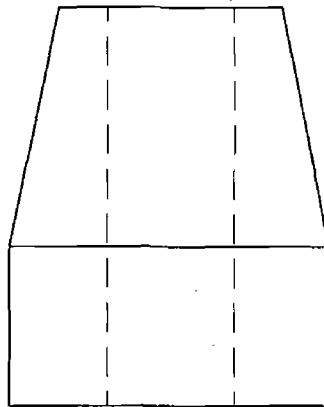
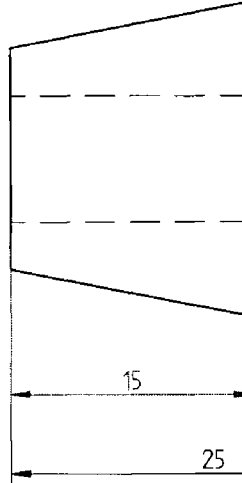
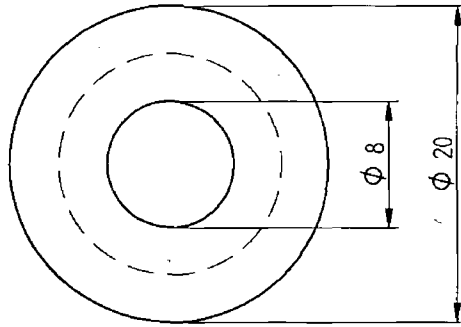
Mechanical drawings



REVISION HISTORY			
REV	DESCRIPTION	DATE	APPROVED

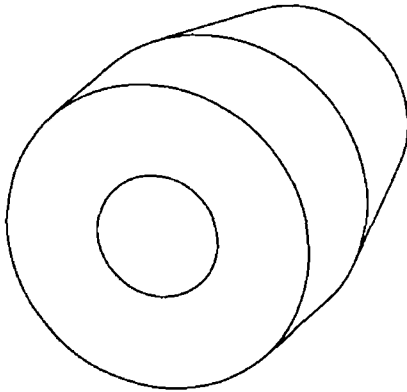
DRAWN	NAME	DATE	SOLID EDGE	
CHECKED	REF: 2	06/05/05	EDS-PLM SOLUTIONS	
ENG APPR			TITLE	
MGR APPR			Goniometer	
UNLESS OTHERWISE SPECIFIED DIMENSIONS ARE IN MILLIMETERS ANGLES °XX'			SIZE	DWG NO
2 PL. *XXX 3 PL. *XXXX			A2	
			FILE NAME	
			SCALE	WEIGHT
				SHEET 1 OF 1

SOLID EDGE ACADEMIC COPY



SOLID EDGE ACADEMIC COPY

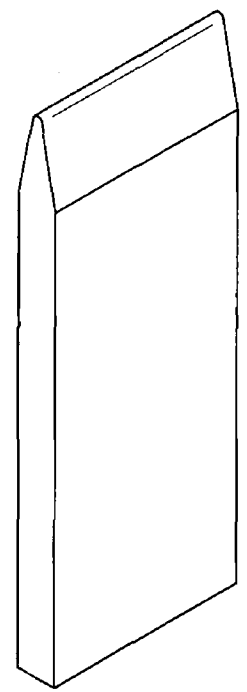
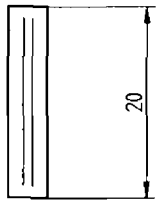
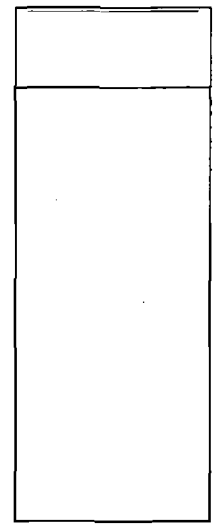
REVISION HISTORY			
REV	DESCRIPTION	DATE	APPROVED



tsigo
 An Intelligent Technological Solution

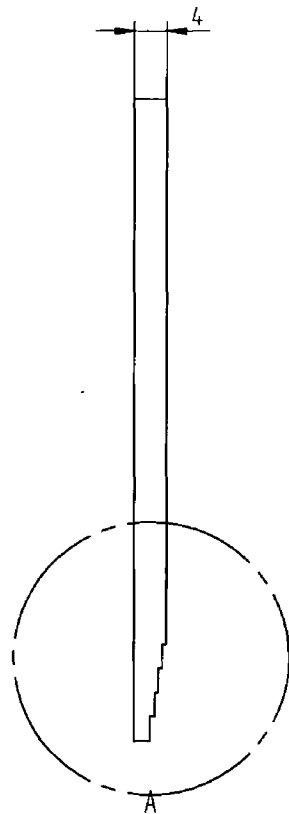
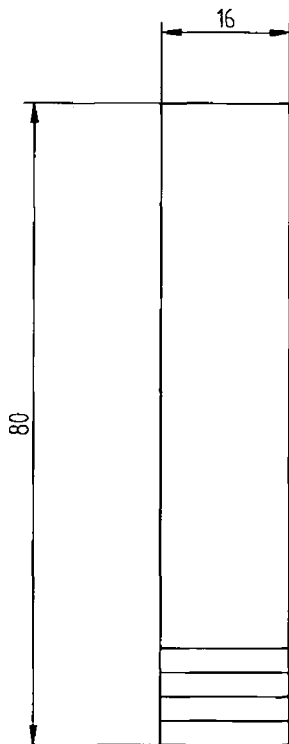
DRAWN	NAME	DATE	SOLID EDGE EDS-PLM SOLUTIONS TITLE: Spacer SIZE: A2 DWG NO: _____ REV: _____ FILE NAME: Spacer.dwg SCALE: _____ WEIGHT: _____ SHEET 1 OF 1	
CHECKED	OFFICE	DATE		
ENG APPR				
MGR APPR				
UNLESS OTHERWISE SPECIFIED DIMENSIONS ARE IN MILLIMETERS ANGLES = XX° 2 PL = XXXX 3 PL = XXXX				

REVISION HISTORY			
REV	DESCRIPTION	DATE	APPROVED



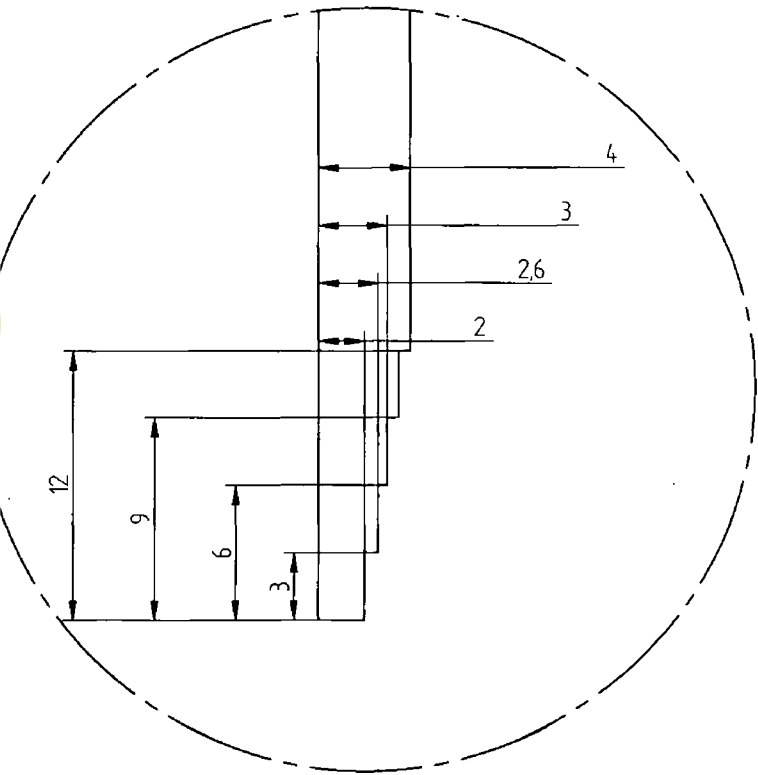
SOLID EDGE ACADEMIC COPY

DRAWN	edp:ce	DATE	08/15/03	SOLID EDGE EDS-PLM SOLUTIONS TITLE Sample blade	
CHECKED					
ENG APPR					
MGR APPR					
UNLESS OTHERWISE SPECIFIED DIMENSIONS ARE IN MILLIMETERS ANGLES °XX'				SIZE	A2
2 PL #XXXX 3 PL #XXXX				TITLE NAME	Eds:ce:01
				SCALE	WEIGHT
				SHEET 1 OF 1	



SOLID EDGE ACADEMIC COPY

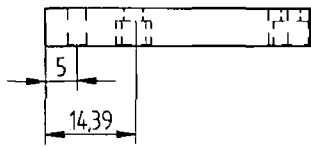
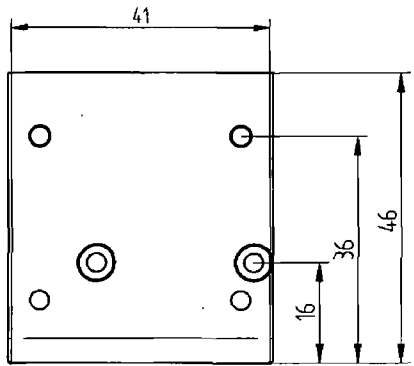
REVISION HISTORY			
REV	DESCRIPTION	DATE	APPROVED
1	Calibration Plate in steps of 0.5mm	29/09/04	



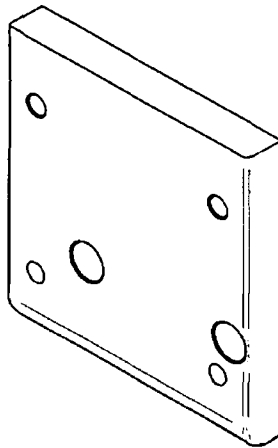
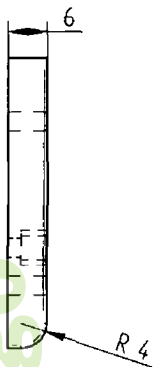
DETAIL A

DRAWN		NAME	DATE	SOLID EDGE EDS-PLM SOLUTIONS	
CHECKED					
ENG APPR				TITLE	Calibration Plate
MGR APPR				SIZE	A2
UNLESS OTHERWISE SPECIFIED DIMENSIONS ARE IN MILLIMETERS ANGLES °XX'				DRG NO	
				FILE NAME	Calibration.dwg
2 PL +XXX 3 PL +XXXX				SCALE	
				WEIGHT	
				SHEET	1 OF 1

Eds |igo
 An Integrated Manufacturing Solution



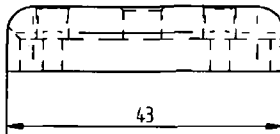
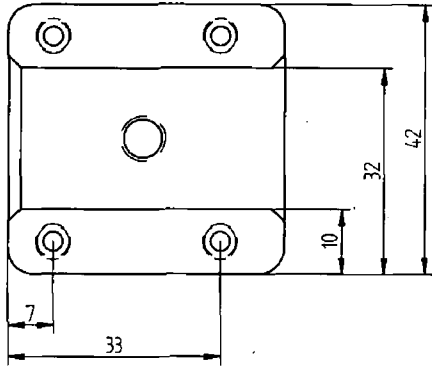
REVISION HISTORY			
REV	DESCRIPTION	DATE	APPROVED



An Instituid Teicmeolaíochta, Sligeach
 TSI
 An Instituid Teicmeolaíochta, Sligeach

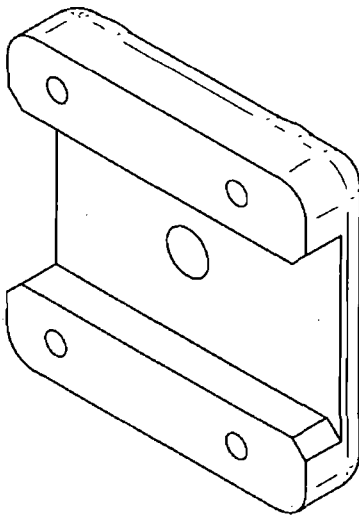
OPY

	NAME	DATE	SOLID EDGE EDS-PLM SOLUTIONS	
DRAWN	garise	08/04/05		
CHECKED			TITLE	
ENG APPR			Base Plate (original clamp)	
MGR APPR			SIZE	DWG NO
UNLESS OTHERWISE SPECIFIED DIMENSIONS ARE IN MILLIMETERS ANGLES = XX° 2 PL = XX XX 3 PL = X XXX			A2	
			FILE NAME	plate (original clamp)
			SCALE	WEIGHT
				SHEET 1 OF 1



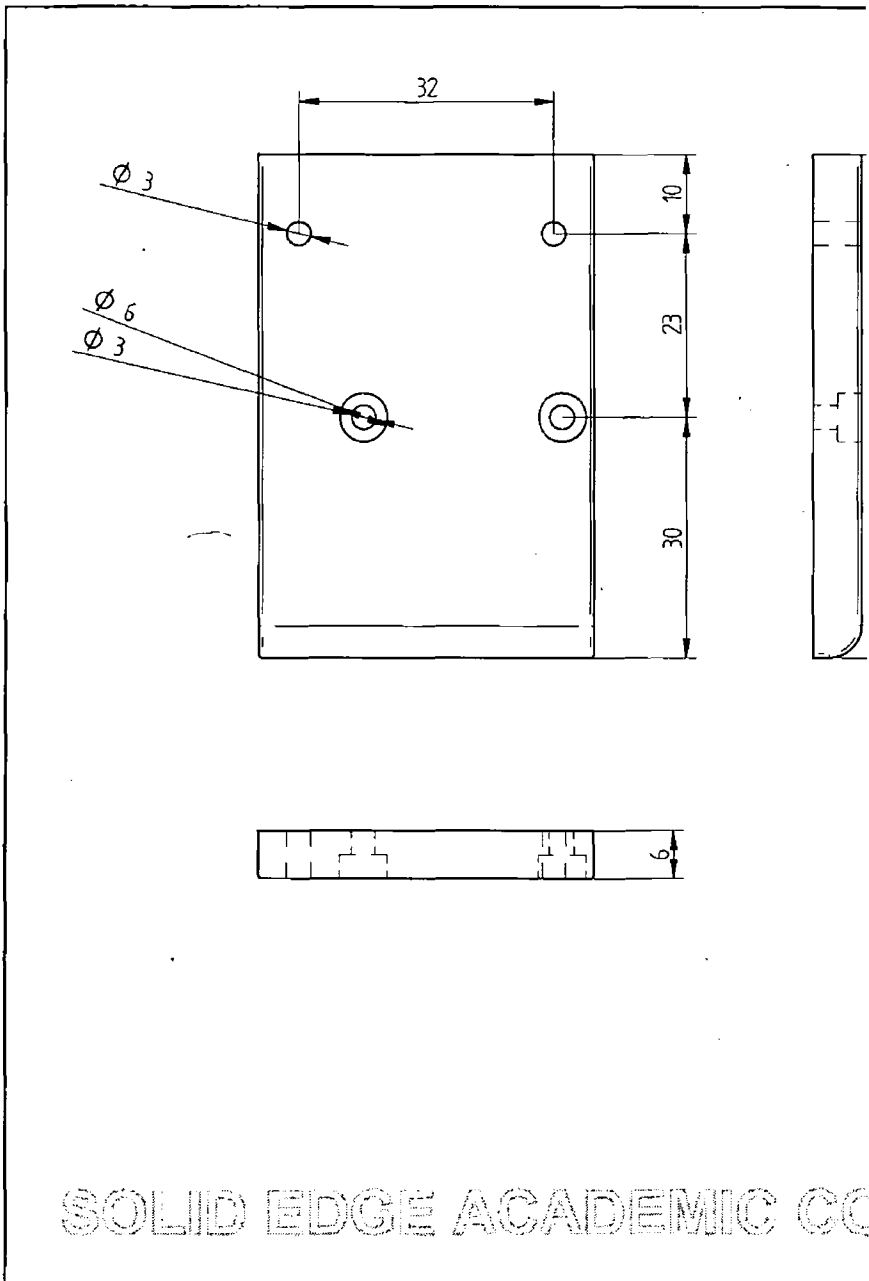
SOLID EDGE ACADEMIC COPY

22



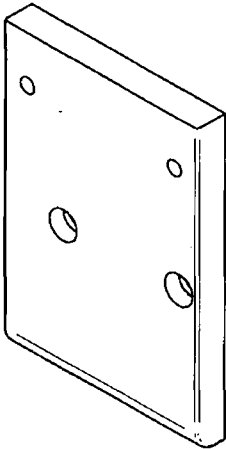
REVISION HISTORY			
REV	DESCRIPTION	DATE	APPROVED

DRAWN	NAME	DATE	SOLID EDGE EDS-PLM SOLUTIONS		
CHECKED	PERICE	22/05/25			
ENG APPR			TITLE		
MGR APPR			Top Plate (original clamp)		
UNLESS OTHERWISE SPECIFIED DIMENSIONS ARE IN MILLIMETERS ANGLES -XX° 2 PL -X.XX 3 PL -X.XXX			SIZE	DWG NO	REV
			A2		
			FILE NAME: Top plate (original clamp).dft		
			SCALE	WEIGHT	SHEET 1 OF 1



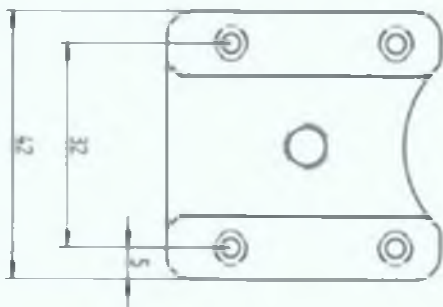
63

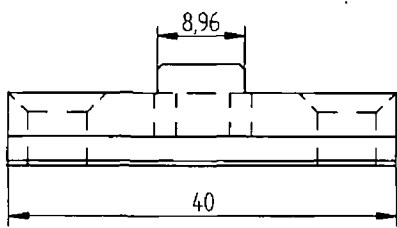
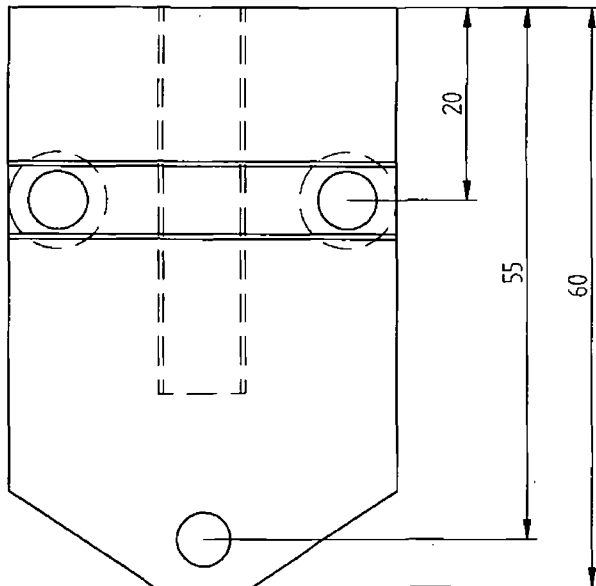
REVISION HISTORY			
REV	DESCRIPTION	DATE	APPROVED



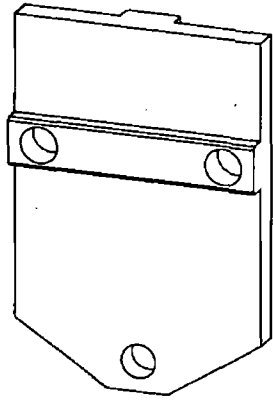
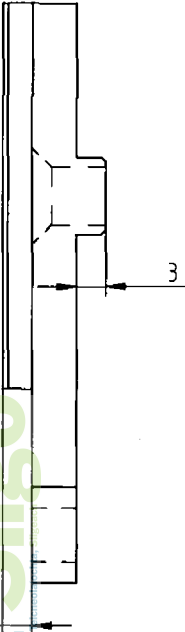
COPY

DRAWN	NAME	DATE	SOLID EDGE EDS-PLM SOLUTIONS	
CHECKED				
ENG APPR			TITLE	
MGR APPR			Base Plate (modified)	
UNLESS OTHERWISE SPECIFIED DIMENSIONS ARE IN MILLIMETERS ANGLES =XX° 2 PL =XXXX 3 PL =XXXX			SIZE	KEY
			AZ	
SCALE:			WEIGHT:	SHEET 1 OF 1



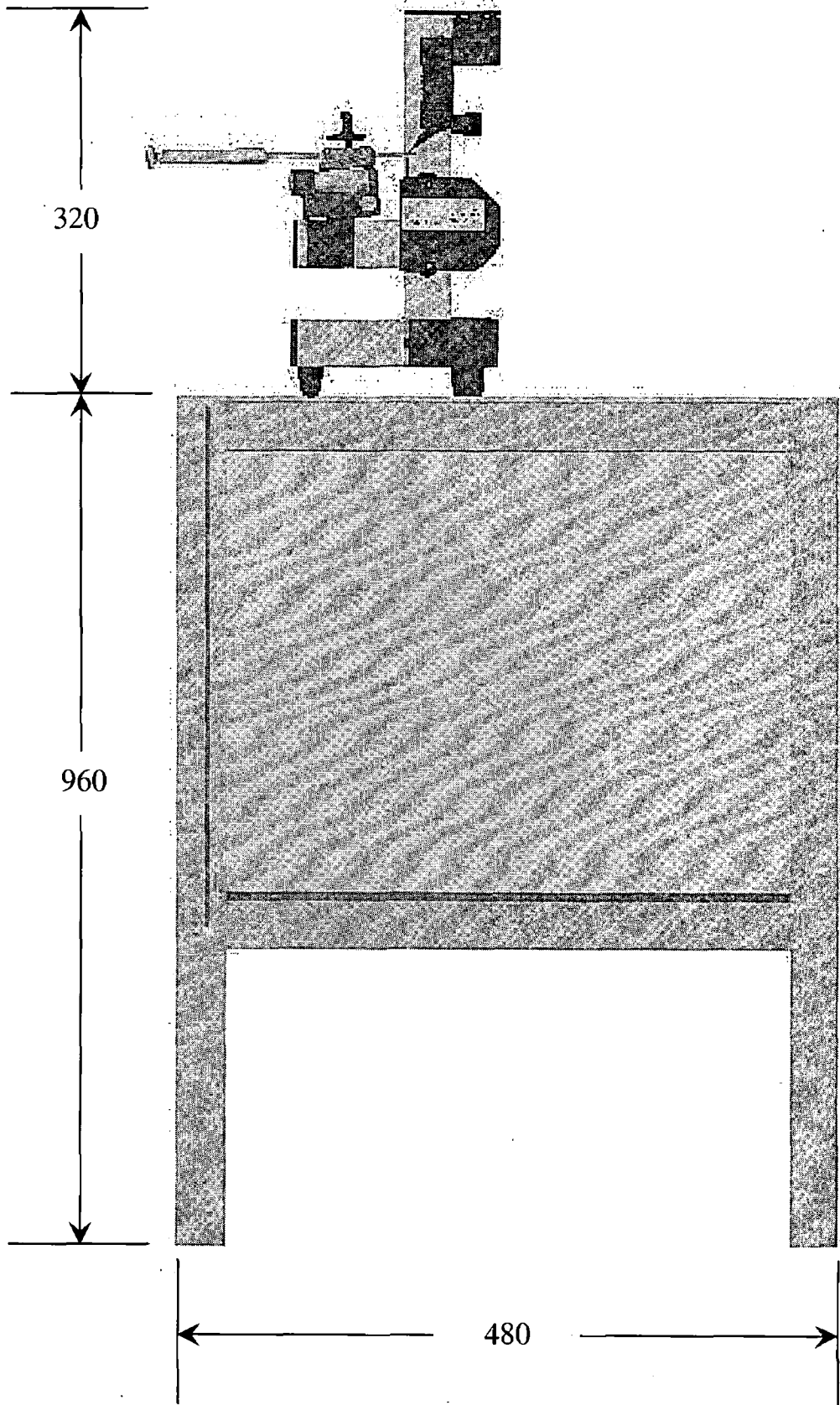


REVISION HISTORY			
REV	DESCRIPTION	DATE	APPROVED



Solid Edge
 An Institution

DRAWN	NAME	DATE	SOLID EDGE EDS-PLM SOLUTIONS TITLE: Spacer plate					
CHECKED	DATE	DATE				SIZE	DWG NO	REV
ENG APPR						A2		
MGR APPR						FILE NAME: Spacer plate for drawing		
UNLESS OTHERWISE SPECIFIED DIMENSIONS ARE IN MILLIMETERS ANGLES =XX° 2 PL +XXXX 3 PL +XXXX			SCALE:	WEIGHT:	SHEET 1 OF 1			



Overall dimensions of measurement instrument

